Technische Universität München
Lehrstuhl für Zoologie

Sound Localization in Birds

-

Physical and Neurophysiological Mechanisms of Sound Localization in the Chicken

Hans A. Schnyder

Vollständiger Abdruck der von der Fakultät Wissenschaftszentrum Weihenstephan für Ernährung, Landnutzung und Umwelt der Technischen Universität München zur Erlangung des akademischen Grades eines

Doktors der Naturwissenschaften

genehmigten Dissertation.

Vorsitzender: Prof. Dr. Rudolf Fries
Prüfer der Dissertation: 1. Prof. Dr. Harald Luksch
2. Prof. Dr. Bernhard Seeber

Die Dissertation wurde am 09.08.2017 bei der Technischen Universität München eingereicht und durch die Fakultät Wissenschaftszentrum Weihenstephan für Ernährung, Landnutzung und Umwelt am 22.01.2018 angenommen.

Summary

Accurate sound source localization in three-dimensional space is essential for an animal's orientation and survival. While the horizontal position can be determined by interaural time and intensity differences, localization in elevation was thought to require external structures that modify sound before it reaches the tympanum. Here I show that in birds even without external structures such as pinnae or feather ruffs, the simple shape of their head induces sound modifications that depend on the elevation of the source. A model of localization errors shows that these cues are sufficient to locate sounds in the vertical plane. These results suggest that the head of all birds induces acoustic cues for sound localization in the vertical plane, even in the absence of external ears. Based on these findings, I investigated the neuronal processing of spatial acoustic cues in the midbrain of birds. The avian midbrain is a computational hub for the integration of auditory and visual information. While at early stages of the auditory pathway time and intensity information is processed separately, information from both streams converges at the inferior colliculus (IC). There, a map of space is created in the external nucleus (ICx) and combined with a visual map of space in the optic tectum (OT). While this integration has mostly been investigated in the barn owl, a hearing specialist, much less is known about these processes in hearing generalist birds. I investigated shape and location of auditory spatial receptive fields (aSRFs) and basic response properties of auditory neurons in the chicken midbrain. Neurons in the IC, the recently identified formatio reticularis externalis (FRLx), and the OT showed spatially confined aSRFs in both azimuth and elevation. These neurons displayed either round or annular aSRFs and were centered lateral to the head. In general, the size of the aSRFs decreased toward spatial positions lateral to the head. These data suggest that in hearing generalist birds, such as the chicken, auditory spatial tuning is sharpest at lateral positions, the position of the visual axis.

Zusammenfassung

Eine exakte Schalllokalisierung im dreidimensionalen Raum ist für die Orientierung und das Überleben eines Tieres unerlässlich. Während die horizontale Position durch interaurale Zeit- und Intensitätsunterschiede (ITDs oder IIDs) bestimmt werden kann, wurde bislang angenommen, dass die Lokalisierung in der Vertikalen von Außenohr-Strukturen abhängig ist, die Geräusche verändern bevor diese das Trommelfell erreichen. Die vorliegende Arbeit zeigt dagegen, dass allein der Kopf der Vögel ausreicht um Geräusche abhängig von deren Elevation zu verändern. Ein Modell, welches Lokalisierungsfehler berechnet, zeigt, dass die erzeugten ITDs und IIDs ausreichen, um Töne in der Vertikalen zu lokalisieren. Diese Ergebnisse deuten darauf hin, dass der Kopf aller Vögel akustische Cues zur Schalllokalisierung in der Vertikalen generiert, gänzlich ohne äußere Ohren. Basierend auf diesen Erkenntnissen habe ich die neuronale Verarbeitung von räumlich akustischen Cues im Mittelhirn der Vögel untersucht. Das Mittelhirn ist ein Zentrum für die Integration von auditorischen und visuellen Informationen. In der aufsteigenden Hörbahn werden Zeit und Intensität zunächst getrennt verarbeitet und konvergieren erst auf der Ebene des Inferioren Colliculus (IC). Im äußeren Teil des IC, dem ICx, wird eine Karte des Raumes erzeugt und daraufhin mit der visuellen Raumkarte im Optischen Tektum (OT) kombiniert. Während dies bis ins Detail in der Schleiereule, einem Hörspezialisten, untersucht wurde, ist bei einfacheren Vögeln hingegen viel weniger darüber bekannt. In dieser Arbeit zeige ich Untersuchungen zur Gestalt und dem Vorkommen auditorisch räumlich rezeptiver Felder (aSRFs) und charakterisiere grundlegende Antwort-Eigenschaften auditorischer Neurone im Mittelhirn von Hühnern. Neurone im IC, dem kürzlich identifizierten formatio reticularis externalis (FRLx) und im OT weisen sowohl in der Horizontalen als auch Vertikalen räumlich begrenzte aSRFs auf. Diese aSRFs waren entweder rund oder ringförmig und immer seitlich zum Kopf ausgerichtet. Im Allgemeinen nahm die Größe der aSRFs bei räumlichen Positionen seitlich zum Kopf hin ab. Dies legt nahe, dass das

Richtungshören nicht-spezialisierter Vögel, wie dem Huhn, zur Seite hin am Schärfsten ist, nämlich dort wo sich auch deren Sehachse befindet.

Contents

Summary 1

Zusammenfassung 2

1 Sound localization in birds 6

1.1 Sound localization facilitates survival in animals 6

1.2 Sound localization cues in mammals, owls and birds 9

1.3 Hearing range in mammals, owls and birds 12

1.4 Neuronal processing of sound localization cues in birds 13

1.5 Representation of auditory space in the midbrain of birds 14

1.6 Directional hearing integrates into the visual space in the optic tectum 15

1.7 Aims 17

2 The Avian Head Induces Cues for Sound Localization in Elevation 20

2.1 Methods 20

2.1.1 Head related impulse response measurement 20

2.1.2 Estimation of the localization error 22

2.2 Results 27

3 Auditory spatial receptive fields in the midbrain of the chicken 42

3.1 Methods 42

3.1.1 Animals 42

3.1.2 Surgery 42

3.1.3 Stimulation 43

3.1.4 Recording 44

3.1.5 Histology 45

3.1.6 Analysis 46

3.1.7 Explaining aSRFs by ILDs and ITDs 47

3.2 Results 50

3.2.1 Auditory recordings in the chicken midbrain 50

3.2.2 Overview of auditory units along the midbrain structures and their responsiveness to noise and pure tones 51

3.2.3 Frequency response fields (FRFs) 54

3.2.4 Response properties of auditory units in the midbrain 56

3.2.5 Spatially confined auditory receptive fields in the chicken midbrain 58

3.2.6 aSRFs can be explained by either ITD or ILD 62

3.2.7 Percentage of spatially confined auditory spatial receptive fields by midbrain structures 65

3.2.8 Topographic distribution of annular aSRFs in the optic tectum 67

4 Discussion 68

4.1 Sound localization cues in birds 68

4.2 The hearing range of birds is connected to the perception of sound localization cues 69

4.3 Increasing sound localization cues without external ears 73

4.4 Auditory spatial receptive fields in the midbrain of the domestic chicken 74

4.5 The chicken midbrain displays two different types of spatially confined aSRFs 75

4.6 Whole spatial surround covered by aSRFs in the chicken 77

4.7 Topography of annular aSRFs in the optic tectum 77

4.8 Differences between auditory responses in the different midbrain structures 78

4.9 Auditory responses in the bird FRLx reported for the first time 78

4.10 Sound localization in symmetrically eared birds 79

4.11 Comparing auditory systems in tetrapods 82

4.12 Conclusion 84

Bibliography 86

Appendix 99

1 Sound localization in birds

Imagine standing in a dense forest with your eyes closed. What do you hear? Even though you do not feel the wind on your skin you notice the leaves of the beech trees rustling above you. A small creek announces itself, even though hidden, you hear its gentle rippling. Tok, tok, tok you hear a woodpecker working on one of the trees you just passed. A chaffinch's unmistakable song reaches your ear, it may soon start to nest. And a crack far in front of you followed by fleeing steps gives away a deer you might just have chased away.

We constantly analyze our environment in a similar way, even if we might not realize it. Hearing provides us with vital information from all directions of our environment: If we were hungry or thirsty, fish and water would be found at the creek. Our sense of hearing warns us also of dangers, long before we face them. In our modern environment, for example, if a car approaches from the rear, one might consider staying on the sidewalk a little longer.

And all of this works easily in situations where bigger distances, poor lighting conditions or fragmented environments are involved. The key for this system to function properly is: we need to locate a sound’s source.

This doctoral thesis focuses on the unique mechanisms of sound localization in birds.

1.1 Sound localization facilitates survival in animals

Animals locate sounds under the widest variety of conditions for different purposes, all of which have been developed and proven over the course of evolution. The common goal is to secure the species’ survival. For example, directional hearing allows for the exploration of foreign areas, which are potentially full of unused food sources, and thus to avoid starvation. For carnivores, it could mean that it stalks

prey using its hearing. In turn, this leads to a corresponding response in the course of evolution: potential prey use sound localization to avoid their predators. Reproduction and thus the propagation of one's own genes is another driving force in evolution. The directional hearing helps not only in finding a partner, but also in searching and retrieving lost offspring.

Many of these strategies have been studied and demonstrated in numerous species. A prime example of directional hearing for the purpose of hunting is the marsh hawk (*Circus cyaneus*). This bird of prey knows exactly where a mouse hides in dense scrub. It flies over the rampant vegetation in a few meters height and swoops down to catch its prey with 1-2° accuracy (Rice 1982). The towhee, a North American song bird, displays its own strategy to secure reproductive success. It depends on its ears to aggressively defend its territory. Upon hearing a rival’s mating calls it locates the singing competitor and drives it off (Nelson and Suthers 2004). On the other hand, there are also examples of animals that avoid their aggressive conspecies. The corncrake (*Crex crex*) makes sure to keep its distance upon hearing the songs of conspecifics (Rek 2014). "Glucke" in German means a particularly caring mother. This word is borrowed from nature and is actually used for a hen who takes care of its offspring. When the chicks are separated from the mother, the hen finds them without difficulty by locating their beeping calls (Engelmann 1928). When an animal crosses larger distances to open up new sources of food, the hearing helps to navigate through its environment. Birds for example quite commonly hear infrasound (<20 Hz) (Hill et al. 2014, Theurich et al. 1984, Schermuly and Klinke 1990). It is hypothesized that pigeons use infrasound sources as landmarks for navigation. A natural source for infrasound are oceanic breakings of waves, which pigeons are known to hear over great distances (Hagstrum 2000, Yodlowski et al. 1977). A particularly striking form of orientation evolved among both birds and mammals: echolocation. These animals scan their surroundings via sound. By emitting calls and analyzing the returning echo they gain information about their environment. Among avian species cave-dwelling and nocturnal birds use echolocation. Their calls are audible in the human hearing range and are primarily used for orientation (Brinklov et al. 2013, Coles et al. 1987, Konishi

and Knudsen 1979, Thomassen et al. 2007). Echolocation among mammals evolved prominently in toothed whales (*Odontoceti*) and in bats (*Microchiroptera*). The echolocation calls of both taxa are in the ultrasonic range and are used for hunting and orientation (Au 2012, Schnitzler and Kalko 2001). Unfortunately for these predators, some of their prey also evolved ultrasonic hearing (Miller and Surlykke 2001). Bats have a hard time to catch moths as these respond to such calls with evasive maneuvers (Roeder 1962), and crickets avoid sound sources in the ultrasonic range (Moiseff et al. 1978). The same occurs under water: If herrings hear ultrasonic calls they steer away from its source (Popper et al. 2004, Anglea et al. 2004). Herrings do not seem to communicate in ultrasonic range or use it for other purposes. So their ability to hear these sounds is seen as an adaptation to avoid being caught by toothed whales.

Finally the barn owl (*Tyto alba*) has to be mentioned. This nocturnal bird of prey catches its quarry even under the most difficult conditions; it is able to strike prey even in the complete absence of light (Payne 1962). Its sound localization behavior is clearly observable: It first approaches and then catches the source of the sound. This allows to evaluate the sound localization performance of the barn owl in behavioral experiments, making it an ideal organism for the investigation of sound localization. In the field of sound localization there is no other species that is so well studied till today. However during my doctoral thesis I focused on a bird which is not as specialized in sound localization as the barn owl. The chicken (*Gallus gallus*) is an avian species with hearing abilities like any other common bird. And as you will see in this work, both the physical and neurophysiological mechanisms of sound localization in the chicken are quite different from the barn owl.

1.2 Sound localization cues in mammals, owls and birds

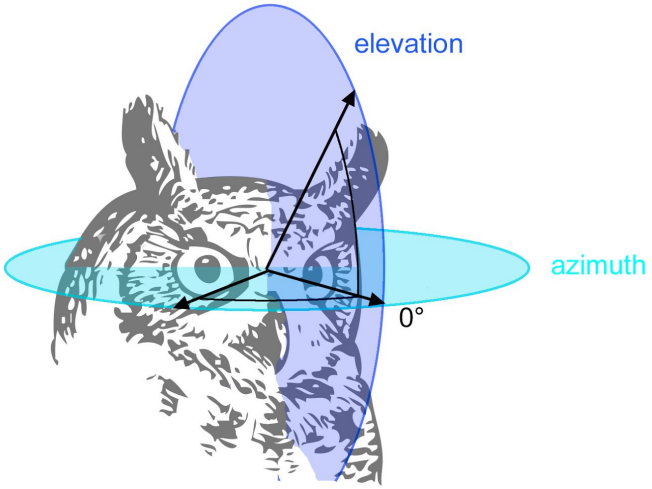

Figure 1.1: The location of a single sound source is described by its azimuth and elevation. The azimuth (turquoise) describes the angular difference along the horizontal plane, the elevation (blue) the vertical height of a sound source compared to the head. (Illustration: Ulrike Schnyder)

The auditory system requires special cues to determine the direction of a sound source. But what are these cues and where do they come from? In vertebrates two spatially separated ears provide the cues needed for sound localization. They compare the differences in sound between both ears (Blauert 1997). For example, a sound originating from the left reaches the left tympanum earlier and with higher intensity. The differences in time (or phase) are induced by the distance between both receiving eardrums, the differences in intensity are due to the head diffracting, reflecting and refracting sound. In vertebrates, localization of sound in the horizontal plane (azimuth, Fig. 1.1) is primarily achieved by comparing phase and intensity differences between both ears (IPDs and IIDs, respectively) (Grothe et al. 2010, Schnupp and Carr 2009). In contrast, sound localization in the vertical plane (elevation, Fig. 1.1) requires structures that modify sound before it reaches the tympanum (Middlebrooks 1991). In mammals this is typically achieved by external ears (pinnae) (Koka et al. 2011). Due to their complex morphology, pinnae absorb, reflect and diffract sound depending on direction and frequency. Thus, the sound that reaches the tympanum has characteristic notches and peaks in the frequency spectrum. These spectral cues are used to locate sound in elevation (Blauert 1997, Gardner and Gardner 1973) (Fig. 1.2). Such a spectral analysis has to be learned in mammals, usually guided by their visual system (Hofman et al. 1998). In

consequence individuals who were born blind struggle to locate sounds along elevation (Lewald 2002). Also, if the pinna is strongly deformed by injuries, individuals lose this ability but recover it again with training (Hofman et al. 1998).

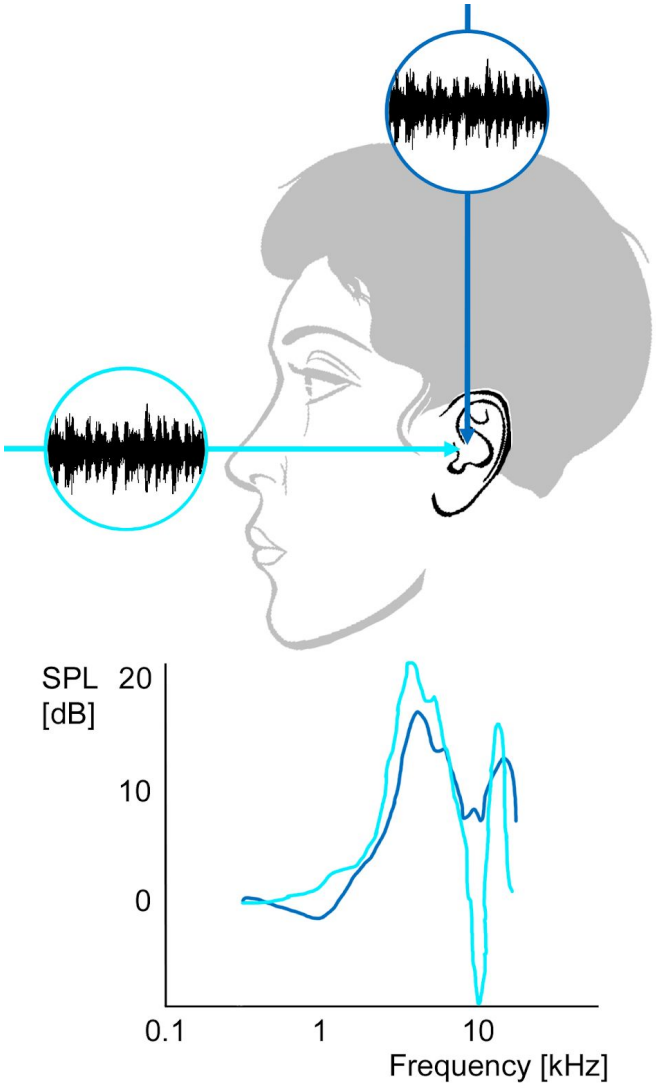

Figure 1.2: The pinna allows sound localization along elevation. The same sound once played from the front (turquoise) and from above (blue). The outer ear modulates the sound as a function of sound position, resulting in different frequency spectra on the eardrum. The frontal position (turquoise) results in a clear notch at 10 000 Hz. From above (blue) the notch is not as pronounced at 10 000 Hz. These differences in the frequency spectrum allow sound localization along elevation. (Illustration: Ulrike Schnyder)

This solution is however only possible for animals with pinnae, a structure that perplexingly only evolved in mammals. Birds, reptiles and amphibia lack pinnae, with one notable exception among birds being owls. These hearing specialists have a similar approach to sound localization as mammals: They possess a feather ruff, which consists of densely packed feathers (“reflector feathers”) (see Fig. 1.3). These feathers reflect sound and therefore serve a similar purpose as the pinna of

mammals (Campenhausen and Wagner 2006). Together with the frontally shifted position of the eyes, this is seen as a unique adaptation for hunting under dim light conditions. The barn owl is a nocturnal predator that strongly relies on auditory localization of prey (Payne 1971). Both the feather ruff and asymmetric ears (a vertical offset of the outer ear openings, Fig. 1.3) introduce IIDs that change systematically with elevation (Keller et al. 1998).

Figure 1.3: The asymmetric ears of the barn owl (*Tyto alba*) consist of external ear structures and a vertical offset of the outer ear openings. Auricular and reflector feathers and two “ear flaps” form the external ears of the owl. Here, the auricular feathers are removed up to the "ear flap", uncovering the reflector feathers. (Artist: Elizabeth Roen Kelly)

This allows for localization in elevation (Moiseff 1989, Pena and Konishi 2001), especially in front of the animal (Hausmann et al. 2009). As virtually all other birds lack such specializations, they were considered largely incapable of sound localization in elevation (Rice 1982, Klump 2000, Christensen-Dalsgaard 2005), even though this was obviously at odds with the richly structured three-dimensional world of birds (Larsen 2004).

1.3 Hearing range in mammals, owls and birds

The avian and mammalian hearing varies significantly in its frequency range. The avian ear is insensitive to frequencies above 7000 Hz, but is still sensitive to infrasound. In mammals, on the other hand, sensitivity for frequencies above 7000 Hz is common, whereas infrasound can only be detected by very large mammals. For example, the human ear is sensitive to frequencies from 20 to 20000 Hz, the chickens' from 7 to 7000 Hz (Hill et al. 2014, Theurich et al. 1984, Schermuly and Klinke 1990, Fay 1988), extending in both cases over 10 octaves. In terrestrial mammals it is assumed that high-frequency hearing evolved in adaptation to pinna-based localization cues (Heffner and Heffner 2008). Only high-frequency components of sound are sufficiently modulated by the pinnae to produce usable cues. In humans, for example, frequencies above 7000 Hz must be present in sounds, so that they can be located along elevation with the aid of the pinnae (Roffler and Butler 1968). This interaction between the pinna and the sound depends on the size of the pinnae and the wavelength of the sound. The smaller the pinnae, the shorter are the wavelengths (i.e., higher in frequency) that sufficiently induce spectral cues and IIDs. The result is that smaller mammalian species, with smaller ears, also have better sensitivity for high frequencies (Heffner and Heffner 2008). Interestingly, there are also some bird species that show an increased sensitivity for high frequencies (Fay 1988). However they are all owl species, which like mammals possess external ear structures. This is well studied in the barn owl, where asymmetric ears (consisting of external ear structures and asymmetric ear openings) introduce IIDs especially at high frequencies that change systematically with elevation (Campenhausen and Wagner 2006). Due to an elongated basilar membrane in the cochlea, the organ that perceives sound, the barn owl hears up to 12000 Hz (Fischer et al. 1988, Manley 1990, Dyson et al. 1998). Without this sensitivity to high frequencies, the barn owl would be unable to use the cues induced by its asymmetric ears. Until now it is not clear why the remaining birds are insensitive to higher frequencies.

1.4 Neuronal processing of sound localization cues in birds

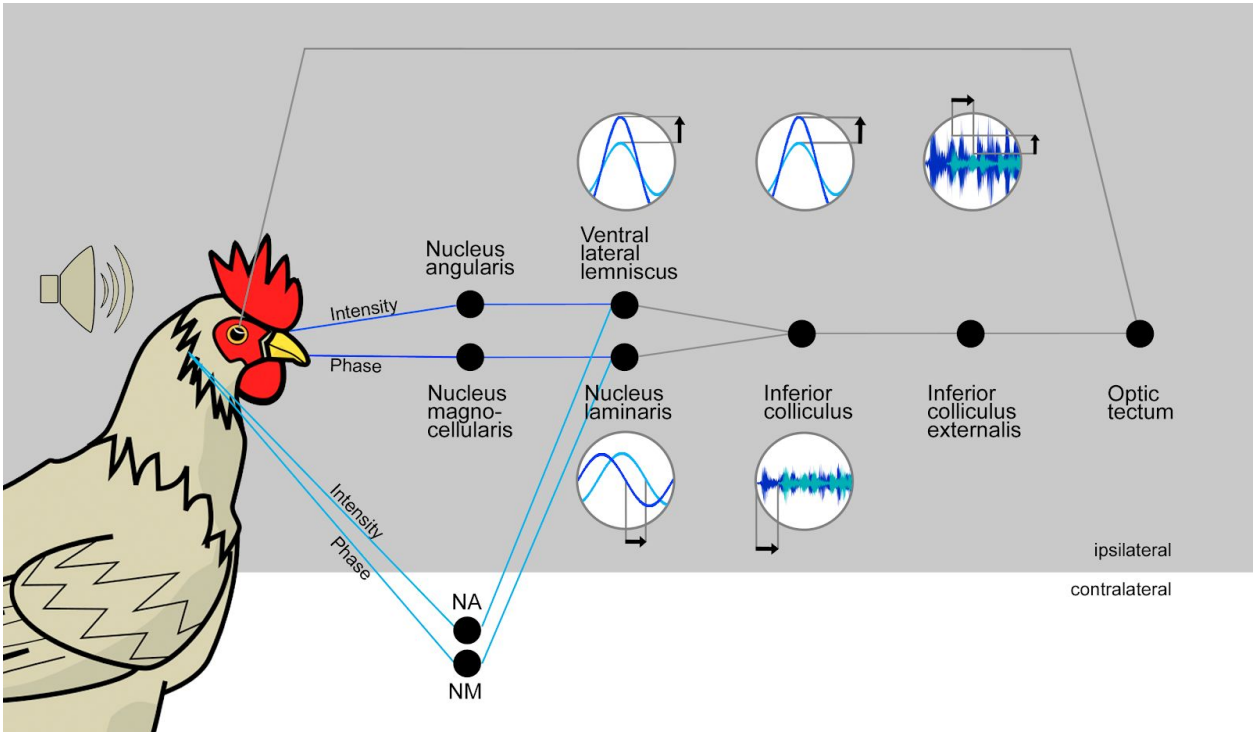

Figure 1.4: The avian brain processes sound localization cues in different structures. In the first step phase (nucleus magnocellularis (NM)) and intensity (nucleus angularis (NA)) is processed separately for each ear. The sound-facing side (ipsilateral) is shown in blue, the sound-turned side (contralateral) in turquoise. In the next step, the differences of phase and intensity for each ear result in IPDs and IIDs. The inferior colliculus (IC) then calculates "real" ITDs from IPDs. In the external IC, the neurons simultaneously process ITD and IID, while for the first time displaying complete auditory spatial receptive fields. The optic tectum (OT) combines auditory and visual information and processes them together. (Illustration: Ulrike Schnyder)

At first the auditory pathway processes phase and intensity of the sound separately (Fig. 1.4). Starting from the inner ear, auditory nerve fibers enter the primary auditory nuclei, the nucleus angularis (NA) and the nucleus magnocellularis (NM). The lateral part of the auditory nerve innervates the NA. The medial part transmits information about the phase to the NM (Carr 1991), but does not respond to intensity differences (Fukui et al. 2010, Sullivan and Konishi 1984). Afferents of the ipsilateral and contralateral NM bilaterally innervate the nucleus laminaris (NL). Their axons serve as so-called delay lines and thus form a neural map of ITDs in the NL (Carr and Konishi 1988). The NL neurons work as coincidence detectors, meaning proper ITDs

from both NMs activate the NL neurons strongly. At the same time NL neurons are strongly frequency-selective and phase-dependent (Carr and Konishi 1990). The NL projects to the inferior colliculus (IC), which is part of the midbrain (Wang and Karten 2010). In the IC, IPDs across frequencies are merged based on the same time differences (Wagner et al. 1987; Konishi 2000), although not across the entire audible range (Vonderschen and Wagner 2009; Cazettes et al. 2014) and the frequency dependency is lost (Konishi 2000, Wagner et al. 1987). The contralateral and ipsilateral NA connects binaurally to the ventral lateral lemniscus (LLDp / VLVp), which processes IIDs (Klump, 2000). In the LLDp, IIDs form a map and the LLDp projects this to the IC (Manley et al. 1988, Mogdans and Knudsen 1994). ITDs and IIDs converge in the lateral shell of the IC (Takahashi et al. 1989) and are processed simultaneously from there on (e.g.in the external part of the IC, the ICx; Takahashi et al. 1984). This processing of ILDs and ITDs in the brainstem is comparable in all birds.

1.5 Representation of auditory space in the midbrain of birds

Most of the work on the representation of auditory space in birds has been performed in the barn owl. However, as mentioned before, the barn owl is a unique bird as it possesses specializations (feather ruff, asymmetric ears, high frequency hearing) that facilitate excellent sound localization (Moiseff 1989; Keller et al. 1998). Other avian species lack such specializations. Their auditory system differs in the availability of binaural cues and consequently in the representation of auditory space.

For example, ICx neurons of the barn owl are maximally active when the sound exhibits the right IID and ITD combination (Moiseff and Konishi 1981; Takahashi et al. 1984; Pena and Konishi 2001). If one cue is a bit off, the unit does not respond. In the barn owl ITDs code azimuth and IIDs code elevation (Moiseff 1989), giving rise to auditory spatial receptive fields (aSRFs). aSRFs recorded from the IC are spatially confined with an excitatory center and an inhibitory surround (Knudsen and Konishi

1978a). The spatial tuning of ICx neurons is topographically arranged, i.e., their aSRFs represent the area surrounding the bird along azimuth and elevation (Knudsen and Konishi 1978b). The barn owl, therefore, possesses as spatiotopic map of sound positions in the ICx. This map is then transferred onto the OT via a direct projection (Knudsen 1982, 1984; Olsen et al. 1989).

In other birds however, the burrowing owl (*Athene cunicularia*) and the pigeon (*Columba livia*), both parameters seem to encode azimuth in the IC (Volman and Konishi 1990; Lewald 1987, 1990). Likewise, the shape of the aSRFs in the IC differs between the barn owl and other bird species, including owls without ear asymmetries: They lack a narrow spatial tuning in elevation (hawks: (Calford et al. 1985); great horned owl (*Bubo virginianus*): (Volman and Konishi 1989, 1990) and burrowing owl: (Volman and Konishi 1990)). Likewise, a topography of sound position was only found for azimuth (great horned owl: (Volman and Konishi 1989), burrowing owl and long-eared owl: (Volman and Konishi 1990)) or not at all (Coles and Aitkin 1979). Since the measured fields are spatially unconfined, it is still unclear how unspecialized birds, i.e. auditory generalists, can locate sound in space.

1.6 Directional hearing integrates into the visual space in the optic tectum

Objects, especially alive ones, transmit signals in a wide range of modalities, often stimulating several senses simultaneously. An approaching dog, for example, is seen and heard first. If it is close enough, one can feel and probably smell it too. The opportunity to recognize and locate an object increases with every available sense (Stein and Meredith 1993). It even goes so far that integrating across senses provides performances that a single sense would not. Humans, e.g., recognize objects faster and with higher accuracy when exposed to multisensory stimuli compared to unisensory stimulation (Giard and Peronnet 1999, Forster et al. 2002). Chickens discriminate audiovisual objects better than visual objects alone (Verhaal and Luksch 2015). To facilitate this, vision and hearing is processed together for the first time on the level of the optic tectum in the midbrain. As the name implies, this

midbrain structure primarily processes visual sensory information. Thus, the superficial layers of the tectum receive direct topographic input from the contralateral retina. Tectal units respond to visual stimuli from specific spatial positions, displaying visual spatial receptive fields (vSRFs). Stimulation from other directions however inhibits these units (Stein et al. 1993, Knudsen and Brainard 1995). The vSRFs arrange systematically along the surface of the tectum and form a map that represents the entire retinal input. However the tectum also receives auditory input from the inferior colliculus (Knudsen 1982; Niederleitner et al. 2017). It thus represents the first structure which processes both the visual and auditory world. In the barn owl units in the deep layers respond also to auditory stimulation, displaying aSRFs (Knudsen 1982). These fields are much larger in comparison to the vSRFs (Middlebrooks and Knudsen 1984). The aSRFs also arrange topographically along the surface of the tectum and form an auditory spatial map. This map roughly aligns with the visual map (Knudsen 1982) and is dynamically adapted if a mismatch to the visual map occurs (Witten et al. 2006). Consequently, the OT compares and processes hearing and seeing together, enabling the animal with a more complete picture of its environment, resulting in a faster and better identification of stimuli with a multimodal signature.

1.7 Aims

It is essential for animals to locate the direction of a sound – not only in the horizontal plane, but also in elevation. In mammals external ears induce the necessary spectral cues at high frequencies. In the barn owl a feather ruff and asymmetric ears induce IIDs at high frequencies that change along elevation. Their aSRFs are spatially confined both in azimuth and elevation. But birds, which lack these specializations, have long puzzled science (Fig. 1.5). Pinnae or ear asymmetries were assumed to be essential to induce cues for sound localization in elevation. Neurophysiological experiments seemed to support this assumption: So far aSRFs that were spatially confined in elevation could not be demonstrated in birds without ear asymmetries. Until now it was not clear how elevation information can be derived in birds such as chickens, pigeons or sparrows. However behavioral experiments and observations in nature show that birds can accurately locate sounds in the vertical (Marti 1974; Kretzschmar 1982; Rice 1982). The necessary cues must therefore be available and be processed accordingly in the brain.

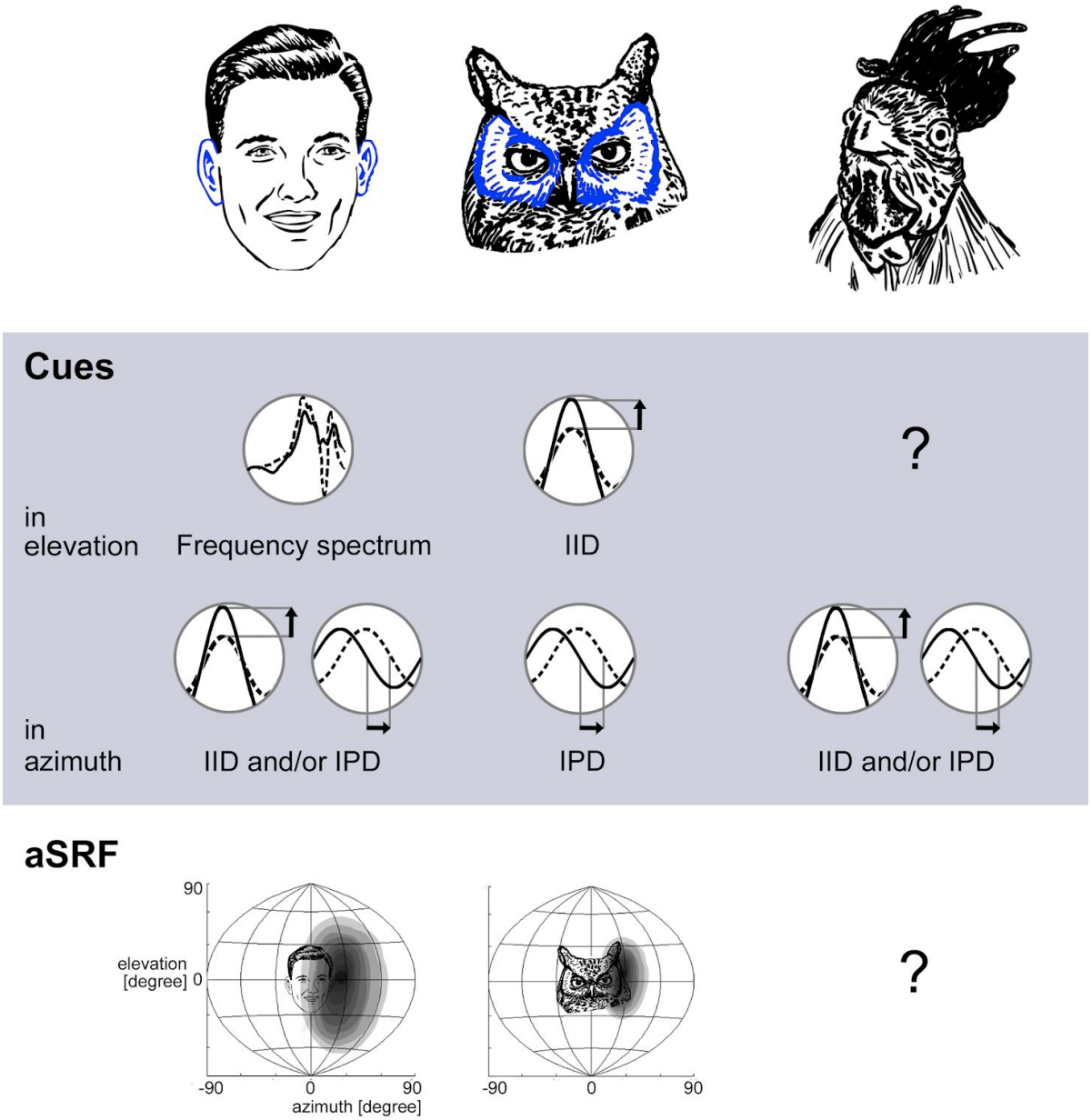

Figure 1.5: The cues for sound localization in elevation are unknown and the neuronal representation of elevation is unclear in birds without asymmetrical ears. In mammals and owls with asymmetric ears, external structures (in blue) induce at high frequencies cues for sound localization in elevation. The pinna induces spectral cues in mammals, a feather ruff in combination with asymmetrical ears IIDs in owls. It is unclear how similar cues could be induced in birds with symmetrical ears. Furthermore, aSRF are spatially confined both in mammals and owls with asymmetrical ears. So far such a spatial confinement could not be demonstrated in birds with symmetrical ears. Illustration: Ulrike Schnyder

In the work presented here, I investigated the physical and neurophysiological

mechanisms of sound localization in a generalist bird, the chicken. But compared to previous attempts, I made some significant changes to my experimental approach.

A possible role of the bird's head in creating cues for sound localization in elevation was previously underestimated. The animal's head will also absorb, reflect and diffract sound depending on sound direction and frequency. All of these modifications are described by the head related impulse response (HRIR) (Young et al. 1996). To prove the existence of direction-dependent peaks and notches in the sound spectrum even in the absence of pinnae, I investigated the HRIR in three bird species which lack external ears. To characterize a general effect irrespective of lifestyle or phylogeny, I selected the chicken, the rook (*Corvus frugilegus*) and the duck (*Anas platyrhynchos*). These species are not auditory specialists, nor are they closely related or share similar ecological niches. I calculated the HRIR by cross-correlating white noise stimuli presented from various positions with the signals recorded in the ear canal close to the tympanum.

In addition, I have significantly adapted the approach for measuring aSRFs. I was particularly interested in the extent and the shape of aSRFs lateral to the animals. Auditory localization in hearing generalists might be directed rather laterally than frontally (Nelson and Suthers 2004), an aspect that has been overlooked in previous attempts. I therefore investigated aSRFs not only frontally but also laterally and recorded basic response properties of auditory neurons in the chicken midbrain.

2 The Avian Head Induces Cues for Sound Localization in Elevation[1]

2.1 Methods

2.1.1 Head related impulse response measurement

We conducted all experiments in a sound reduced environment. We measured the directionality of sound pressure transformation (HRIR, head related impulse response) in heads of three species of three different avian orders, Galliformes, Anseriformes and Passeriformes (*Gallus gallus*, *Anas platyrhynchos* and *Corvus frugilegus*, respectively). All tested specimen were fully grown adults. We measured head widths of 30 mm for the chicken, 34 mm for the duck and 30 mm for the rook. The necks were still attached and intact, therefore influences on the HRIR by the neck were included as well. The work was done in accordance with the *Directive 2010/63/EU of the European Parliament and of the Council of 22 September 2010 on the protection of animals used for scientific purposes*, but was not subject to official approval by the local authority the Regierung von Oberbayern. Chicken heads were obtained from the Versuchsstation Thalhausen, duck heads from the Geflügelhof Lugeder and the crow from the Klinik für Vögel, Reptilien, Amphibien und Zierfische of the Ludwig-Maximilians-Universität München. Chicken and duck heads were slaughterhouse waste. The crow was brought to the clinic as a casualty in an accident in Landkreis München. No animal was killed for the purpose of this study. Specimens were freshly dead or deep frozen. We fixated the heads in 4 % paraformaldehyde solution for one week and made a small incision from behind towards the ear canal on both sides of the head. Then we inserted a small microphone (Knowles, EM-D65) through this incision into the hearing canal just in

[1] Schnyder HA, Vanderelst D, Bartenstein S, Firzlaff U, Luksch H (2014) The Avian Head Induces Cues for Sound Localization in Elevation. PLoS ONE 9(11): e112178. doi:10.1371/journal.pone.0112178

front of the tympanic membrane. To ensure that the microphone only received sound from the ear entrance it was placed into a tightly fitting metal tube. This tube was cemented into the incision and all remaining openings were sealed. In our experiments we did not investigate the influences of fixation on the HRIR. However in experiments with owls the fixation did not influence the HRIR measurements compared to anesthetized animals for frequencies below 7 kHz (Hausmann et al. 2010).

We placed the thus prepared head into the center of a rotatable semicircular loudspeaker array with a diameter of 102 cm and 27 speakers covering -73.125° to 73.125° in elevation in 5.625° steps. The array was rotated from – 180° to 180° in 5.625° steps azimuth. We measured the directionality of hearing at a total of 1755 positions. The midpoint between both ears was in the center of the semicircle. The beak faced the central speaker in its zero position, which was defined as elevation and azimuth 0°. Vertical positions of beak, ear entrances and the central speaker defined the horizontal plane. This position resembles the head position observed under natural conditions.

We based the measurement of HRIRs on methods described in (Young et al. 1996, Firzlaff and Schuller 2003). We digitally generated white noise between 60 – 10000 Hz of 2 seconds duration (MATLAB R2013b, Florida, USA) and emitted it after DA conversion (Fireface 400, RME, samplerate 44100 Hz) sequentially from each of the 1755 possible speaker positions. Signal to noise ratio was about 50 dB. We then recorded the noise signal with the microphones inside both ear canals and cross-correlated it with the original signal to establish the impulse response. To cancel the influence of individual speakers and the tube/microphone assembly, we calibrated each speaker before every recording session with the tube/microphone assembly in the same positions as when implanted in the birds' head under test conditions.

We cut the impulse responses from all positions with a rectangular window to remove any undesired reflection which might have originated from metal parts of the speaker array. We padded the impulse responses with zeroes to the final length of

256 points and performed a Fourier transformation (MATLAB). By dividing the Fourier transformation of the ear canal response by the Fourier transformation of the calibration response we obtained a proper HRIR. The FFT window of 256 points yielded a spectral line resolution of 172.3 Hz.

We processed all data with in-house developed programs written in MATLAB. We organized the mHRIR data, which is the magnitude spectrum of the HRIR, in a three-dimensional azimuth-by-elevation-frequency array. Data were smoothed in azimuth and elevation with a standard MATLAB function (Box convolution kernel (size = 3)). We graphed the data as two-dimensional contour plots (2 dB contour spacing) using a Hammer projection. We defined the sound intensity (dB) as the gain relative to the calibration measurement. By subtracting the mHRIR obtained from the right and the left ear we calculated interaural intensity differences (IIDs).

2.1.2 Estimation of the localization error

We estimate the likelihood that a broadband noise burst (with a known spectrum) will be correctly located with an approach that has been used to estimate the echolocation performance in bats (Reijniers et al. 2010, Vanderelst et al. 2011) and sound localization in humans (Reijniers et al. 2014). In parallel, we estimate the errors birds will make in localizing white noise bursts. Noise bursts are commonly used in behavioural experiments (Klump 2000). This makes it interesting to model the localization of these particular stimuli although more complex stimuli could add additional cues and cue variability that might influence the localization performance of the model.

Our estimation of localization errors is based on the head related impulse response (HRIR) and the known temporal resolution and intensity discrimination of the common birds hearing apparatus. We estimate the localization errors in elevation. Moreover, localization performance is estimated including and not including the mHRIR. This allows us to assess the contribution of the mHRIR, which includes IIDs, in reducing the errors in the vertical plane. The parameters used in calculating the

localization errors are derived from behavioural experiments (Welch and Dent 2011). In the following we describe the model used to estimate the localization errors.

Let $\vec{v}_{\varphi,\theta}$ be the vector describing the HRIR as measured at the left and the right tympanic membrane for azimuth φ and elevation θ. The parameter α denotes the gain of the noise burst. The vector $\vec{v}_{\varphi,\theta}$ is constructed as given in the following equation,

$$\vec{v}_{\varphi,\theta,\alpha} = [\vec{I}_{\varphi,\theta,\alpha},\ \vec{A}_{\varphi,\theta,}]$$

with

$$\vec{I}_{\varphi,\theta,\alpha} = [I_1^L, \ldots, I_n^L, \ldots, I_1^R, \ldots, I_n^R] + \alpha\ ;\ \vec{A}_{\varphi,\theta} = [, A_1^L, \ldots, A_n^L, \ldots, A_1^R, \ldots, A_n^R]$$

In this equation I_f^L and I_f^R denote the sound intensity (in dB_{SPL}) for frequency f at the left and the right tympanic membrane respectively. Likewise, A_i^L and A_i^R denote the phase (in radians) for frequency i at the left and the right tympanic membrane respectively. These intensities have been normalized such that the maximum across all frequencies, positions and both ears E is zero ($max_{\varphi,\theta,f,E}\, I^E_{\varphi,\theta,f} = 0$). Values of $\vec{I}_{\varphi,\theta,\alpha}$ smaller than zero are set to zero as these are below the hearing threshold.

Due to noise, the hearing apparatus of the bird has a limited ability to encode the phases and intensities. Therefore, assuming Gaussian noise modelled by the covariance matrix Σ, the hearing system will only have access to a noisy version of vector $\vec{v}_{\varphi,\theta,\alpha}$ given by $\vec{m}_{\varphi,\theta,\alpha}$ defined as follows, $\vec{m}_{\varphi,\theta,\alpha} = \vec{v}_{\varphi,\theta,\alpha} + N(0,\Sigma)$

The probability of a vector $\vec{m}_{\varphi\theta,}$ to originate from azimuth φ and elevation θ is given by,

$$P(\varphi,\theta|\vec{m}_{\varphi,\theta,\alpha}) = \sum_{\alpha} \frac{P(\vec{m}_{\varphi,\theta,\alpha}|\varphi,\theta,\alpha)\cdot P(\varphi,\theta)}{\sum\limits_{\varphi,\theta} P(\vec{m}_{\varphi,\theta,\alpha}|\varphi,\theta,\alpha)\cdot P(\varphi,\theta)} \cdot P(\alpha)$$

with

$$P(\vec{m}_{\varphi,\theta,\alpha}|\varphi,\theta,\alpha) = \frac{1}{(2\pi)^{n/2}|\Sigma|^{1/2}} exp[-\tfrac{1}{2}(\vec{m}_{\varphi,\theta,\alpha} - \vec{v}_{\varphi,\theta.\alpha})^T \Sigma^{-1} (\vec{m}_{\varphi,\theta,\alpha} - \vec{v}_{\varphi,\theta,\alpha})]$$

As the gain α of the noise burst is not directly accessible to the animal, it is

considered as a nuisance parameter that is removed from the equations by integration.

The probability to perceive a noise burst originating from direction φ, θ as coming from direction φ', θ' is given by $\underline{P}(\varphi', \theta' | \vec{m}_{\varphi,\theta}, \alpha)$, I.e. $P(\varphi', \theta' | \vec{m}_{\varphi,\theta,\alpha})$ averaged across many realizations of $\vec{m}_{\varphi,\theta}, \alpha$. However, to reduce the computational load, we approximate $\underline{P}(\varphi', \theta' | \vec{m}_{\varphi,\theta,\alpha})$, as follows [see (Reijniers et al. 2010) for a justification],

$$\underline{P}(\varphi', \theta' | \vec{m}_{\varphi,\theta,\alpha}) \cong \sum_{\alpha} \frac{P(\vec{v}_{\varphi,\theta,\alpha} | \varphi', \theta') \cdot P(\varphi', \theta')}{\sum_{\varphi,\theta} P(\vec{v}_{\varphi,\theta,\alpha} | \varphi', \theta') \cdot P(\varphi', \theta')} \cdot P(\alpha)$$

with

$$P(\vec{m}_{\varphi,\theta,\alpha} | \varphi, \theta, \alpha) = \frac{1}{(2\pi)^{n/2} |\Sigma|^{1/2}} exp[-\frac{1}{2}(\vec{v}_{\varphi,\theta,\alpha} - \vec{v}_{\varphi',\theta',\alpha})^T \Sigma^{-1} (\vec{v}_{\varphi,\theta,\alpha} - \vec{v}_{\varphi',\theta',\alpha})]$$

This equation allows us to estimate both the probability of correct localization and the expected localization errors. The probability of correct localization is given by $\underline{P}(\varphi', \theta' | \vec{m}_{\theta,\varphi,\alpha})$ for $\varphi = \varphi'$ and $\theta = \theta'$. The localization errors in azimuth and elevation are given by,

$$E_{\varphi} = \sum_{\varphi} \underline{P}(\varphi', \theta' | \vec{m}_{\varphi,\theta',\alpha}) \cdot D(\varphi, \varphi')$$

and

$$E_{\theta} = \sum_{\theta} \underline{P}(\varphi', \theta' | \vec{m}_{\varphi',\theta,\alpha}) \cdot D(\theta, \theta')$$

With $D(\varphi, \varphi')$ and $D(\theta, \theta')$ the great circle distance between the real azimuth φ and elevation θ and each of the other azimuth φ' and elevation θ' positions considered.

The calculation of the localization performance as outlined above depends on the HRIR and the covariance matrix modelling the additive noise. The HRIR for frequencies from 1000 Hz to 5500 Hz were used as they are consistent with the typical hearing range in birds (Fay 1988). We model the auditory channels of the bird using equivalent rectangular band pass filters (ERB) with a bandwidth of 500 Hz, which is a good fit for higher frequencies but is overestimating the bandwidth for

lower frequencies (Dooling et al. 2000). As such, our model is more likely to underestimate the localization performance than to overestimate it. The spacing of the frequencies supports the assumption that the noise in different frequency channels is independent. To the best of our knowledge, there is no data suggesting the noise on the two neural channels is correlated. Correlated noise would imply that any overestimation (/underestimation) of the intensity at the left and right ear would be systematically associated with an overestimation (/underestimation) of the interaural phase difference. However, both neural channels are encoded by different neural substrates. While the magnitude of the signal at the left and the right ear are encoded on the level of the cochlear nucleus, the phase information (i.e. difference in phase at both ears) is encoded at the level of the nucleus laminaris using delay lines (McAlpine and Grothe 2003). Moreover, IPD and intensity cues are processed independently in birds: intensity cues are found to not influence the encoding of the IPD (Viete et al. 1997). This makes it unlikely that the noise of the two channels is correlated. Therefore, in the absence of any evidence suggesting differently, we model the noise independently. Therefore, the off-diagonal elements of Σ were set to 0. The diagonal elements of the matrix Σ represent the additive noise on the intensities and phases. These values were deduced from behavioral experiments (Welch and Dent 2011).

Welch and Dent (2011) measured interaural level and time difference discrimination thresholds in budgerigars. Interestingly, they report the discrimination thresholds for d'= 1.5. The d' gives the distance between distributions in units of the standard deviation of the noise distribution. Therefore, these data allow to directly parameterize the matrix Σ. The minimal interaural time difference discrimination thresholds reported by Welch & Dent 2011 is about 20 μs 2000 Hz, which implies Gaussian noise on the phase for frequency f with a standard deviation given by:

$$\sigma(A)_f = 2\pi f \cdot \frac{20\ \mu s}{1.5}\ .$$

Welch and Dent 2011 report a minimal discrimination threshold of 3 dB. Therefore, the standard deviation of the noise on the intensity was set to:

$$\sigma(I) = \frac{3dB}{1.5}$$

Finally, as the avian auditory system is unable to phase-lock for frequencies above 4000 Hz (Klump 2000) no phase information was included for frequencies above 4000 Hz.

2.2 Results

Elevation-dependent sound modifications could be found in all avian heads (Fig. 2.1a-c). As expected, sound presented ipsilateral to the examined ear resulted in a smooth intensity gain distribution along both the vertical and horizontal axis. Moving the sound source towards the contralateral side around the head resulted in decreasing sound levels, as the head increasingly shielded the ear from the sound source. However, when the sound was presented from the contralateral side, an intensity peak occurred at a distinct vertical and horizontal position. Along the vertical axis, intensity notches flanked the contralateral intensity peak in elevation (Fig. 2.1d, Figs. 2.2-2.4). This notch/peak/notch distribution was observed from 3500 Hz up to 5500 Hz (Fig. 2.1d, see Figs. 2.5-2.7 a-e), which is in the high frequency hearing range of the species examined (Fay 1988, Hill et al. 2014). Therefore strong monaural spectral cues are present for contralateral azimuth positions and change systematically along elevation (Figs. 2.8-2.10 b-d). In contrast to this, for ipsilateral azimuth positions, the spectral profile did not change for different elevations and thus no spectral cues for sound localization would be available (Figs. 2.8-2.10 a). Such elevation dependent cues for contralateral sound were found in all three investigated species.

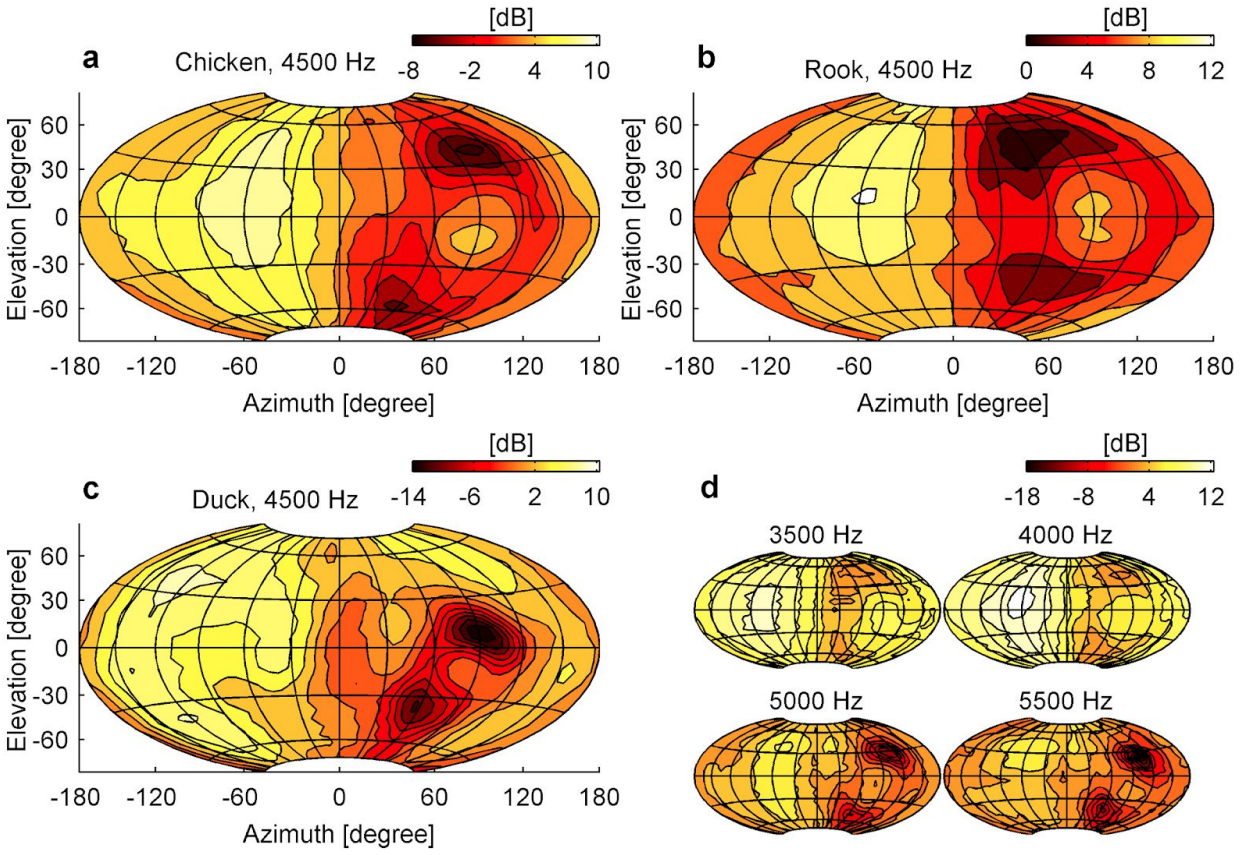

Figure 2.1: Bird heads [chicken (a, d), rook (b) and duck (c)] modify sound intensity dependent on elevation. Monaural gain [dB] is displayed at the right ear for multiple sound positions. Coordinates of 0° azimuth and 0° elevation face the beak, -90° azimuth and 0° elevation face the right ear. Sound intensity is projected according to the Hammer projection. Meshgrid spacing is 30°, iso-contourline spacing is 2 dB. Axes correspond to the x- and y-midline coordinates.

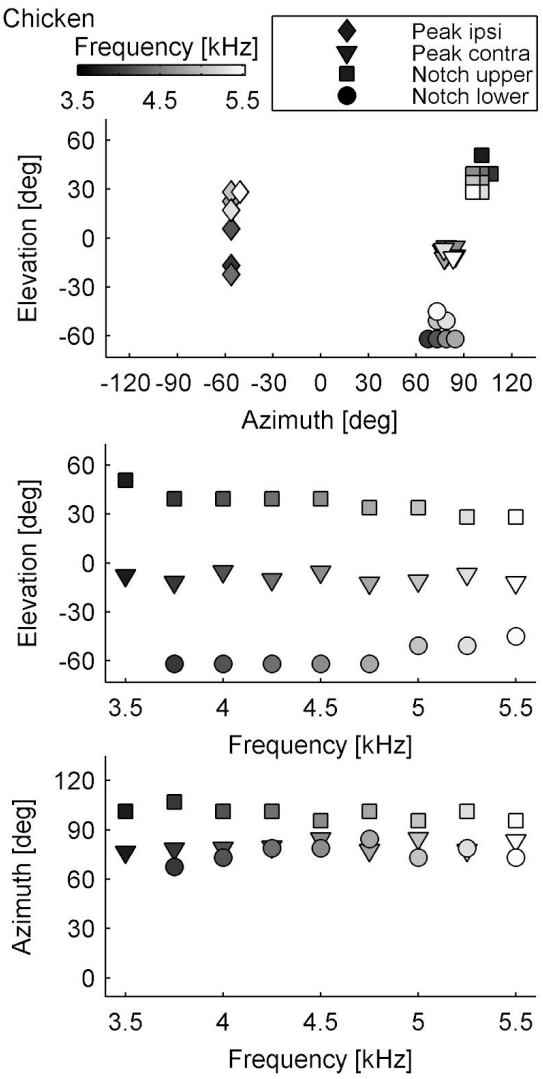

Figure 2.2: Contralateral peak position is stable over a wide frequency range. Positions of the minimum of the upper and lower notch and position of the maximum of the contralateral and ipsilateral peak from 3500 Hz to 5500 Hz in the chicken.

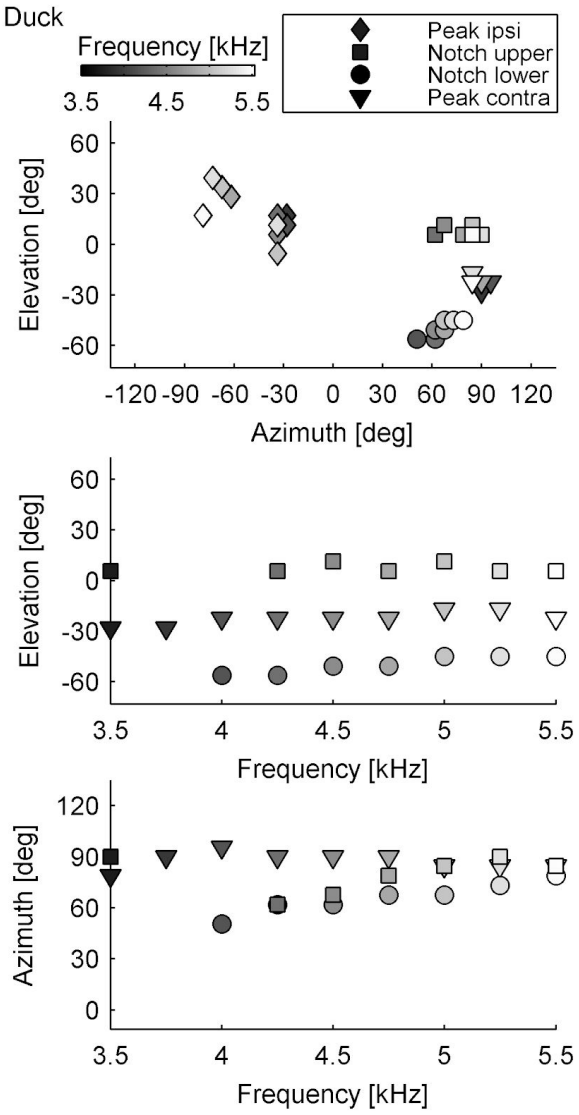

Figure 2.3: Contralateral peak position is stable over a wide frequency range. Positions of the minimum of the upper and lower notch and position of the maximum of the contralateral and ipsilateral peak from 3500 Hz to 5500 Hz in the duck.

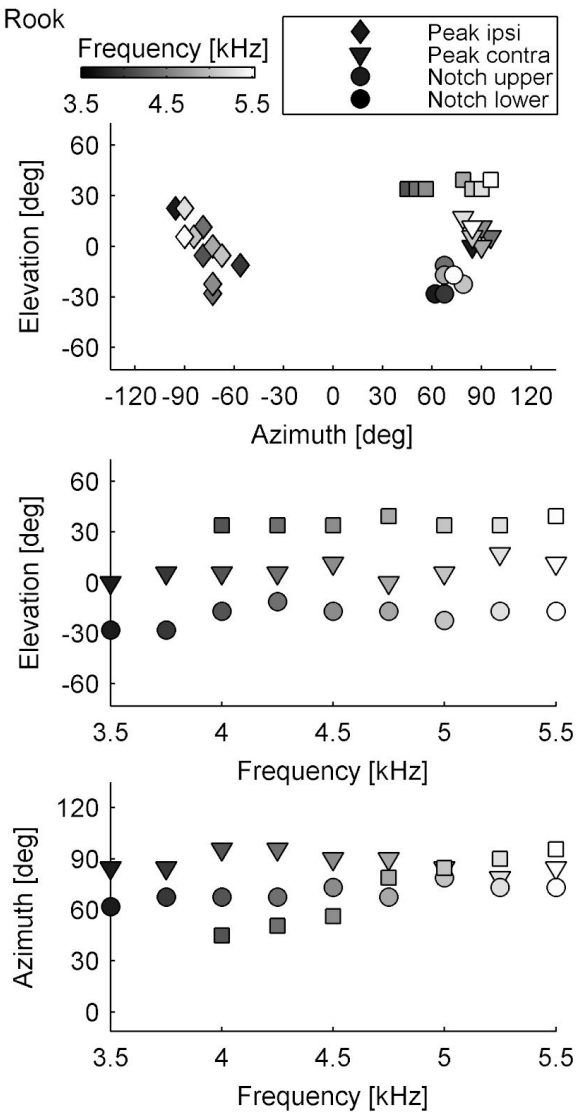

Figure 2.4: Contralateral peak position is stable over a wide frequency range. Positions of the minimum of the upper and lower notch and position of the maximum of the contralateral and ipsilateral peak from 3500 Hz to 5500 Hz in the rook.

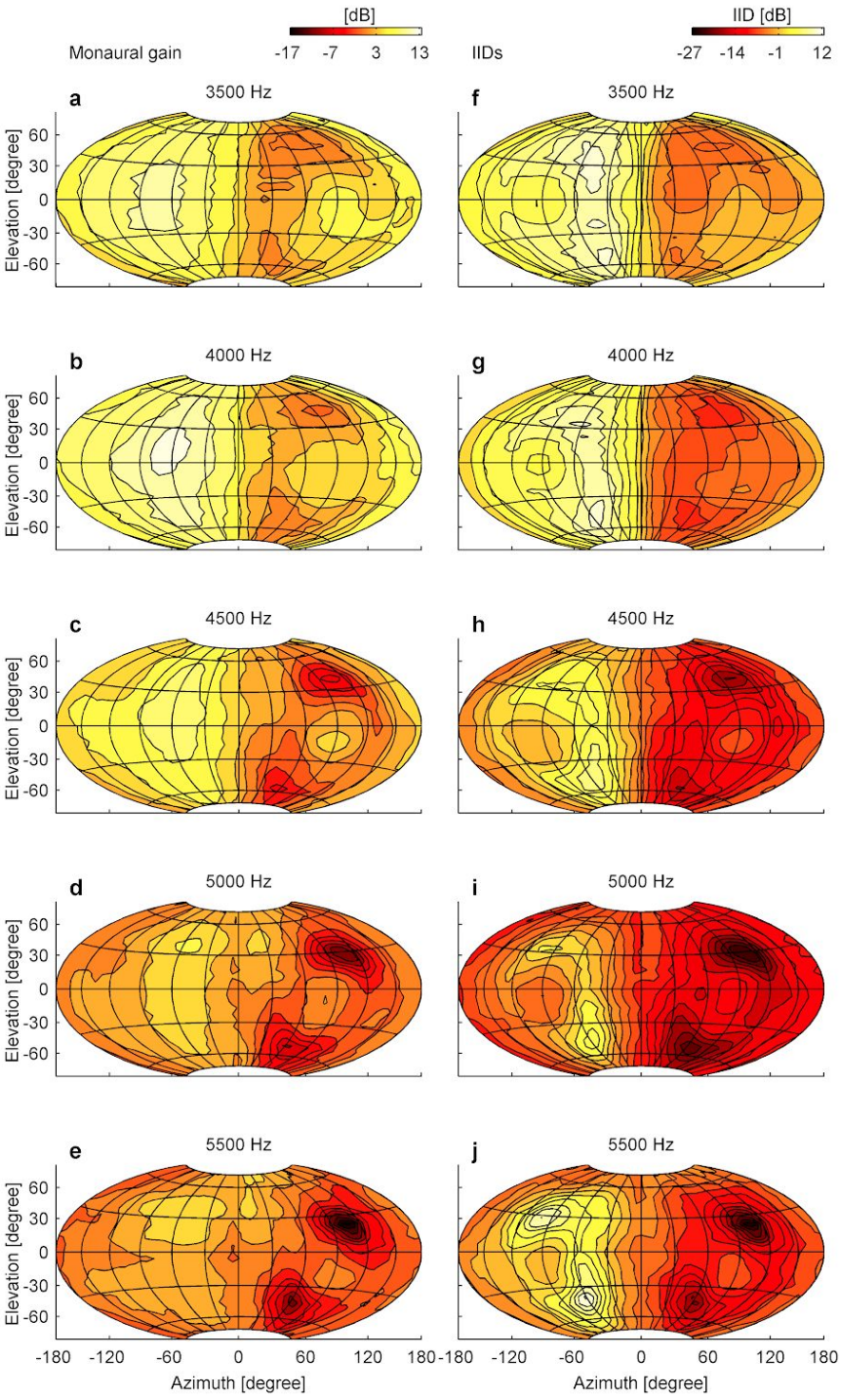

Figure 2.5: (**a-e**) Monaural gain at the right ear and (**f-j**) interaural intensity differences (IIDs) of a chicken between 3500 and 5500 Hz.

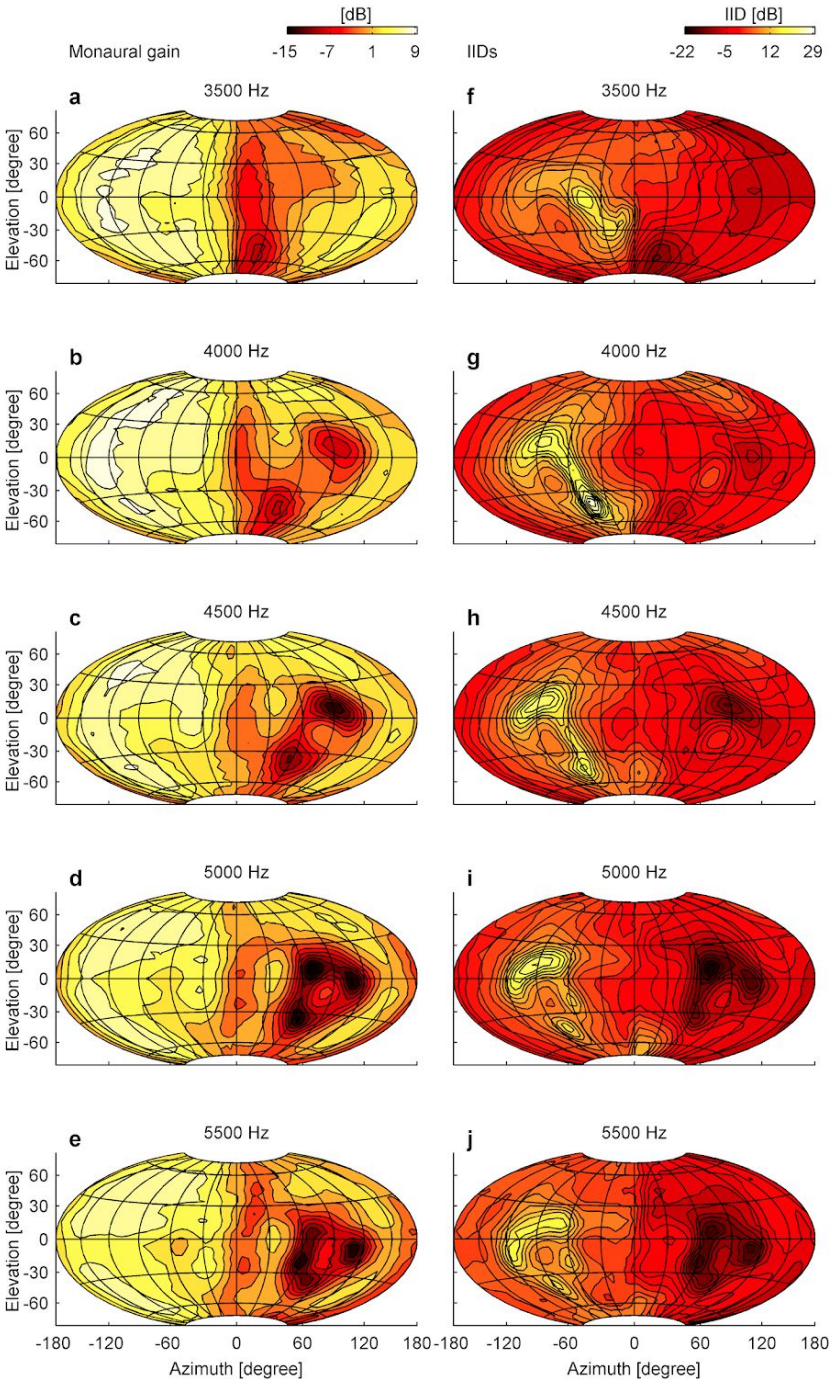

Figure 2.6: (**a-e**) Monaural gain at the right ear and (**f-j**) interaural intensity differences (IIDs) of a duck between 3500 and 5500 Hz.

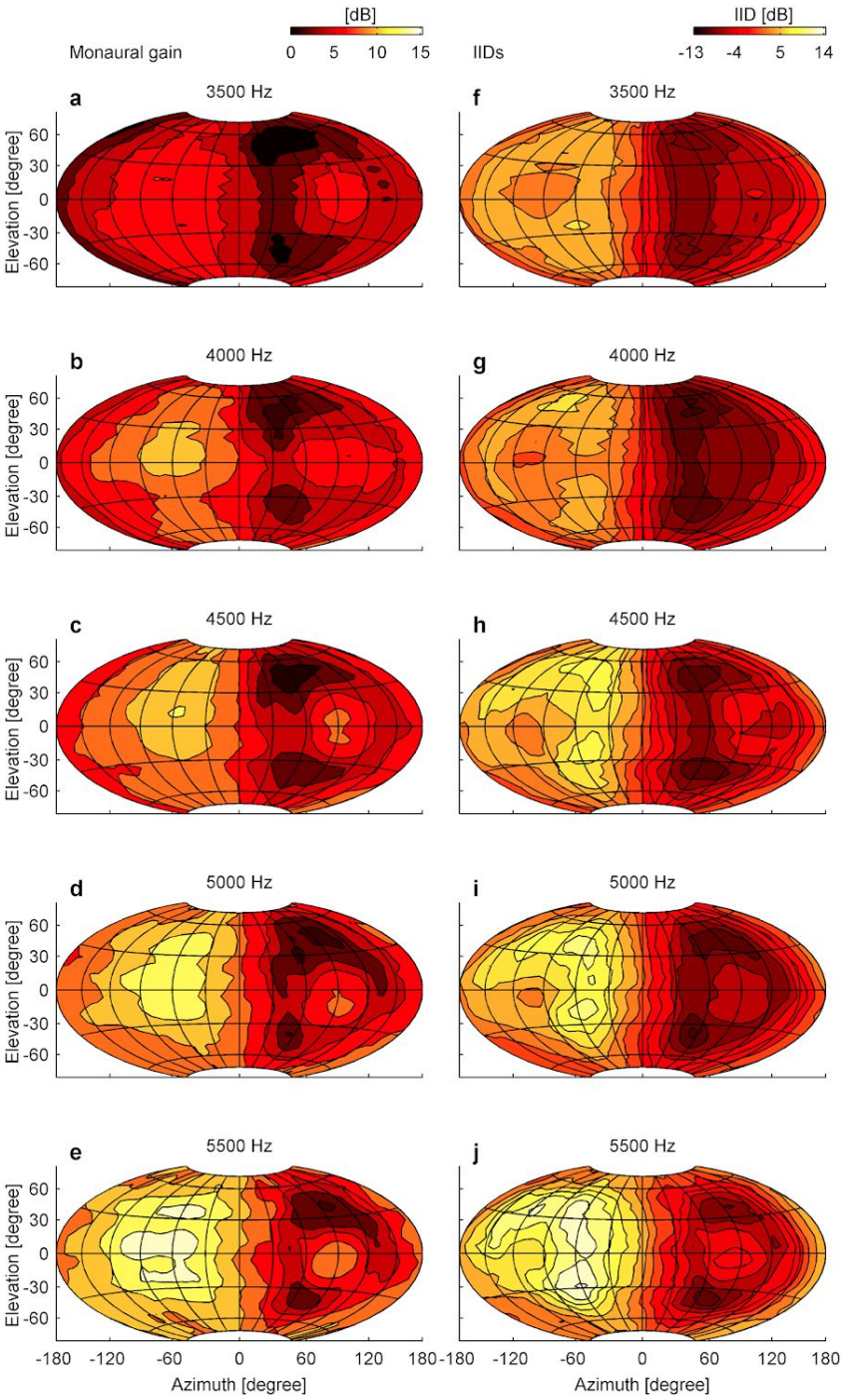

Figure 2.7: (**a-e**) Monaural gain at the right ear and (**f-j**) interaural intensity differences (IIDs) of a rook between 3500 and 5500 Hz.

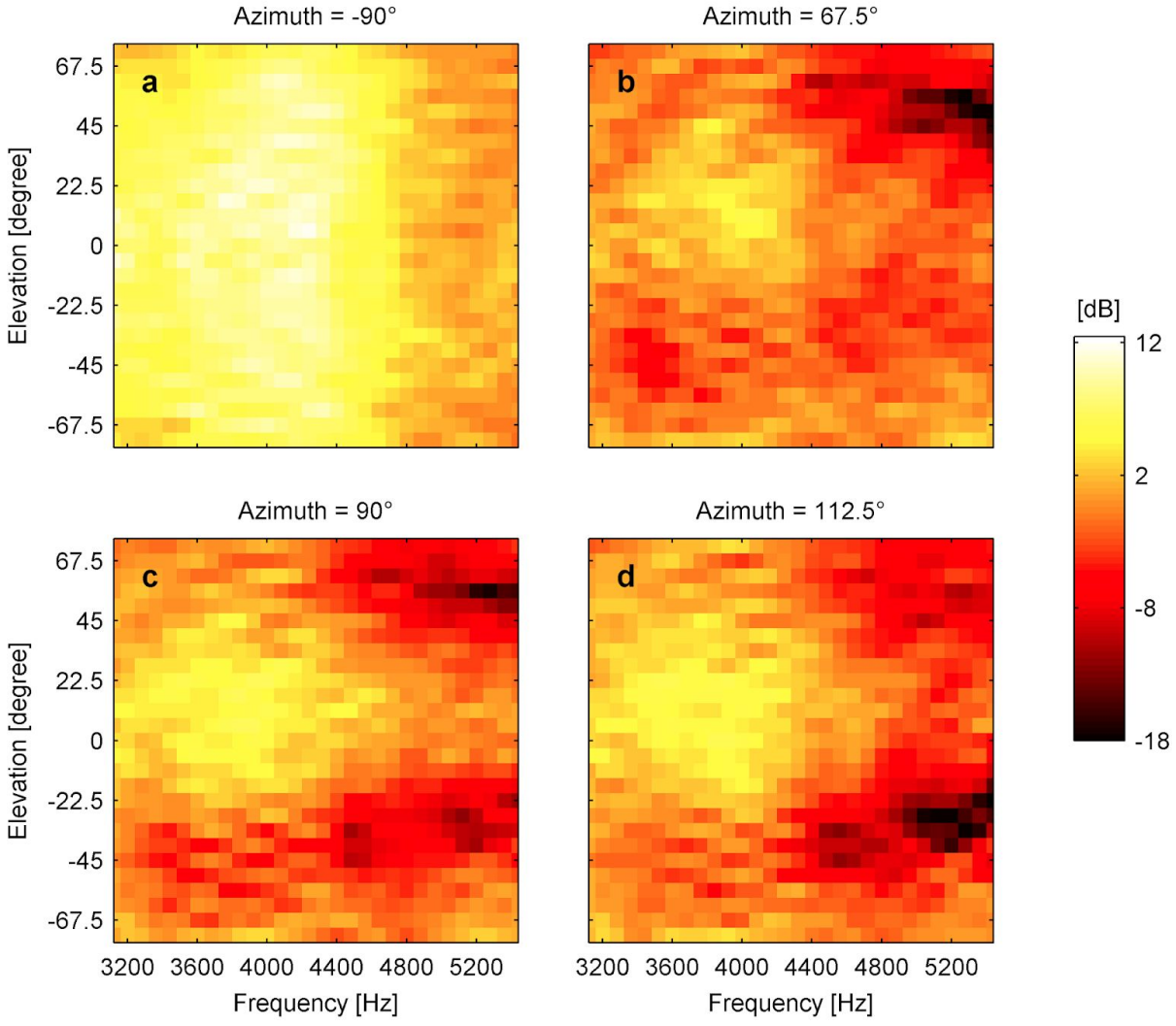

Figure 2.8: Monaural spectral cues change systematically along elevation. Monaural spectral cues between 3000 and 5500 Hz at a specified azimuth position for different elevation positions in the chicken.

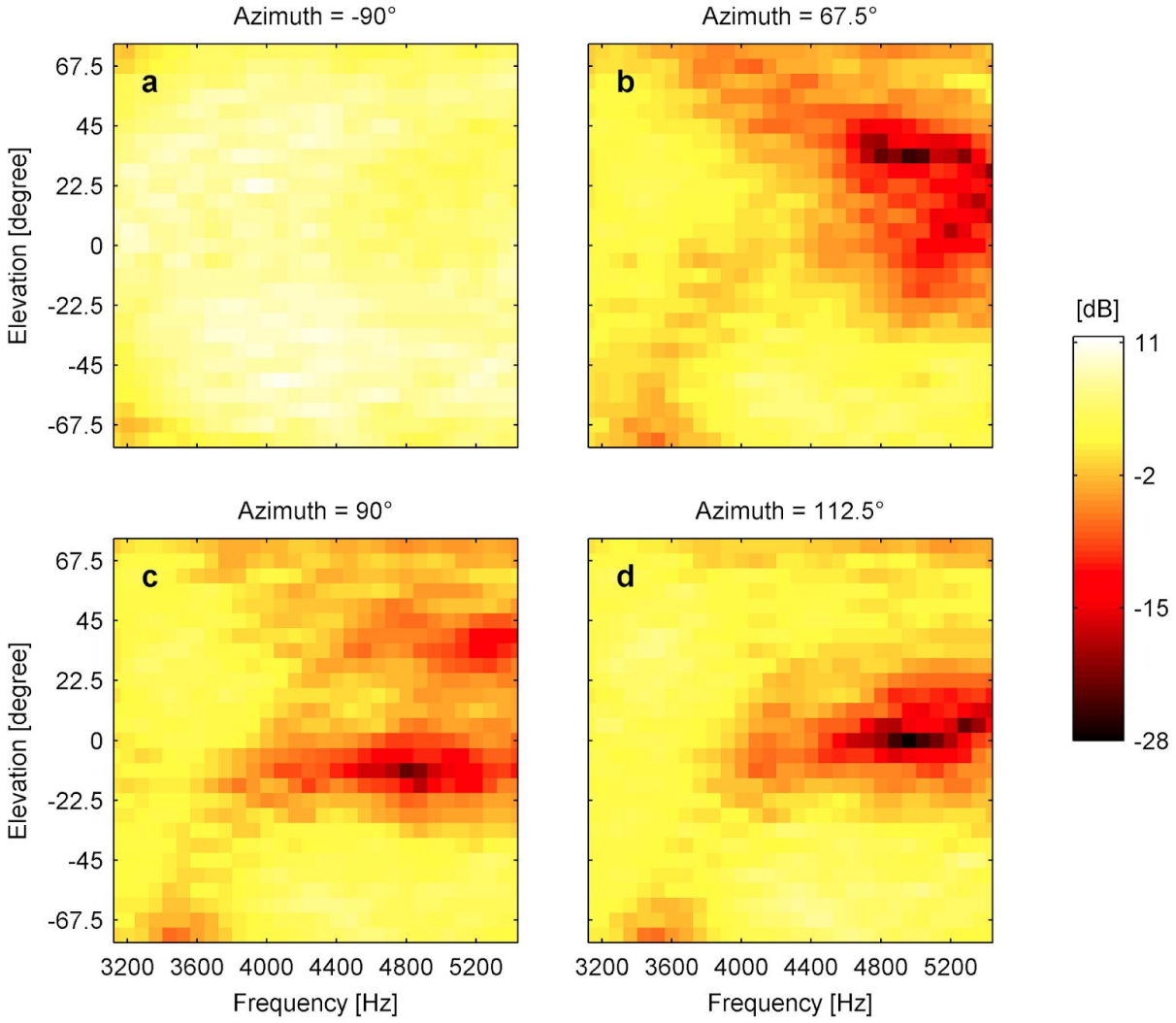

Figure 2.9: Monaural spectral cues between 3000 and 5500 Hz at a specified azimuth position for different elevation positions in the duck.

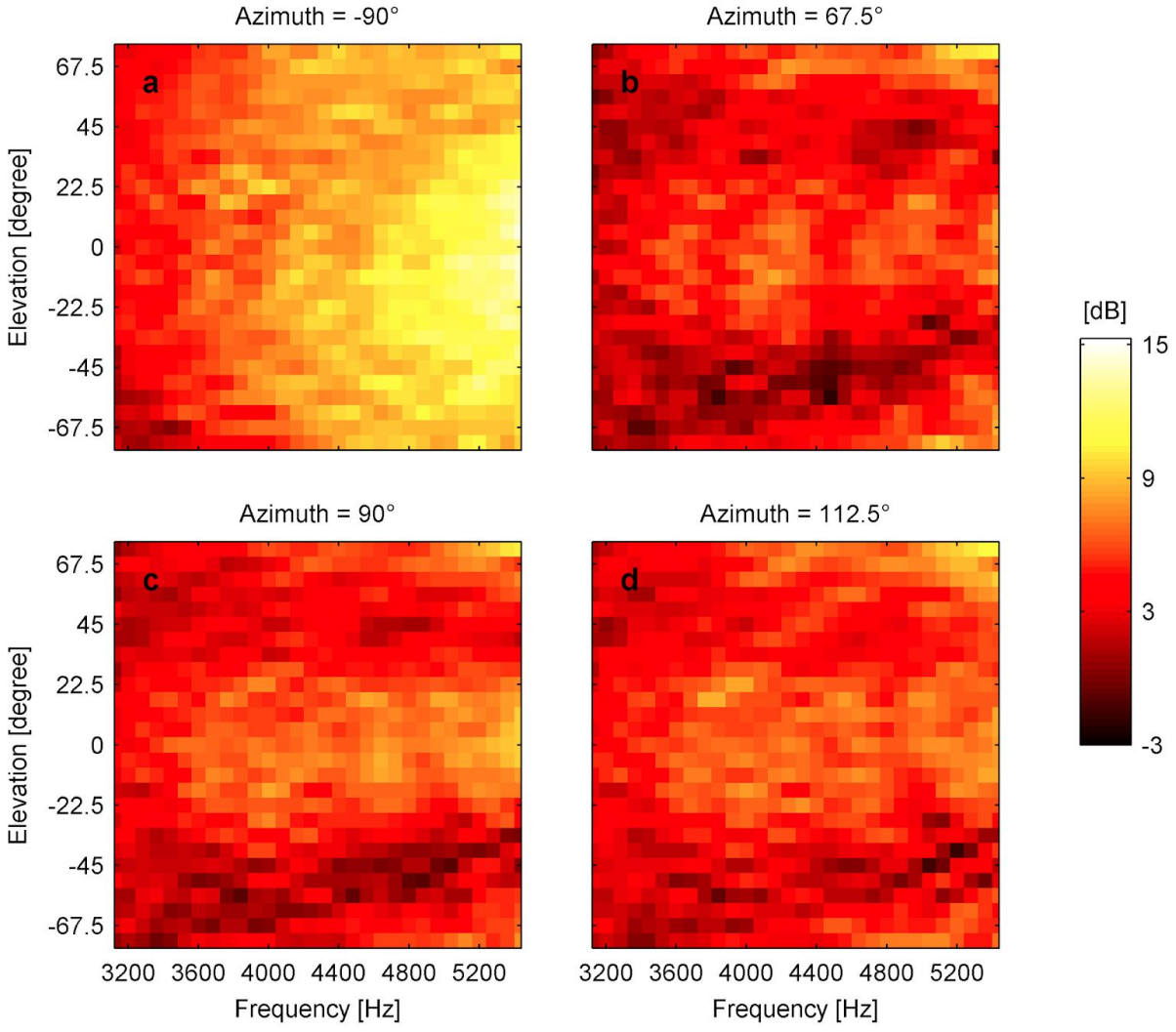

Figure 2.10: Monaural spectral cues between 3000 and 5500 Hz at a specified azimuth position for different elevation positions in the rook.

But what causes these cues? Interestingly, no complex mechanism or structure is needed to explain our observation. In a certain frequency range, spherical objects not only produce an acoustic shadow, but diffract sound to add up on the opposite side (Wiener 1947). This well-known phenomenon (‘bright spot’) also applies to the head of birds, but has thus far never been linked to their hearing. The ‘bright spot’ in the midst of an acoustic shadow resembles the notch/peak/notch configuration we described above.

To quantify the contribution of the HRIR to sound localization, we used a model of vertebrate sound localization (Reijniers et al. 2010, Reijniers et al. 2014). Localization errors were estimated based on either the phase spectrum of the HRIR (pHRIR), the magnitude spectrum of the HRIR (mHRIR) or both combined (HRIR). Parameterizing the model with behavioural data in birds (Welch and Dent 2011), we estimated the probability of sound originating from a given direction to be perceived as originating from any other direction. The localization error was expressed as the average angular deviation between the true origin of the sound and the perceived origin. Comparing the localization errors with and without mHRIR cues enables us to quantify how much the mHRIR contributes in reducing the ambiguity about the origin of a sound source. As mHRIRs were similar for all the species tested (Figs. 2.5-2.7 a-e), we selected the chicken data as representative.

As expected, pHRIR localization error in elevation is lowest at the sides of the head (Fig. 2.11a). This is because the region where equal IPDs are found (called the 'cone of confusion', also indicated by the contourlines in Fig. 2.12) decreases for lateral positions (Fig. 2.12) (Mills 1972). The mHRIR reduces the localization error in elevation even further (Fig. 2.11b). At the position where the notch/peak/notch distribution is located, the area of lowest error is enlarged. This effect is quantified in Fig. 2.11c which shows the combined contribution of both mHRIR and pHRIR, and Fig. 2.11d where the differential contribution of the mHRIR in reducing localization error is shown. Magnitude cues are most important for positions above 30° and below –30° in elevation for azimuth positions around ±90° (Fig. 2.11d). From these positions the localization error based on phase is increasing again (Fig. 2.11a) whereas the localization error based on the magnitude spectrum stays stable (Fig. 2.11b). It is noteworthy that such an enlargement of low error regions resembles the effect of increased localization acuity in elevation generated by external structures like the feather ruff in barn owls (Hausmann et al. 2009). The lowest predicted error across the complete space using the pHRIR, mHRIR or both was 9°, 7° and 7° respectively. However, the typical errors are higher than these values. For example, the average angular error in the frontal hemisphere (-90° to +90° azimuth) was 35°.

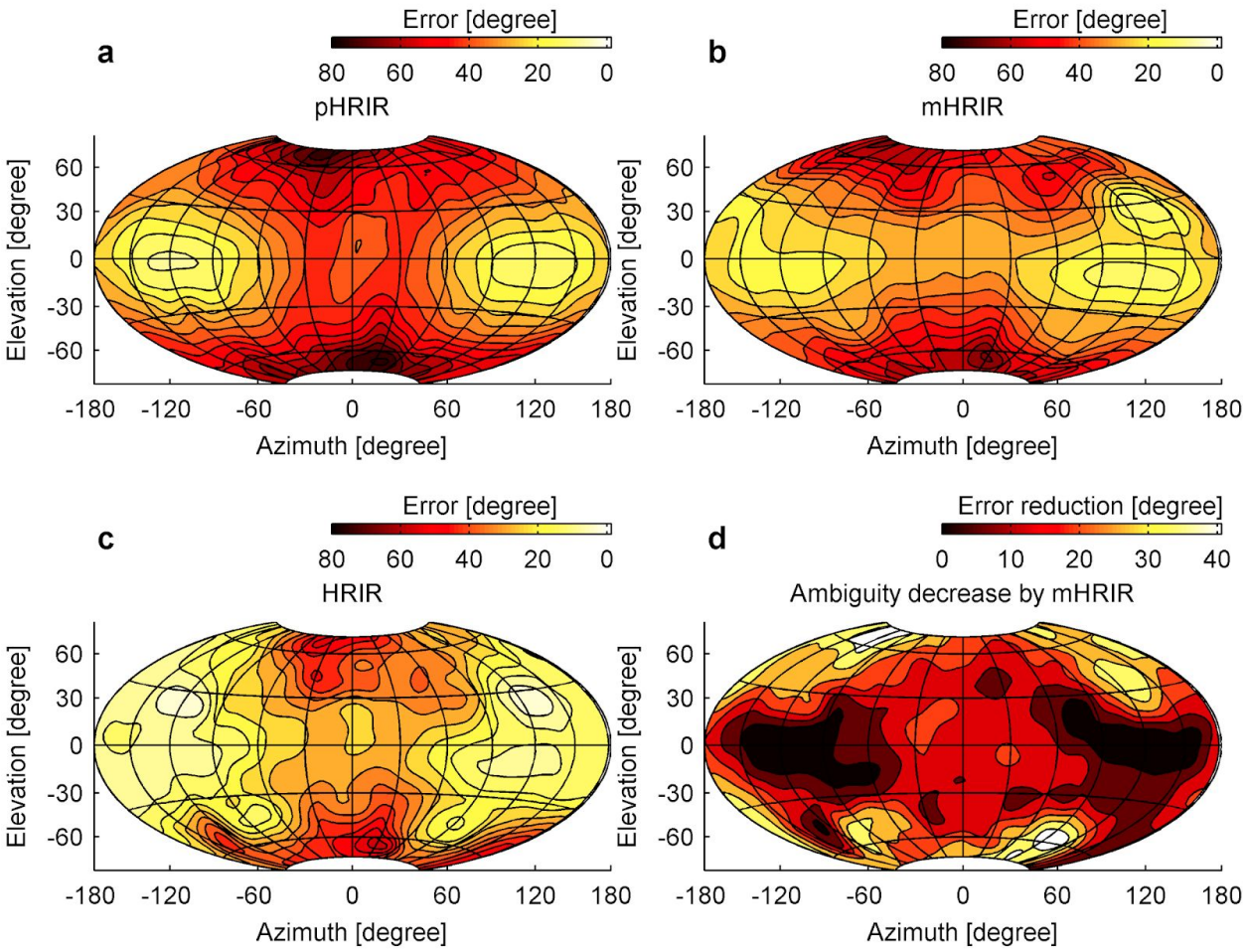

Figure 2.11: Localization error in elevation is lowest at spatial positions lateral to the head. The localization error in elevation is based on either the chicken‘s pHRIR (a), mHRIR (b) or both combined (c). The mHRIR‘s differential contribution to reduce elevation error (d) is calculated by subtracting (a) from (c). Spacing of error-contourline is 5°, map orientation in relation to the head and map projection are the same as in Fig. 1. Axes correspond to the x- and y-midline coordinates.

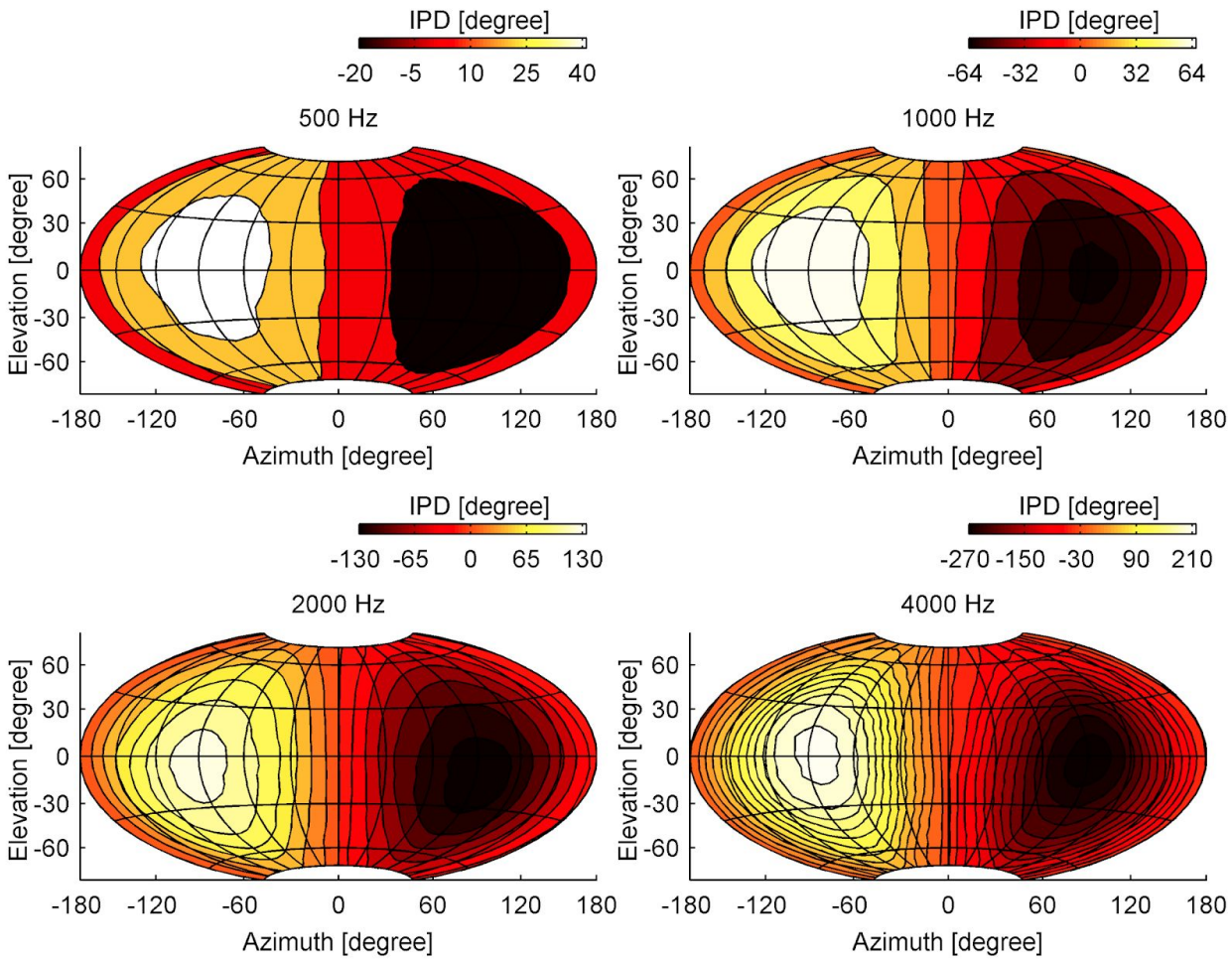

Figure 2.12: Interaural phase differences (IPDs) at 500, 1000, 2000 and 4000 Hz in the chicken. Spacing of iso-contourline is 20°, map orientation in relation to the head and map projection are the same as in Fig. 1. Axes correspond to the x- and y-midline coordinates.

The increase in localization performance when using the mHRIR in addition to the pHRIR can be explained by the fact that (1) the mHRIR provides the chicken with two additional sources of information and (2) the assumption that the neural noise on the mHRIR and the pHRIR are uncorrelated.

The mHRIR provides the chicken with two sources of localization information in addition to the pHRIR. Indeed, the mHRIR can be rewritten as follows (Reijniers et al. 2014),

$$\vec{I}_{\varphi,\theta,\alpha} = [\vec{I}^{R}_{\varphi,\theta,\alpha} - \vec{I}^{L}_{\varphi,\theta,\alpha}] + \frac{[\vec{I}^{L}_{\varphi,\theta,\alpha} + \vec{I}^{R}_{\varphi,\theta,\alpha}]}{2}$$

The first term in this equation denotes the IID. The second term is the average intensity (i.e. average power spectrum) across the two ears. Each of these two components of the mHRIR supplies the chicken with additional localization information.

First, a priori, in our data, 84% of the variation in the IID could be explained by the pHRIR. This indicates that the correlation between the pHRIR and mHRIR was large but not perfect. This means that errors are further reduced when adding the mHRIR. Second, for a sound source with a known spectrum, such as the white noise modelled in this paper or sound sources familiar to the bird, some localization information is encoded in the average spectrum across the two ears (Reijniers et al. 2010). The correlation between the spectral component of the mHRIR and the pHRIR was only limited (26% of explained variance).

In addition to the two components of the mHRIR, there is a third reason why the mHRIR reduces the localization error. In our simulations, the noise on the neural encoding of the mHRIR and pHRIR cues is assumed to be uncorrelated. This is modelled by setting the off-diagonal elements of matrix Σ to zero. Therefore, even if both the IID and the average spectrum would correlate perfectly with the pHRIR (which is not the case) the mHRIR would increase performance because it is an additional channel with uncorrelated noise.

3 Auditory spatial receptive fields in the midbrain of the chicken

3.1 Methods

3.1.1 Animals

Nine fully grown hens (*Gallus gallus domesticus*) were used for this study. Adult animals were used as their hearing is fully developed in contrast to young chickens (from 9 Hz to 7000 Hz from (Hill et al. 2014)), HRIRs (measured in our previous study) were available, and the size of the ear canal allowed easy presentation of sounds via in-ear headphones.

Animals were obtained from a local breeder or reared from fertilized eggs in our own animal facility and kept in social groups, with free access to sand baths, roosts, nesting sites, water and food.

3.1.2 Surgery

Our surgical procedures were a slightly modified version of the one described in (Verhaal and Luksch 2013). Hens were anesthetized with a mixture of Ketamine (40 mg/kg ketamin, Inresa) and Xylazine (12 mg/kg rompun, Bayer) administered intramuscularly. The depth of the anesthesia was kept constant with a perfusion pump (B. Braun Melsungen) that continuously administered Ketamine (20 mg/h/kg) and Xylazine (6 mg/h/kg) intramuscularly. During all procedures the heart rate was constantly monitored by ECG. Sudden increases in heart rate were taken as a sign that the anesthesia was too light, sudden decreases of heart rate as a sign that anesthesia was too deep. To maintain body temperature (above 39.8°C) animals

were positioned on a heating pad and covered in blankets. During surgery and recordings the head was fixed in a custom made stereotactic apparatus. Custom made ear bars, which fitted snugly into the ear canal, and a beak holder kept the head at a tilt of 60° (beak to ear). Usually a head tilt of 45° is used in comparable studies and in the chicken brain atlases (avianbrain.org). However we realized that the brain is less tilted in adult chickens than in the younger animals that were used for the brain atlases. To compensate for this we tilted the heads 15° further than in young birds. To get access to the midbrain, a small part of the head medial to the ear canal was shaved, the scalp incised, a hole was drilled into the skull and parts of the dura were removed. To compensate for an increased intracranial air pressure during anesthesia (Larsen et al. 1997) we vented the middle ear by drilling a hole into the middle ear cavity.

3.1.3 Stimulation

Acoustic stimuli were generated with MATLAB (MathWorks), digital-analog converted with an RX6 (Tucker Davis Technologies) at a sampling rate of 48828 Hz, attenuated with a PA5 (Tucker Davis Technologies) and presented binaurally via commercial headphones (AH-C260R, DENON). The stainless-steel ear bars of the head-holder were hollow and transmitted sounds directly to the ear of the chicken. We calibrated the entire system to ensure a flat frequency response (between 350 Hz up to 5600 Hz) at the ear-entrance of the chicken.

Stimuli consisted of either noise or pure tones. To present sounds via headphones in virtual acoustic space we filtered frozen noise with the chickens' HRIR. The HRIRs were not individualized; for all recordings we used the HRIR obtained in one female adult chicken as earlier HRIR measurements (data not shown) from different female chickens had yielded only a minor degree of inter-individual variability.

The HRIRs used in the present study were measured directly at the position of the ear drums (Schnyder et al. 2014). Therefore, all properties of the sound reaching the eardrum under natural conditions were fully captured. The measured HRIRs were in

good correspondence to the simulated HRIR based on laser scans of a chicken head (supplied by Dieter Vanderelst). Keller et al. (1998) showed that neuronal response to acoustic free-field stimulation were in good correspondence to the responses obtained from stimulation in virtual acoustic space using HRIRs in the barn owl.

Pure tones were presented in the same frequency range as noise, in a band from 350 Hz up to 5600 Hz, which covers almost all of the chickens mid to high hearing range (Hill et al. 2014). During recordings we stimulated from 198 different spatial positions. In azimuth the positions ranged from -180° to 174.375° and in elevation from -67.5 to 67.5° (with a stepwidth of 16.875°). When a unit responded to acoustic stimulation the following protocol was executed: To map aSRFs the response to noise presented in virtual acoustic space was recorded, with noise stimuli presented at 10dB above the auditory threshold. Each spatial position was presented 10 times. The recording window had a duration of 500 ms, with a 50 ms pause before the stimulus, 150 ms of noise stimulus and 300 ms after the stimulus. To determine the frequency response fields (FRFs) of the units pure tones in 1/8 octave steps were presented with different sound pressure levels (SPL). The pure tones had a duration of 150 ms, with a 50 ms pause before and 300 ms after the stimulus.

3.1.4 Recording

All recordings were performed in a dark sound-attenuated chamber (IAC, Niederkrüchten). We recorded extracellularly from the optic tectum (OT), the inferior colliculus (IC) and the external formatio reticularis lateralis (FRLx) (Niederleitner et al. 2016). A tungsten electrode (~2 MΩ, Alpha Omega) was positioned with a 2-axis micromanipulator arm (51602, Stoelting) and advanced with a microdrive (IVM-1000, Scientifica). Signals were amplified (DAM80, World Precision Instruments), bandpass filtered between 300 and 3000 Hz, and recorded with an RP2 (Tucker Davis Technologies) analog-digital converter (sampling rate 25 kHz) and the Software Brainware (Tucker Davis Technologies). We additionally monitored the neural activity both visually on a virtual oscilloscope and acoustically via headphones

outside of the sound-insulated chamber.

Neuronal responses were evaluated by spike shape and interspike interval. However as it was not always possible to relate the measured activity to a single neuron, we use the term unit. Even though we recorded mostly from single units, we cannot exclude the possibility that we recorded from multiple units (2-3 units) as well.

To reconstruct the recording sites later, the coordinates of the penetration on the micromanipulator arm and stereotactic apparatus were noted, as well as the tilt of the microdrive and the advancement of the electrode. At the end of each experiment a lesion was made with a 20 µA DC current of 10 seconds duration at depths of 3000 µm, 1500 µm or 0 µm and its position on the surface was noted. Alternatively we labeled the electrode tracks with DiI stainings according to a published protocol (Dicarlo et al. 1996). Shortly, the electrode was coated with DiI, lowered into the brain, advanced to 1500 µm and the coordinates were noted for subsequent reconstruction. Coordinates of the recordings sites in relationship to the lesion and DiI stainings allowed us to reconstruct the different recording positions in the brain.

After recording animals were euthanized with an intrapulmonary injection of 200 mg/kg Pentobarbital (Pentobarbital-Sodium, Merial) and decapitated with poultry scissors.

3.1.5 Histology

The head was put overnight in 4 % paraformaldehyde (PFA) at 6° C. The next morning the bone was removed above the brain, the head was put back into the stereotactic apparatus (at the exact angles from the experiment before) and the brain was incised rostral to the OT. The resulting coronal plane ensured that during later sectioning of the midbrain, the brain slices would be parallel to the electrode tracks. The brain was then removed, post-fixed in 4 % PFA for at least two days, cryoprotected by immersion in a 30 % sucrose solution in 0.1 M phosphate-buffered saline, and subsequently sectioned at 75 µm on a cryostat (Slee). Slices were transfered onto glass slides coated with chromalaungelatinge. After drying we

examined the sections for DiI stainings. Slices without DiI stainings were counterstained with cresyl violet and coverslipped with Depex mounting medium. To reconstruct the recording tracks pictures of the DiI sections were taken with a fluorescence microscope (Olympus BX 63). The recording sites were determined in relation to the lesion site or the DiI tract and reconstructed onto the standardized coordinates of the chicken brain atlas (avianbrain.org). To account for the shrinking of the tissue during fixation, we calculated with a 10 % shrinkage factor.

3.1.6 Analysis

We processed all data with in-house developed programs written in MATLAB. To create a peristimulus time histogram (PSTH), neuronal activity over 10 repetitions was summed for each spatial position. Before stimulus presentation 50 ms of baseline activity was recorded. To determine if a unit was responsive or not, we moved a 10 ms window in 1 ms steps over the recording window and compared the responses in each window with the first window (containing only spontaneous activity). The first two consecutive windows with a significant change in activity (0.01 significance p-value, Wilcoxon signed-rank test, MATLAB) were taken as the start of the response and the last two as the end of the response. A significant change could both mean an increase or a decrease in activity. We normalized the response to the overall maximum activity. If there was no significant response we discarded the unit as unresponsive. We organized the aSRF data in a three-dimensional azimuth-by-elevation-spike activity array. The data were smoothed in azimuth and elevation with a standard MATLAB function (moving_average2 (size = 2)). We graphed the data as contour plots (10 % activity contour spacing) using a Hammer projection.

We calculated area sizes of the aSRFs on the basis of the 67% activity contour line. To ensure equally sized areas even on different positions on the sphere, we projected everything according to the Hammer projection, which is an equal-area projection. This also allowed us to calculate the exact position of the centroid of the

area. Most centroids were on the contralateral side to the recording. Due to the nature of the projection, centroids on the lateral side, exceeding a distance of 180° to the centroids of the contralateral side, are actually getting closer to the contralateral centroids. The projection is two-dimensional; the stimuli however were presented on a spherical surface. To account for these periodic boundary conditions, we excluded the few centroids to the opposite side as they would unproportionally factor into the mean.

FRF visualizes the summed activity of auditory units in response to frequency and amplitude combinations. Double-tuned FRFs are characterized by two distinct response fields, single-tuned FRFs by one response field. CF, thresholds at best frequency (BF) and Q10dB values are directly based on the FRF. Q10dB values result from the BF divided by the bandwidth 10 dB above threshold.

To qualify as an annular aSRF, the unit's local minima had to be at least 30 % less active than the bordering two local maxima (along elevation and or azimuth). The local maxima had to be at or above 30 % of the maximum activity. The distance between the local maxima through the local minima gave the dimensions of the aSRF in elevation and azimuth. As the distances between local minima and maxima were typically the same, the position of the center of the annular aSRF was given by the local minima position.

All statistical analysis were performed with MATLAB.

3.1.7 Explaining aSRFs by ILDs and ITDs

The shape of the aSRFs in the barn owl results from specific combinations of both ILDs and ITDs (Moiseff 1989). In contrast, the spatially selective units in other birds respond to either specific ILDs or ITDs (Volman and Konishi 1990; Lewald 1987, 1990). Auditory generalists have relatively simple HRIRs with multiple redundant cues, i.e., highly correlated ILDs and ITDs (Schnyder et al. 2014).

To evaluate the hypothesis that auditory space in hearing generalist bird species is encoded using multiple redundant cues we used a neural network analysis to fit

aSRFs on ITDs and ILDs derived from the chicken HRIR. In detail, we tested whether the observed aSRFs can be explained by both the ITDs and ILDs as measured by (Schnyder et al. 2014). These authors measured the HRIR of the chicken from -73.125° to 73.125° in elevation in 5.625° steps and from -180° to 180° in 5.625° steps in azimuth. In the current analysis, we used the HRIR for frequencies from 1 to 5 kHz in 250 Hz steps. As the avian auditory system is unable to phase-lock for frequencies above 4 kHz no ITD information was included for frequencies above 4 kHz (Klump 2000). In several units it was possible to record FRFs. For these units, we only used the frequencies up to 500 Hz below and above their center frequency.

Both the ILDs and ITDs correlate highly across frequencies. To reduce the number of inputs while maximizing the input information, we performed a principal component analysis on the ILDs or ITDs. For each unit, the five first principal components were retained (explaining over 99% of variance in each case).

Next, we assessed whether the five principal components were able to fit the units' measured spike rate as a function of azimuth and elevation. In a first attempt, we fitted a multiple linear regression model with the spike rate as dependent and the five PCs as independent variables. However, this approach ignores the fact that, for some units, we found the spike rate to be a non-linear function of both ILD and ITD. To allow for this non-linear relationship, we used a simple neural network instead of linear regression.

The neural network consisted of six artificial neurons: five artificial input neurons (i_1 to i_5) and a single artificial output neuron o. Each artificial input neuron transformed the value $p_{n,\theta}$ for principal component n for direction θ into a non-linear response r_n as follows,

$$r_{n,\theta} = f(w_{1,n} \times p_{n,\theta} + b_n)$$

with $w_{1,n}$ and b_n weight and bias parameters, respectively. The function f denotes the log-sigmoid transfer function. Finally, the output o_θ of the artificial output neuron o for

direction θ was given by,

$$o_\theta = f[\sum_{n=1}^{5}(w_{2,n} \times r_{n,\theta}) + b_o]$$

The values of the weights $w_{.,n}$ and biases $b_.$ were fitted using the Levenberg-Marquardt backpropagation algorithm as implemented in MATLAB. The goodness of fit was evaluated by calculating the correlation between the output of the neural network o_θ and the spike rate of the unit s_θ across all directions θ.

For each unit, two networks were trained: one using principal components derived from the ILDs as input and one using principal components derived from the ITD as input. Hence, for each recorded unit we obtained two correlation measures ρ_{ILD} and ρ_{ITD} expressing how well its receptive field could be approximated using the ILDs or ITDs, respectively.

3.2 Results

3.2.1 Auditory recordings in the chicken midbrain

In total we recorded 81 auditory units extracellulary from the left midbrain of 9 adult female chickens. 42 units were located in the IC, 7 in the FRLx and 32 units in the OT (Fig. 3.1). All auditory units in the OT were exclusively located in the deep layers (stratum griseum centrale (SGC) and stratum album centrale (SAC)), layer 13 to 15 (see (Luksch 2003) for review). Recordings in the OT were restricted in the rostral-caudal dimensions to the accessible tectum, which extended from 2.6 to 3.8 mm (in accordance to the chicken brain atlas of avianbrain.org). Auditory units in the OT were sparse compared with the IC. While a single penetration in the IC yielded numerous auditory units, penetrations in the OT seldom even yielded one unit.

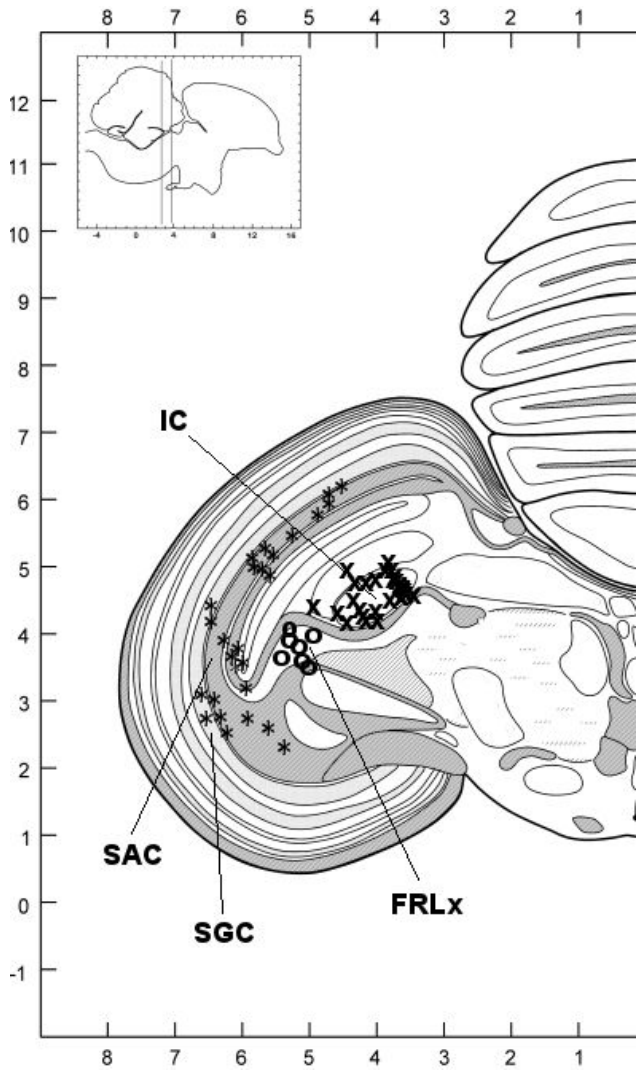

Figure 3.1: Recording sites in the chicken midbrain. Different symbols indicate recording sites in different structures: OT (asterisk), IC (cross) and FRLx (circle). Note that the rostro-caudal dimension is collapsed here. The section is a slightly modified version of the chicken brain atlas from avianbrain.org (avianbrain.org). All recordings were made from the left hemisphere. IC = inferior colliculus, FRLx = formatio reticularis lateralis mesencephali externalis, SAC = stratum album centrale, SGC = stratum griseum centrale;

3.2.2 Overview of auditory units along the midbrain structures and their responsiveness to noise and pure tones

The majority of the auditory units in the IC, FRLx and OT were responsive to noise (note that this finding might be biased as we searched for auditory units with noise presented in a virtual acoustic space. All units not responding to noise, meaing responding only to pure tones, were accidentally recorded). In the IC, the majority of auditory units were responsive to pure tones (75%) and to white noise (90%). In the FRLx, more than half of the units responded to pure tones and every unit in this area responded to white noise. In the OT almost half of the units responded to pure tones and almost all to white noise. When all structures are compared, the responsiveness

to pure tones decreased from the IC over the FRLx to the OT (see Table 1).

Based on the PSTHs, two different types of response to pure tones and noise could be observed. PSTHs either showed On-responses, responding to sound onset only, or tonic response, responding during the whole duration of the stimulus (Fig. 3.2). For pure tones mainly On-responses were observed (Fig. 3.2a). Responses to noise were always tonic (Fig. 3.2b).

Table 1: Overview of auditory units by midbrain structure and responsiveness to pure tones or noise.

Structure	IC (n=42)	FRLx (n=7)	OT (n=32)
Responsive to pure tones (%)	78.7 (n=33)	58.0 (n=4)	43.8 (n=14)
Responsive to noise (%)	90.4 (n=38)	100.0 (n=7)	87.5 (n=28)

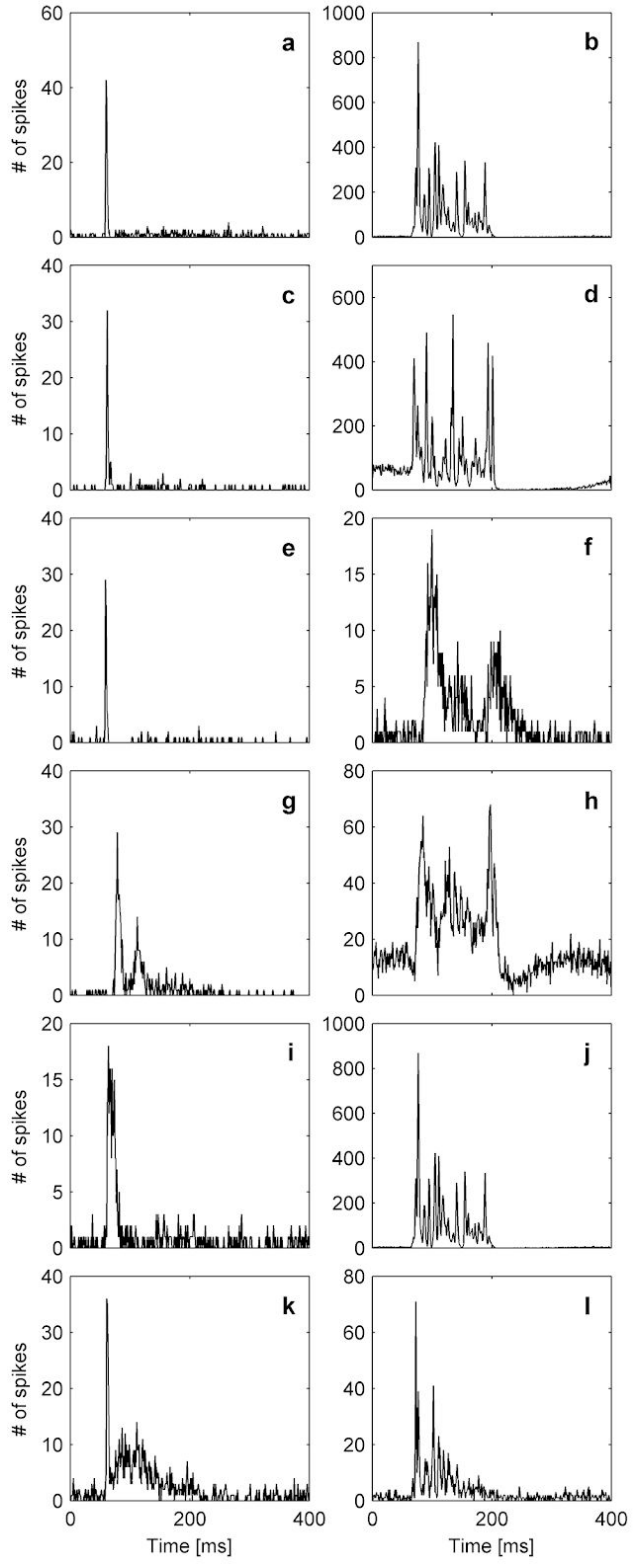

Figure 3.2: Peristimulus time histograms (PSTHs) of the neuronal activity of auditory units in response to stimulation with pure tones (left column: a, c, e, g, i, k) or noise (right column: b, d, f, h, j).

3.2.3 Frequency response fields (FRFs)

To characterize auditory units in the different structures we recorded frequency response fields (FRFs) in the IC (Fig. 3.3 a, b), FRLx (Fig. 3.3 c, d) and the OT (Fig. 3.3 e, f). Units of the IC, FRLx and OT displayed single-tuned FRFs (Fig. 3.3 a, c, e). The IC also showed double-tuned FRFs, that were characterized by two threshold minima at different frequencies separated by a threshold maximum (Fig. 3.3b). Units in the OT responded to pure tones as well, but only a few displayed a broad distinct FRF (Fig. 3.3e). Most of them responded to few frequency-level combinations only (Fig. 3.3f). Differences between FRFs in IC and OT suggest that pure tones are not the preferred stimulus for neurons in the optic tectum.

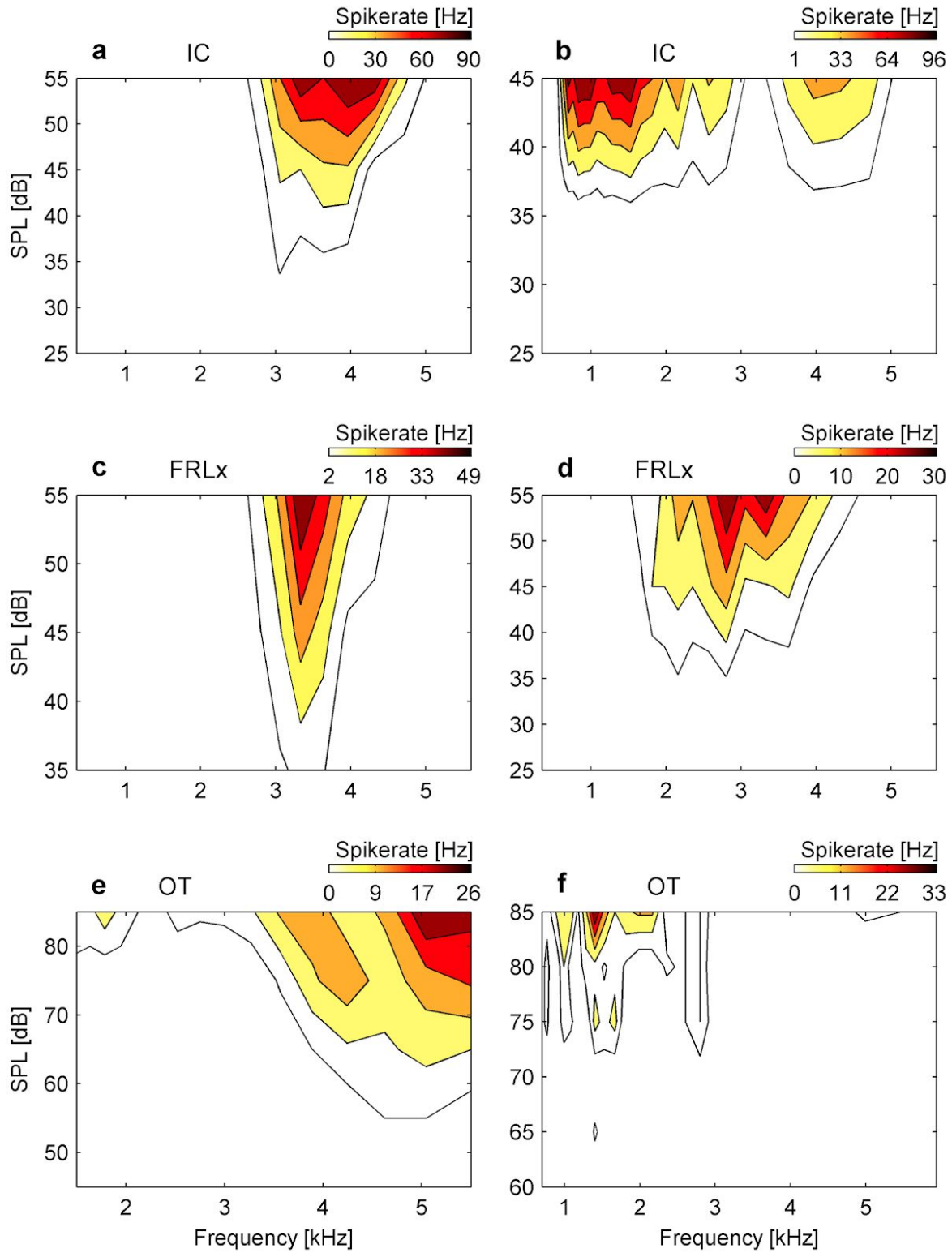

Figure 3.3: Frequency response fields (FRFs) of auditory units from the IC (a, b), FRLx (c, d) and the OT (e, f). Iso-contourline spacing is 20 % of the maximum spike rate.

3.2.4 Response properties of auditory units in the midbrain

To quantify response properties further we compared Q10dB, center frequency (CF) and thresholds for all units measured in the different midbrain structures. In general the threshold for noise was lower than for pure tones (Fig. 3.4 i, m) (Wilcoxon rank sum test $p<0.05$). Also the thresholds for both noise and pure tones of units in the OT (Fig. 3.4 l, p) were higher than for units in the IC (Fig. 3.4 j, n) (Wilcoxon rank sum test $p<0.05$).

The sharpness of the frequency tuning was quantified by the Q10dB value. Q10dB values over all structures covered a range between 0.3 and 5 (median 2.0, Fig. 3.4a). The lowest Q10dB values were found in the IC. There the Q10dB values ranged from 0.3 to 4.7 (median 1.8, Fig. 3.4b), in the FRLx from 1.4 to 4.7 (median 3.3, Fig. 3.4c) and in the OT from 1.3 to 5 (median 2.6, Fig. 3.4d).

The CF over all structures ranged from 0.66 kHz to 5.2 kHz (median 2.0 kHz, Fig. 3.4e). The CFs in the IC and OT did not differ significantly (Wilcoxon rank sum test $p>0.05$). In the FRLx units with a low frequency tuning were missing, which could be due to the low numbers recorded. In the IC the CF ranged from 0.66 kHz to 5.2 kHz (median 2.0 kHz, Fig. 3.4f). In the FRLx the CF ranged from 2.8 kHz to 4.7 kHz (median 3.3 kHz, Fig. 3.4g). In the OT the CF ranged from 0.9 kHz to 5.6 kHz (median 2.0 kHz, Fig. 3.4h).

The threshold in response to pure tones over all structures ranged from 20dB to 73dB SPL (median 41dB, Fig. 3.4i). Thresholds in the IC were lower than in the OT (Wilcoxon rank sum test $p<0.05$), with the lowest thresholds in the FRLx. In the IC the threshold ranged from 20dB to 70dB (median 38dB, Fig. 3.4j). In the FRLx the threshold ranged from 26dB to 37dB (median 34dB, Fig. 3.4k) and in the OT from 30dB to 73dB (median 54dB, Fig. 3.4l).

The threshold in response to white noise over all structures ranged from 13dB to 85dB (median 35dB, Fig. 3.4m). Again thresholds in the IC were lower than in the OT (Wilcoxon rank sum test $p<0.05$), with the lowest thresholds found in the FRLx. In the IC the threshold ranged from 15dB to 74dB (median 35dB, Fig. 3.4n), in the

FRLx 15dB to 65dB (median 50dB, Fig. 3.4o) and in the OT from 13dB to 85dB (median 40dB, Fig. 3.4p).

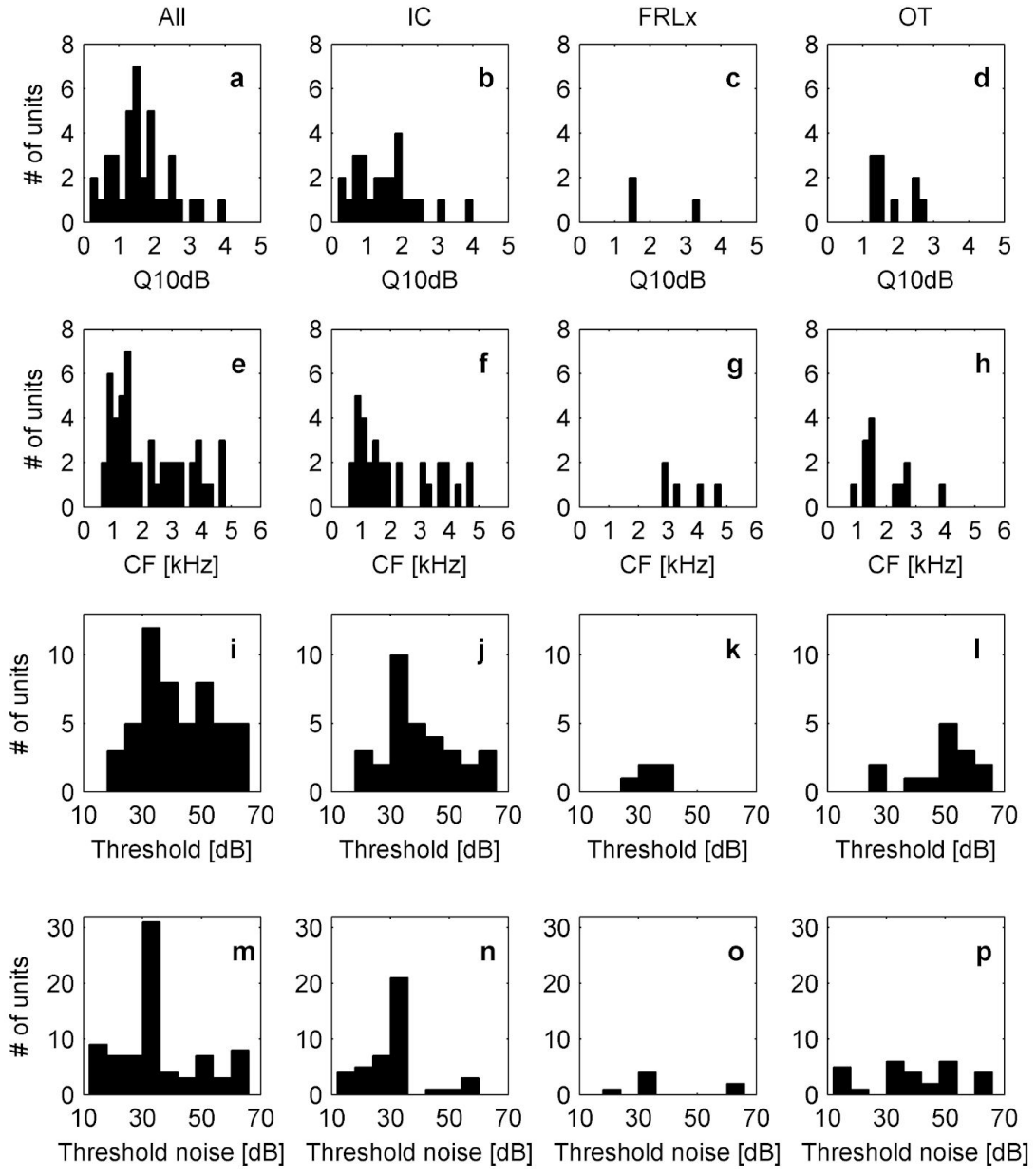

Figure 3.4: Basic response properties of auditory units in the chicken midbrain. The first column shows data summed up over all structures, columns 2-4 show data from the IC, FRLx and the OT, respectively. First row (a-d): Q10dB; second row (e-h) centre frequency (CF); third row (i-l): response threshold at CF; fourth row (m-p): response threshold measured with band-pass noise.

3.2.5 Spatially confined auditory receptive fields in the chicken midbrain

Spatially confined aSRFs could be recorded in the IC, FRLx and the OT of the chicken. Spatially confined aSRFs were defined by an increase in response strength coinciding with an orderly spatial arrangement (Fig. 3.5). In general we found two different types of aSRFs with a confined spatial tuning (Fig. 3.6).

The first type responded to contralateral sounds, was round and had its maximum response at its center (Fig. 3.6, left column) which was located around 90° azimuth and 0° elevation (Fig. 3.7). This aSRF type ranged in size from small (≥34°) to almost hemifield (~180°). The mean position of their centroids was at 90° azimuth and 2° elevation, contralateral to the recording sites. The best frequencies of the units with round aSRFs ranged from 1 kHz to 4 kHz.

The second type responded strongest to spatial positions reminiscent of an annulus and was not responsive to positions within or beyond it (Fig. 3.6, right column). This shape led us to call this type of auditory unit ‘annulus’. Most annular aSRFs had either a high best frequency (above 4 kHz) or did not clearly respond to pure tones at all.

The fact that annular aSRFs were circle symmetric (rho= -0.95, Spearman ranked correlation <0.001, Fig. 3.9a), allowed us to quantify them by diameter. Interestingly, annular aSRFs had the center always at the same position (90° azimuth and 0° elevation, see above) but varied in the outer diameter of their response area (Fig. 3.6, right column). Therefore, the eccentricity of the responsive spatial circular transect with respect to the lateral axis (ear position of 90° azimuth and 0° elevation) was specific for each annular aSRF. In some annular aSRFs the responsive circular transect was located close to the 90° lateral axis (Fig. 3.6b), while others were responsive to positions more closely to the front/back midline and higher/lower elevation (Fig. 3.6f).

In detail, annular aSRFs ranged in azimuth from 6° to 56° (Fig. 3.9a). 6° corresponds to the most frontal position found in azimuth, 56° respectively the most lateral position. In respect to elevation, annular aSRFs ranged from 23° to 67.5°. Note that the range of stimulus presentation in elevation was restricted to 67.5 degree (see

methods).

All centroids of the annular aSRFs were located within ±16° of 90° azimuth and 0° elevation (Fig. 3.9b). The mean location of the centroids was at 88° azimuth and -2° elevation. The diameter of the annular aSRFs ranged from 60° to almost 180° (Fig. 3.9c). The more frontal an annular aSRF is positioned (closer to 0°), the bigger its diameter. The smallest diameter corresponds to azimuth positions lateral to the head, the biggest diameter to azimuth positions in front and in the back of the animal. This correlation is linear (rho= -0.96) and highly significant (Spearman ranked correlation <0.001).

In one occasion we recorded an annular aSRF at more than just one stimulus presentation level. With increasing SPL, spike rate increased and the annular response field broadened. But the position of the maximum response, i.e., the diameter of the annulus did not change. Therefore, it is unlikely that annular aSRF are just a peri-threshold phenomenon.

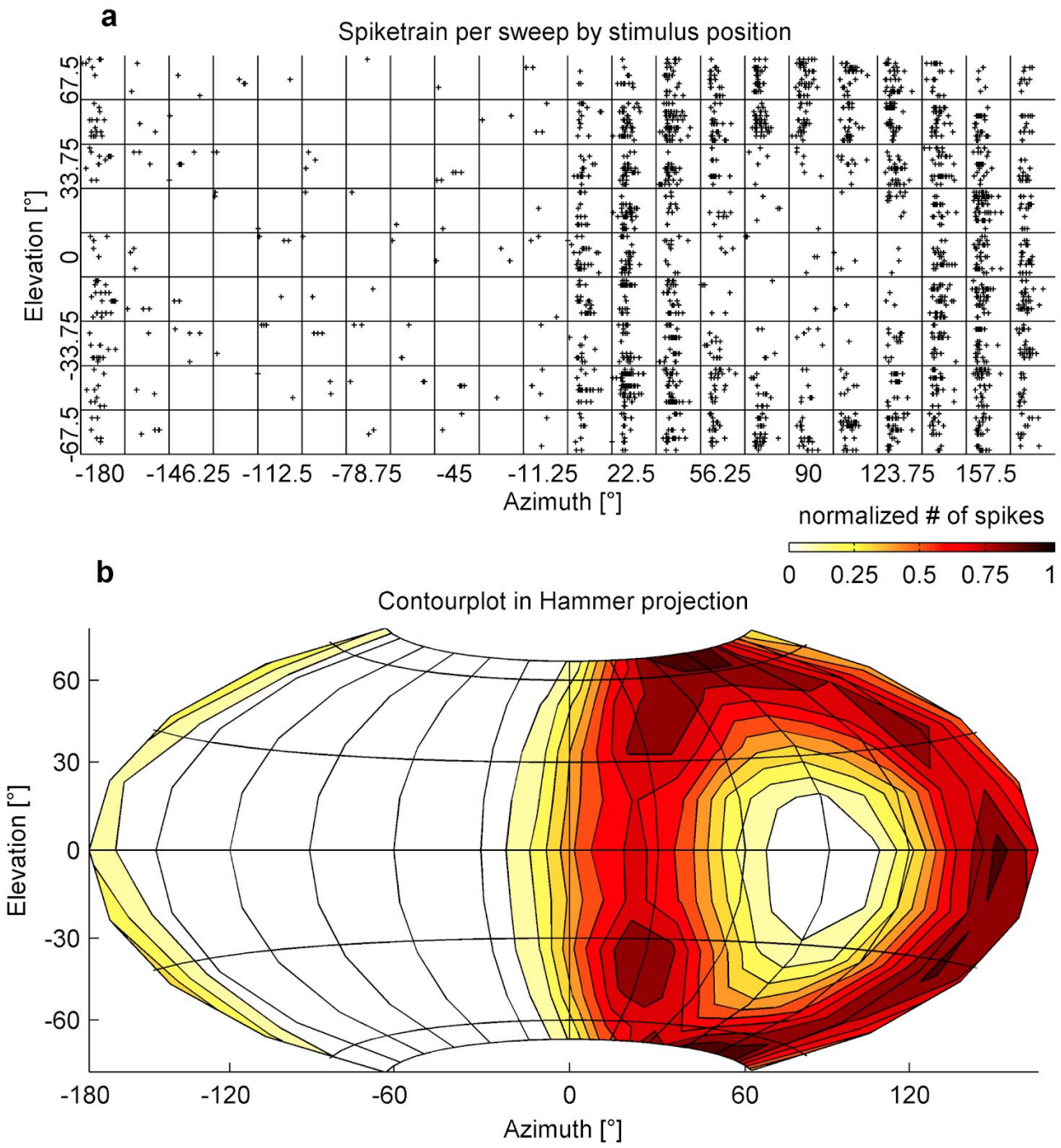

Figure 3.5: A recording from a single auditory unit whose spatial selectivity is indicated by its aSRF. The raster plots show spike activity in response to spatial stimuli. Each plot represents 10 repetitions of 500 ms of recording window duration. The plots are arranged by coordinates of stimulus position in the virtual acoustic space. 0° azimuth and 0° elevation faces the beak, 90° azimuth and 0° elevation faces the left ear (a). Summed neural activity of each stimulus position is represented in a contour plot (b). The positions are projected according to the Hammer projection. Axes correspond to the x- and y-midline coordinates.

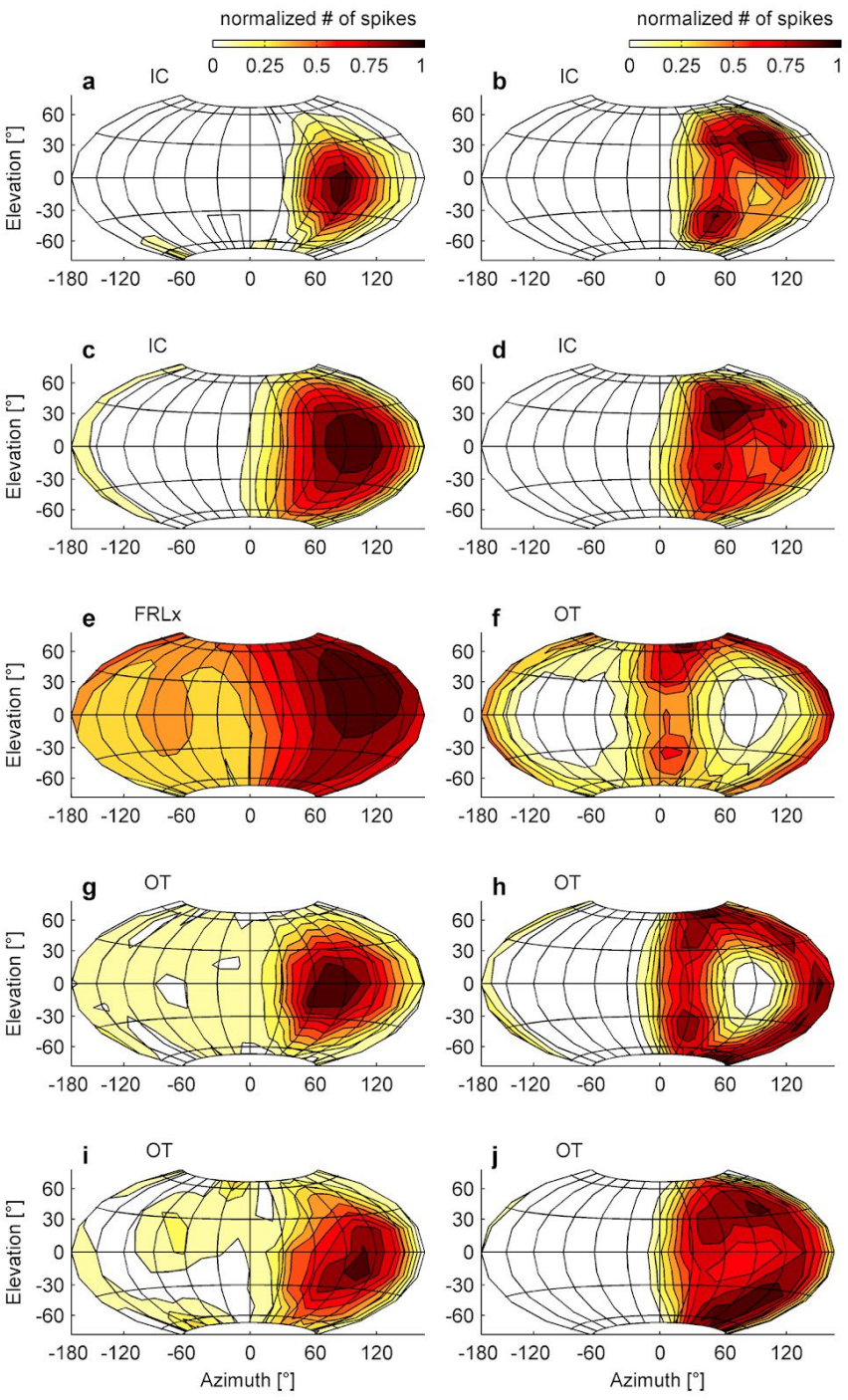

Figure 3.6: The auditory units in the midbrain display two types of auditory spatial receptive fields with a spatially confined tuning: Round (first column, a, c, e, g, i) and annular (second column, b, d, f, h, j) aSRFs. Both types of aSRFs were present in the IC and the OT. Neural activity [normalized to the overall maximum activity] is displayed for multiple sound positions. Coordinates of 0° azimuth and 0° elevation face the beak, 90° azimuth and 0° elevation face the left ear. Neural activity is projected according to the Hammer projection. Meshgrid spacing is 30°, iso-contourline spacing is 10 % activity. Axes correspond to the x- and y-midline coordinates.

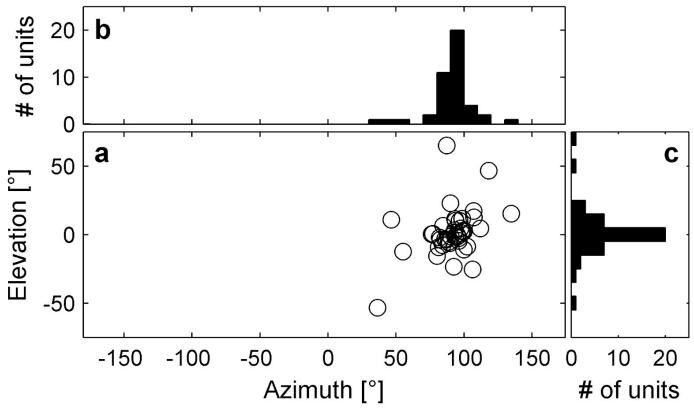

Figure 3.7: Most centroids of round aSRFs are located laterally. (a) Circles indicate the centroids of all round aSRFs measured in the IC, FRLx and OT. Coordinates of 0° azimuth and 0° elevation face the beak, 90° azimuth and 0° elevation face the left ear. Histogram of azimuth (b) and elevation (c) position of the centroids. aSRFs have been exclusively measured in the left brain hemisphere.

3.2.6 aSRFs can be explained by either ITD or ILD

A neural network analysis showed that either ITDs or ILDs can explain the shape of spatially confined aSRFs equally well. We plotted the values of the first principal component (which consists of the essential information of the ITD and ILD) against the respective (meaning the same position in space) spike rate of the neurons with a receptive field. We found three different types of relation: monotonic (Fig. 3.8d), non-monotonic (Fig. 3.8e) or no relation at all (Fig. 3.8f). Non-monotonic relations were only found for annular aSRFs (Fig. 3.8b), monotonic relations were found for round receptive fields (Fig. 3.8a) and no relation between the first principal component and the spike rate was found for unconfined aSRFs.

For each unit, two neural networks were used to fit its response. One network used principal components derived from ILDs as input and one used principal components derived from ITDs as input. For units displaying spatially confined aSRFs, the network fitted the spatial response using either principal components derived from the phase (as in ITDs, Fig. 3.8g, h) or the magnitude (as in ILDs, Fig. 3.8 j, k). The mean of the fit between the measured and predicted units' response was 90.6 % for ILDs and 91.5 % for ITDs, with no significant differences between round and annular aSRFs (Wilcoxon rank sum test $p>0.05$, for both ITDs and ILDs). There were no

significant differences between the networks using the principal components derived from the ITDs or the ILDs (Wilcoxon rank sum test $p>0.05$). Responses of auditory units displaying unconfined aSRFs could not be fitted using the neural network (Fig. 3.8 c, f, i, l). For these units, the mean fit of measured and predicted response patterns was 57.6 % for ILDs and 59.9 % for ITDs.

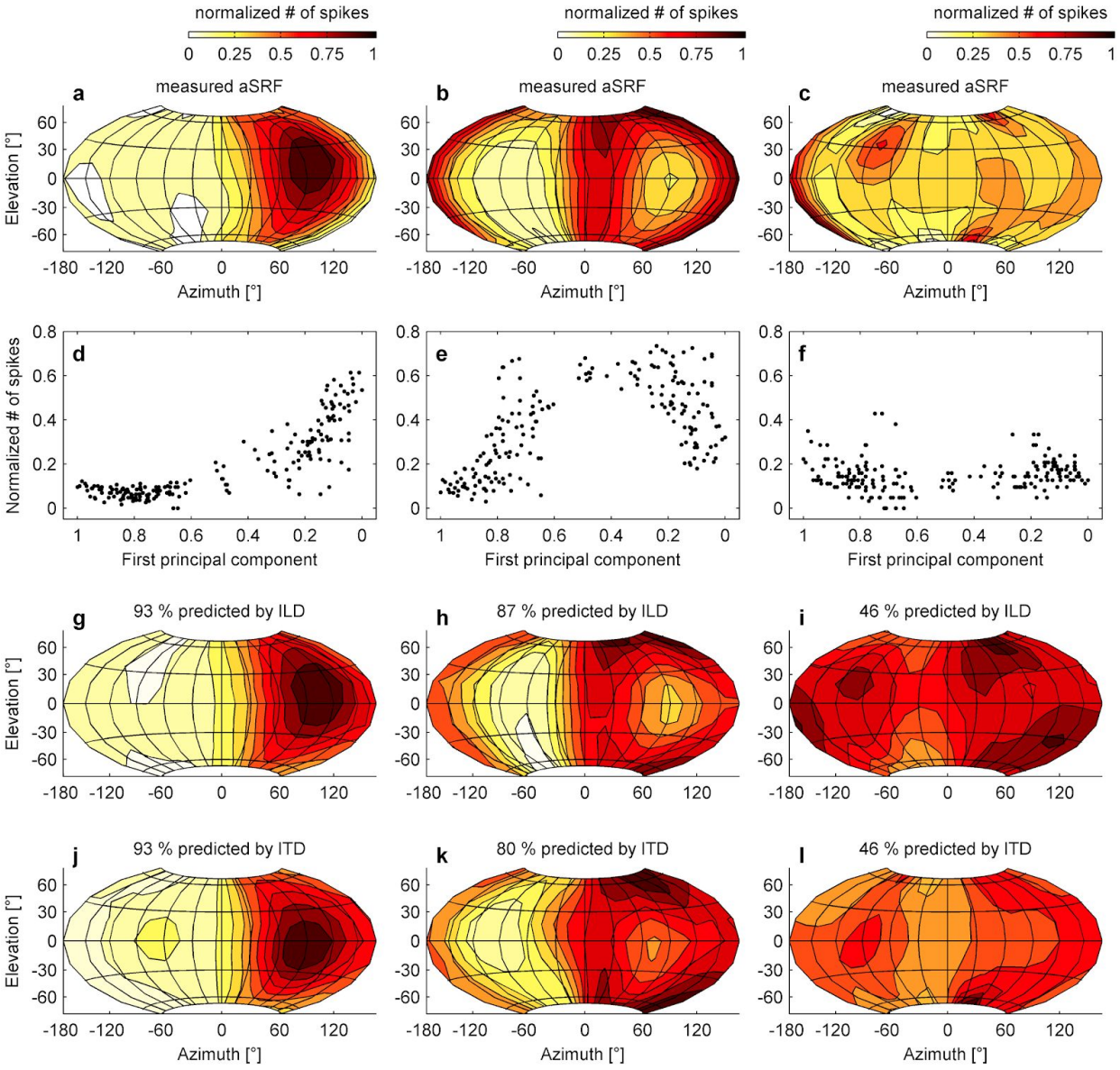

Figure 3.8: Spatially confined aSRFs can be explained by interaural time or interaural level differences (ITD or ILD) carried in the chickens HRIR. Examples show a round (a), annular (b) and unconfined aSRF (c). The first principal component of the HRIR is plotted against the spike rate (d, e, f). They are paired by their respective stimulus position. Fit of the principal components of the ITD (g, h, i) and ILD (j, k, l) to the units' spike rate as a function of azimuth and elevation. The goodness of the fit is indicated by the number above the contour plots.

3.2.7 Percentage of spatially confined auditory spatial receptive fields by midbrain structures

In the following we compare the occurrence of the different aSRF types for neurons in the three different midbrain structures (IC, FRLx and OT).

In general the percentage of spatially confined aSRFs decreased from IC to the OT. The major decrease was due to aSRFs of the round category, which decreased proportionally from IC to the OT. The percentage of annular aSRFs however increased from the IC over the FLRx to the OT.

Almost all units in the IC displayed a spatially confined aSRF (88 %, Table 2). Most of them were part of the round aSRF category (see Fig. 3.6, left column). Only a small percentage of the auditory units in the IC displayed an annular aSRF (8.1 %). Only one unit was responsive to noise, but did not show a spatially confined aSRF.

Table 2: Percentage of aSRF types by structure.

IC (n=42)		FRLx (n=7)		OT (n=32)	
Spatially confined aSRF (%)					
88.0 (n=37)		57.1 (n=4)		43.8 (n=14)	
Round	Annular	Round	Annular	Round	Annular
91.9 (n=34)	8.1 (n=3)	100.0 (n=4)	0.0 (n=0)	21.4 (n=3)	78.6 (n=11)
Responsive to noise but without a spatially confined aSRF (%)					
2.4 (n=1)		42.9 (n=3)		43.8 (n=14)	

Over half of the units in the FRLx displayed a spatially confined aSRF (57.1 %, Table 2). They all belonged to the round aSRF category (see Fig. 3.6, left column) and did not display an annular aSRF. Almost half of the units were exclusively responsive to noise, but did not show a spatially confined aSRF.

The percentage of spatially confined aSRFs is lowest in the OT. Almost half of the units in the OT did show a spatially confined aSRF (43.8 %). Most of them were part of the annular aSRF category (see Fig. 3.6, right column). If units in the OT displayed a round aSRF they were exclusively small. Only one fifth of the auditory units in the IC displayed a round aSRF (21.4 %). The rest did not show a spatially confined aSRF, even though they responded to noise. This type of unrestricted aSRF was (almost) exclusive to the OT.

3.2.8 Topographic distribution of annular aSRFs in the optic tectum

Annular aSRFs were mostly found in OT neurons. As the OT is typically known to display a topographically arranged map of space, we analyzed our data accordingly. Indeed, units with annular aSRFs display a topographic distribution in the OT if they are characterized by their diameter (Fig. 3.9d). The more dorsal an annular aSRF unit was positioned in the OT, the smaller its diameter was. This correlation is significant (Spearman ranked correlation <0.002) and stays significant even if the outlier (at 6.2 mm ventral-dorsal) is removed. Even though we recorded auditory units in the OT in a wide dorso-ventral range (see Fig. 3.1), almost all units displaying annular aSRFs were located in the middle of the OT.

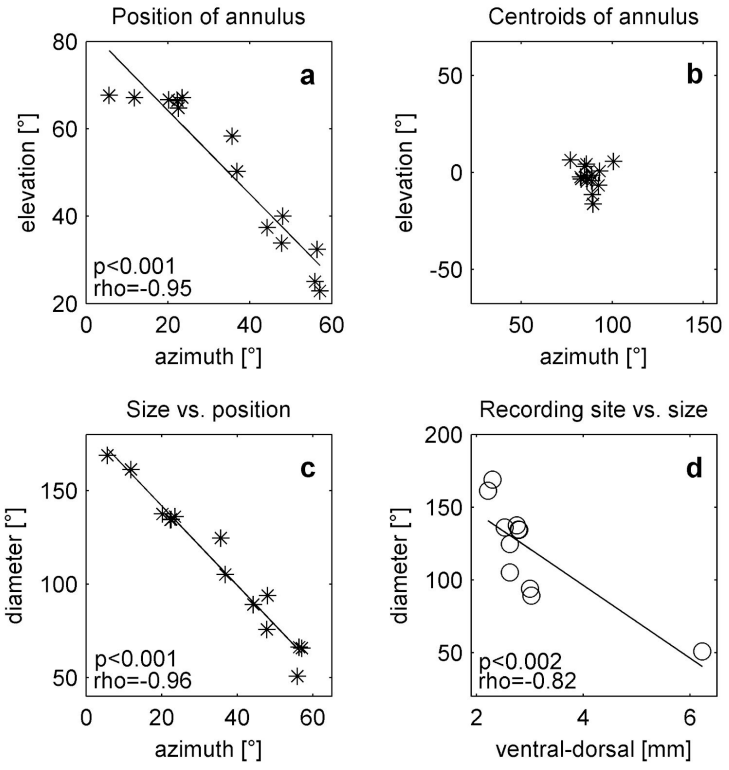

Figure 3.9: Characterization of annular aSRFs and its topographical distribution in the OT. The local maximum response of the annular aSRFs in azimuth is taken at 0° elevation and the local maximum in elevation is taken at 90° azimuth. As annular aSRFs have two local maxima along one dimension, we selected the one closest to the front of the animal for azimuth and the upper one for elevation. Local maxima in azimuth and elevation correlate significantly (a) (Spearman ranked correlation <0.001). Local minima inside all annular aSRFs are located around 0° elevation and 90° azimuth (b). The diameter and the local maximum in azimuth correlate significantly (Spearman ranked correlation <0.001) (c). Diameter and the recording site along dorsal-ventral in the OT correlate significantly (Spearman ranked correlation <0.002) (d).

4 Discussion

4.1 Sound localization cues in birds

The data here show that, even without external ear structures, birds have access to cues for sound localization in elevation. Simple physical diffraction around the bird's head creates frequency-dependent intensity variations that occur on the side contralateral to the sound source. A model shows that a reliable sound localization in elevation is possible and in addition gives us for each sound position the respective localization accuracy. Lateral sounds are modified to such an extent that they are located with highest accuracy (Fig 2.4).

Whereas a lateral focus for sound localization would misalign the acoustic and visual axis in frontal-eyed animals such as primates, for birds with laterally positioned eyes it is advantageous because it aligns the visual with the acoustic axis (Fig. 4.1). This configuration directs both distance senses towards the same spatial location and thus facilitates object detection through multisensory integration (Witten and Knudsen 2005). Most avian species have lateral eye positions (Iwaniuk et al. 2008) that are essential to visually monitor the full extent of the environment – a crucial issue for animals that are preyed upon. For predators however, binocular vision and stereopsis are far more important (Harmening and Wagner 2011). Since the evolutionary pressure towards a larger binocular overlap conflicts with the lateral layout for auditory localization, it is conceivable that some predators (especially those that strongly rely on both vision and audition) developed alternative solutions. Through the formation of a feather ruff and asymmetrical ears, low-light predators such as the barn owl could again align both visual and auditory localization foci (Fig. 4.1), maximizing hunting success at dusk and night.

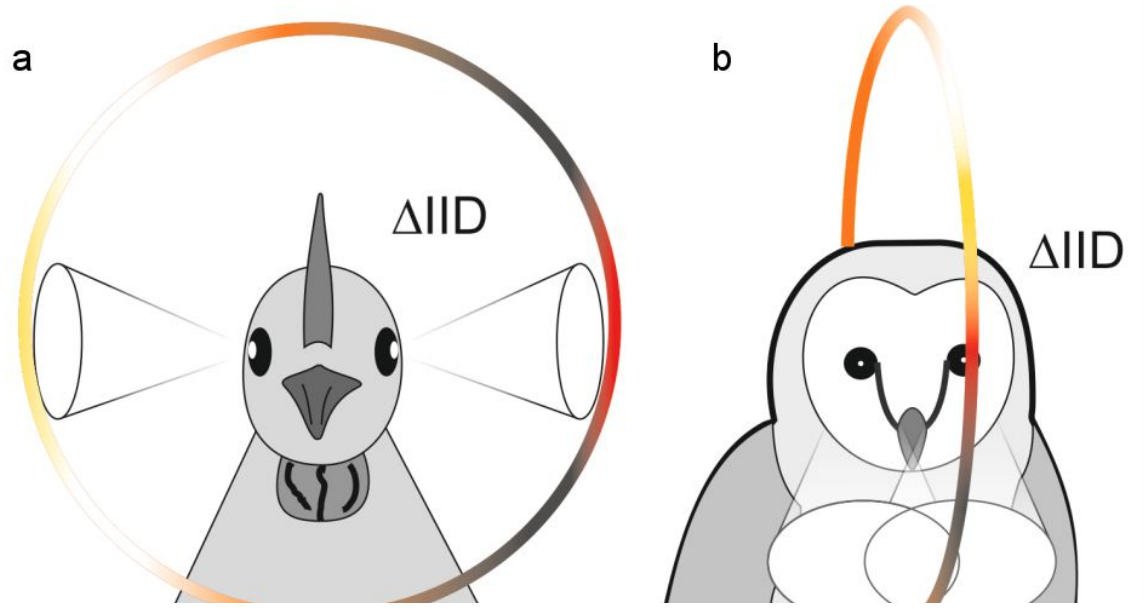

Figure 4.1: Schematic interpretation that directionality of vision and hearing align. Lateral eyed birds like *Gallus gallus* have access to elevation dependent IIDs on both sides (a) (see Figures 2.5 to 2.7). Frontal eyed birds like Tyto alba however have access to their elevation dependent IIDs in front (b) [6]. Colors indicate changing IID values. (Illustration: Harald Luksch)

These results suggest that the majority of birds rely on sound localization cues induced by diffraction of sound by the head of the animal.

4.2 The hearing range of birds is connected to the perception of sound localization cues

It has long been puzzling to science why the avian hearing range is shifted to a lower-frequency range compared to mammals. A common explanation is that the avian ear is subject to evolutionary constraints that limit its high-frequency sensitivity. But this explanation is inaccurate, as there are some avian species, such as small songbirds or owls (Fay 1988, Gleich et al. 2005) which have an increased sensitivity for higher frequencies. Here I offer another explanation for the lower-frequency hearing in birds: As mentioned in the introduction, the high-frequency hearing of mammals allows them to perceive pinna-based intensity cues (IIDs and spectral cues) (Heffner and Heffner 2008). A similar adaptation could also be shown for the barn owl. External structures and asymmetrical ears induce IIDs, especially at high

frequencies (Campenhausen and Wagner 2006). Without their high-frequency hearing they could not use these IIDs. Thus, in both cases, the barn owls' and mammals' high frequency hearing is driven by the perception of sound localization cues in the intensity domain. This suggests that the hearing range of birds, which manage without asymmetrical ears, is also related to sound localization. In the second chapter I could show that the IIDs that normal birds have available are induced by diffraction of sound by the head. If the hearing range of birds adapted to the perception of localization cues, there should be a connection between their hearing range and IIDs. Please note: The smaller the bird's head, the higher the frequencies must be in order to induce the same IIDs. For this I sampled all bird species with known audiograms from the literature and measured their head width at the Zoologische Staatssammlung München (Snow 1961, Coles et al. 1987, Pytte et al. 2004, Gleich et al. 2005, Jensen and Klokker 2006). Ear symmetries / asymmetries of owls are based on a study by Norberg (1977). Owls with unknown symmetries were not considered. All other birds I have classified as symmetrically eared. The frequency of best hearing is plotted against the head width, measured from ear to ear. For comparison, I have indicated how the typical frequency at which the localization cues (IIDs) occur varies as a function of head width, which is described by the following formula:

$$frequency\ (kHz) = \frac{speed\ of\ sound\ in\ air\ (m/s)}{2\pi} \times \frac{IID{-}coefficient}{head\ width\ (mm)}$$

The equation assumes that the head size can be characterized by the head width, i.e. that the skulls of birds with different head widths only differ in scale and not in shape. Then, I used the geometric fact that the wavelength of the sound wave at which the localization cues occur is directly proportional to the head size. Finally:

$$frequency\ (Hz) = \frac{speed\ of\ sound\ in\ air\ (m/s)}{wavelength\ (m)}$$

The IID-coefficient is used for matching the formula to the measurements obtained for the female chicken head.

For the frequency where maximum IIDs of ~ 8 dB occur, the IID coefficient is 1.24; for the frequencies of maximum IIDs of ~ 3 dB, the IID coefficient is 0.908. I chose 3

dB IID, since this is the threshold at which a bird can distinguish between left and right (Welch and Dent 2011).

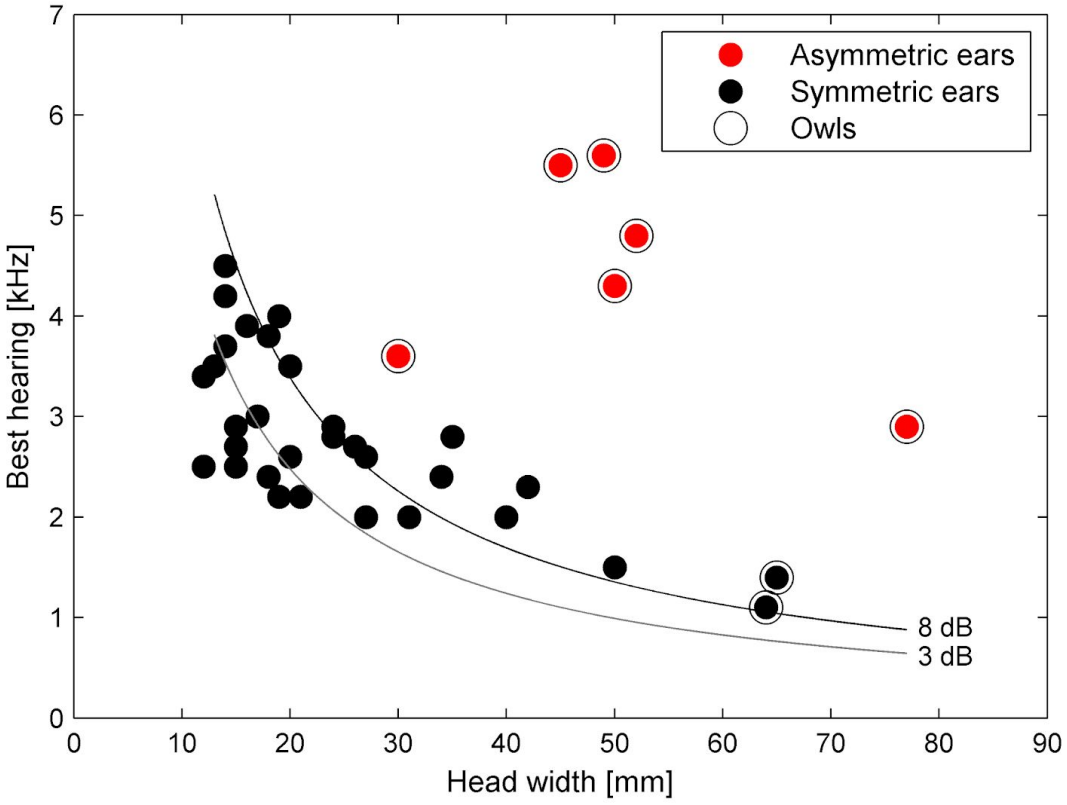

Figure 4.2: Best frequency hearing of birds with symmetrical ears follows the strength of their IIDs. Black dots indicate birds with symmetric ears, red dots birds with asymmetric ears. Circles indicate owls. The curves show the frequencies at which the different head sizes induce specific IIDs. At the gray line the head starts to induce perceptible IIDs, at the black line it already induces strong IIDs.

The best frequency hearing of birds with symmetrical ears follows the strength of their IIDs (Fig. 4.2). Altogether two different clusters distinguish themselves by their ear symmetries. The best hearing of birds with symmetrical ears is in the low frequency range and the best hearing of the birds with asymmetrical ears in the higher frequency range. Owl species are present in both the high and low frequency range. However owls with symmetrical ears follow the trend of the remaining birds. The rest of the owls, all with asymmetrical ears, are the only birds found in the high-frequency range.

This suggests that the difference in hearing range between bird species can be explained by their ear symmetries. For birds with symmetrical ears, a lower frequency hearing is sufficient, since their IIDs are induced at lower frequencies by diffraction by the head. As this principle of inducing IIDs increasingly collapses at higher frequencies (Wiener 1947), a higher-frequency hearing would not make sense for symmetrically eared birds. Diffraction, however, allows strong IIDs only to the sides. As owls possess frontal vision, sound localization based on diffraction (and symmetrical ears) would cause a mismatch between hearing and seeing. As mentioned before, this problem is solved in owls by a feather ruff and asymmetrical ears that induce strong IIDs in front. Because these IIDs are only induced at high frequencies, a high-frequency hearing allows owls with asymmetric ears to use these IIDs.

Sound localization with diffraction as the main source for IIDs also comes with certain advantages. Diffraction works mainly with lower frequencies, which do not interact as much with objects and are less strongly attenuated by air. This allows the animal to locate sound events that are farther away. For an animal that covers great distances in a short amount of time (while flying), this is quite convenient.
This principle, on the other hand, also entails certain limitations. The strength of the IIDs can not be increased arbitrarily as diffraction collapses at higher frequencies (Wiener 1947). A channel that connects the two ears of birds internally and allows for an IID gain appears to be a solution (Vedurmudi et al. 2016).

Last but not least, the relation between best frequency hearing and IIDs has also an application for ornithology. As the size of the head determines IIDs, and IIDs are linked to the best frequency hearing of birds, in a way the head size determines the hearing range. By measuring a bird's head size and applying the above mentioned formula, one could estimate its best hearing. Conveniently the best frequency is also closely related to the upper hearing limit (Gleich et al. 2005). All in all, this approach allows a rough estimation of a bird’s hearing range, without the necessity of time-consuming behavioral experiments.

4.3 Increasing sound localization cues without external ears

Even though it is shown here that birds do not need external ears to induce acoustic cues for sound localization in elevation, the extent of their cues is limited. Some comparable-sized mammals ‘solve’ this problem with larger pinnae and high frequency hearing. This combination not only induces the spectral cues for sound localization in elevation, but also strong IIDs (Koka et al. 2011). In contrast all animals that lack pinnae (including subterranean mammals) share an interaural canal that connects both middle ear cavities with each other (Mason 2016). Indeed simulations show that these internally coupled ears boost sound localization cues. It amplifies IIDs in the high-frequency range and increases IPDs in the low-frequency range (Vedurmudi et al. 2016). This could present a further solution to the challenge of small heads without pinnae (Christensen-Dalsgaard 2005).

It is also conceivable that the bird's head, analogous to the mammalian pinnae, is subjected to an evolutional pressure, to induce particularly strong diffraction patterns. To investigate this I compared the HRIR of a chicken with a similar sized sphere. I chose the sphere as it induces stronger IIDs compared to a similar sized circular cylinder or other comparable geometric bodies (Wiener 1947).

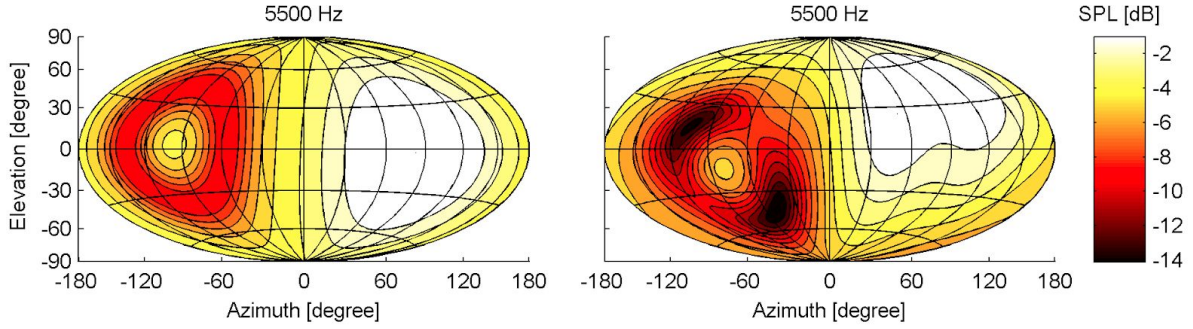

Figure 4.3: Comparison of monaural gain [dB] in the chicken (right) and a similar sized sphere (left). Sound intensity is projected according to the Hammer projection. Meshgrid spacing is 30°, iso-contourline spacing is 1 dB. Dieter Vanderelst supplied HRIRs (methods from De Mey et al. 2008).

Compared to a similar sized sphere, the bird's notches are more pronounced (Fig. 4.3), resulting in stronger IIDs. This makes it plausible that the shape of bird's heads has evolved to some extent to diffract sound more effectively.

4.4 Auditory spatial receptive fields in the midbrain of the domestic chicken

Here I show that the midbrain of a bird with symmetric ears, the domestic chicken, displays auditory spatial receptive fields (aSRFs) which are spatially confined in azimuth and elevation. Based on their shape these aSRFs can be classified into two different types, round and annular aSRFs. I recorded these fields in the inferior colliculus (IC), the formatio reticularis externalis (FRLx) and the optic tectum (OT). In the OT the annular aSRFs displayed a topographic distribution along the dorsal-ventral axis.

ASRFs in the avian midbrain (IC and or OT) have been measured before in asymmetrically eared owls, the barn owl (Knudsen and Konishi 1978a) and the long-eared owl (Volman and Konishi 1990). While neurons in the ICx of owl species with asymmetrical ears typically have aSRFs restricted in both elevation and azimuth, neurons in the ICx of avian species with symmetrical ears were reported to code for azimuth only (Calford et al. 1985; Volman and Konishi 1989, 1990). Birds with asymmetrical ears are however an exception among birds. Their asymmetric ears induce IIDs that change along the elevation in front of the animal. In contrast, the head of birds with symmetrical ears induces IIDs that change along the elevation only to the side of the animal (Fig. 4.1). All previous aSRFs measurements in birds with symmetrical ears were limited to the frontal hemisphere and a lateral extension of the fields was not considered. Volman and Konishi reported aSRFs in the ICx of symmetrically eared owls, the great horned owl, and the burrowing owl (Volman and Konishi 1990). ASRF data are also available for other avian predators, e.g., the brown falcon (*Falco berigora*), the swamp harrier (*Circus approximans*) and the brown goshawk (*Accipiter fasciatus*), all measured in the IC (Calford et al. 1985). Beyond predatory birds, aSRF data were also reported in the IC and OT of the pigeon (Lewald 1990; Lewald and Dörrscheidt 1998). Here I report aSRFs in the chicken midbrain (in the IC, FRLx and OT).

4.5 The chicken midbrain displays two different types of spatially confined aSRFs

As mentioned above, aSRFs have previously also been measured in birds with symmetrical ears (Calford et al. 1985; Volman and Konishi 1989, 1990; Lewald 1990; Lewald and Dörrscheidt 1998). However, aSRFs measured in these species never showed a spatially confined tuning in elevation. This is in contrast to aSRFs in birds with ear asymmetries, most notably the barn owl, which are clearly restricted in all dimensions (Knudsen and Konishi 1978a; Olsen et al. 1989; Volman and Konishi 1990). This difference was explained by the lack of any specializations that introduce elevation-dependent cues in symmetrically-eared birds (Klump 2000; Christensen-Dalsgaard 2005). However as shown in the second chapter, symmetrically eared birds also have access to elevation-dependent cues to the sides of the animal (Schnyder et al. 2014).

Neurons with spatially confined aSRFs in both azimuth and elevation have not been identified in previous studies of symmetrically eared birds, most likely due to a restricted experimental approach. In contrast to previous studies I always recorded the complete surround of the animals and did not limit the measurements to the frontal hemisphere or some selected transects. This was inspired by more recent work by (Nelson and Suthers 2004) and (Schnyder et al. 2014), which indicated that the hearing of symmetrical eared birds is oriented to the sides. In the chicken midbrain two different types of aSRFs can be differentiated based on their extent and shape, namely round aSRFs and annular aSRFs. The center of both types are located to the sides of the animal (at roughly 90° azimuth and 0° elevation). It is noteworthy that, without measuring both lateral hemispheres completely as in these experiments, it would not have been possible to map their full extent and shape. A closer look at the literature reveals that parts of elevation-restricted aSRFs could have been measured earlier if the stimulations had been extended to more lateral positions. Calford et al. (1985, see their fig. 2B) described one aSRF in the brown falcon that is likely to resemble the spatially confined round aSRFs shown in the present study. However Calford et al. (1985) limited their measurements to the

frontal positions. Volman and Konishi (1989) described in one case an annular aSRF in the burrowing owl as a “vertically oriented ring encircling the head”. Moreover other aSRFs described by Calford closely match annular aSRFs found in the chicken (Calford et al. 1985, see their figs. 2C, D). These results suggest that indeed all birds may have access to aSRFs with a spatially confined tuning.

Best frequencies of annular aSRFs typically were in the higher frequency range above 4 kHz. Above 3-4 kHz phase-locking is not possible for generalist bird species (Gleich and Manley 2000; Klump 2000). Therefore, it is most likely that these neurons respond either to envelope ITDs or ILDs. Envelope-ITDs are introduced when stimuli are modulated in their amplitude and presented binaurally. If envelope-modulation-frequencies are slow, also high frequency sounds are accessible for phase-locking (Wang et al. 2014). The shape displayed by the annular aSRFs (especially the ones with larger diameter, Fig. 3.6 F, H) show a strong resemblance to the “cone of confusion”, which is usually associated with sound localization based on ITDs (Mills 1972). Along such a cone stimuli from all positions possess the same ITDs and are therefore ambiguous and not distinguishable in their spatial position.

On the other hand Volman and Konishi (Volman and Konishi 1990) and Lewald (Lewald 1987, 1990) showed that the same auditory units can use both ILD and ITD to encode azimuth. ILD could especially explain the shape of the smaller annular aSRFs (Fig. 3.6 B, D) which might be directly derived from spatial pattern of strong ILDs generated by the HRIR of chicken and other symmetrically eared birds (Schnyder et al. 2014).

4.6 Whole spatial surround covered by aSRFs in the chicken

The aSRFs reported here cover the entire surrounding space of the chicken. For easier comparison the circular annular aSRFs are described in terms of their local maximum response in azimuth (at 0° elevation) and in elevation (at 90° azimuth) (as in Fig. 3.9a). While they have two such local maxima, the description is limited to the one in front of the animal for azimuth and the upper one for elevation.

Annular aSRFs cover space from 6° to 56° in azimuth, and from 23° up to the maximum measureable position at 67.5° in elevation. The more lateral annular aSRFs were located, the smaller their diameters were (Fig. 3.9c). Annular aSRFs did not extend to more lateral positions, i.e. beyond 60° azimuth and below 23° elevation.

(Volman and Konishi 1990) reported a similar range in azimuth (elevational tuning was not reported), with the most lateral aSRF positions at 60° for the burrowing owl and 50° for the great horned owl. They did not find aSRFs at positions more lateral than 60°. As sounds are omnidirectional, this would imply that these birds have an auditory “blind zone”. In natural conditions this could be perilous, as even birds of prey can be predated upon and need to monitor their environment closely. Volman and Konishi (1990) argue that they might have not found cells encoding for this “blind zone”, as they did not record from the most posterior positions in the ICx. In the chicken the round aSRF type (Fig. 3.6, left column) covers this “blind spot”. They are exclusively centered at the most lateral position, the position where I did not find annular aSRFs.

4.7 Topography of annular aSRFs in the optic tectum

I found a topographical distribution of annular aSRF units in the OT. The more ventral an annular aSRF was recorded in the OT, the bigger its diameter was. Spatiotopic auditory maps are well described for the optic tectum in the barn owl (Knudsen 1982), even though they are quite different from what I have found. In the

barn owl, a given position on the tectal auditory space map represents auditory input from a defined position in space. For the chicken I did not find such a map, but a correlation between the recording site and the diameter of the annular aSRF. As diameter is interchangeable with azimuth (see Fig. 3.6C), these findings are in accordance with the topographical distribution of azimuth found in the ICx of the great horned owl (Volman and Konishi 1989). Whether and how this topography is integrated with the visual map of space in the chicken optic tectum (Verhaal and Luksch 2013, 2015) is currently unknown.

4.8 Differences between auditory responses in the different midbrain structures

The percentage of neurons responsive to simple pure tone decreased from the IC to the OT.

While aSRF could be recorded from neurons in all midbrain nuclei tested in this study, one special type of aSRF (“annular”) was mainly observed in OT neurons. In addition, many neurons in the OT were responsive to noise stimuli presented in virtual space but did not show clear spatially confined responses.

A possible explanation is that these OT neurons require more complex acoustic stimuli than IC neurons, such as moving sound sources, stimuli with stronger envelope fluctuations or more complex spectral features (Rauschecker and Tian 2000, Nelken 2004).

4.9 Auditory responses in the bird FRLx reported for the first time

In the present study I recorded for the first time aSRFs in the bird FRLx. The FRLx was only recently described anatomically and hodologically (Niederleitner et al. 2017). This structure is located in close proximity to the ICx and the OT, receives input from the former and projects to the latter, and is discussed as the

plesiomorphic connection between the ICx and the OT (Niederleitner et al. 2017). The involvement of the FRLx in the processing of spatial auditory information could clearly be confirmed by these recordings; I found neurons with spatially confined aSRFs and responses to white noise or pure tones.

4.10 Sound localization in symmetrically eared birds

Although it was shown in behavioral tasks that symmetrically eared birds are quite capable to locate sounds in elevation (Marti 1974; Kretzschmar 1982; Rice 1982), this could not be explained on the basis of the existing data (Klump 2000). So far, it was thought that aSRFs in symmetrically eared birds do not have a spatially confined tuning in elevation. The findings here however suggest that chickens possess the necessary cues for accurate sound localization in elevation (chapter 2, Schnyder et al. 2014). This thesis demonstrates that a symmetrically eared bird, the chicken, indeed has aSRFs with spatially confined tuning in both azimuth and elevation. In addition, using a simple neural network analysis, spatially confined aSRFs can be related to the HRIR: Both ILDs and ITDs can equally contribute to the shape and location of all spatially confined aSRFs. Information about ILDs and ITDs might not need to converge but can be processed independently in the midbrain. This makes sense, as both cues are strongly correlated in the HRIR of symmetrically eared birds. Therefore, a combined use of information from both cues would not be required. This also shows that the neuronal process in the midbrain of chicken is not as specialised as in barn owls. In contrast, the shape of aSRFs in asymmetrically eared birds results from specific combinations of both ILDs and ITDs (i.e. in the barn owl; Moiseff 1989).

Here I show that aSRFs in the chicken are either round or annular. Among those round aSRFs are the smallest. Only if sound is presented lateral to the animal, neurons are stimulated that display round aSRFs. This means that the "response area" of these neurons are the smallest. As a consequence, laterally presented sounds have the lowest ambiguity for the bird. This suggests that symmetrically

eared birds locate sounds with the lowest error for lateral positions, the position where (for lateral-eyed species) the visual axis lies (Iwaniuk et al. 2008). It is therefore obvious that birds try to align their heads laterally to the sound source. The high relevance for the lateral positions is supported by behavioral data, showing that symmetrically eared birds indeed keep their head lateral to the sound source before they approach the source. Which side however, the left or right, seems to depend on the behavioral situation (near field inspection of objects vs. global orientation) and on the individual bird; some always prefer their right side, others their left (Nelson and Suthers 2004). Such side preferences are also well described for the visual system of birds (Güntürkün 1997, Vallortigara et al. 2001). For the sake of simplicity, I call this lateral direction at which a sound has minimal ambiguity 'lateral hearing axis'.

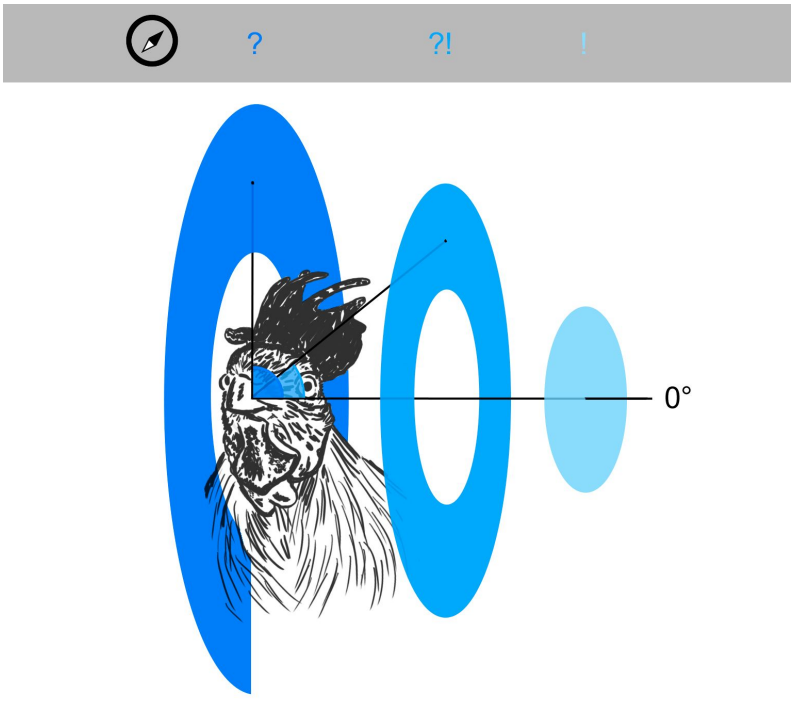

Figure 4.4: Sound sources (shown in shades of blue) with the same angles (relative to the lateral hearing axis) stimulate the same neuron in the brain. The larger the angle, the greater the ambiguity and thus the distance from the lateral hearing axis (90° azimuth and 0° elevation). (Illustration: Ulrike Schnyder)

From the view put forward here that birds are trying to keep their heads lateral to the sound source, it is also easier to explain the importance of annular aSRFs in sound localization. All sound positions which deviate from the side, whether forward, back, up or down, are represented by annular aSRFs (Fig. 4.4). With increasing deviation of the sound source from the side, the response area of the individual neuron, and

consequently the ambiguity for the animal, increases. Specifically, this ambiguity can be described by means of an opening angle (Fig. 4.4). If two sound sources are located at positions with the same opening angle, they also stimulate the same neuron, even if they are far apart in different directions. The larger the angle, the greater the ambiguity and the further the individual sound source is offset from the lateral hearing axis. This angle information alone is not sufficient to locate any sound. Our current understanding of sound localization is based on the mammalian and barn owl approach. In their case a single neuron only responds to sounds from a limited spatial direction. Even a single sound event already gives the animal a rough estimate of direction. The mechanism in birds however has to work differently. If this angle information is combined with head movements, the bird could also locate a sound. If the opening angle decreases during a head movement, this means that the bird moves the sound source towards the lateral hearing axis. If the angle increases, the animal could deduce that it turns away from the source. If the head is ultimately oriented so that the direction of the sound source aligns with the lateral hearing axis, the position of the sound gets unambiguous for the animal (Fig. 4.4, light blue “!”). Such head movements are readily observable in birds during acoustic orientation (Nelson and Suthers 2004). However in comparison to mammals and the barn owl, sound localization based on head movements needs a longer sound event to work properly.

In fact, with the OT, the bird possesses a neural structure that would be ideal for such processing. On one hand annular aSRFs are arranged in angle size along the dorsal-ventral axis of the OT (Fig. 3.9d), on the other hand, visual space and head movements are represented in the OT (Knudsen and Brainard 1995, du Lac and Knudsen 1990). These tectal annular aSRFs may therefore rather signal the distance from the hearing axis than absolute sound source location. The OT could then compute the necessary head movements to align the sound with the lateral hearing axis.

This also has an impact on multimodal integration. At first the integration of the highly ambiguous annular aSRFs with the unambiguous visual spatial receptive fields of tectal neurons seems pointless. However, an explanation could be derived

from the general role of multimodal integration: adding sensory information to get weak unisensory stimuli above threshold. Seen this way, even the ambiguous information derived from responses to annular sound positions could be beneficial for the animal, as it increases the likelihood that weak peripheral stimuli will reach the detection threshold. Possibly this is the only option for hearing generalist birds to integrate vision and hearing at all times, as the auditory system only has access to unambiguous cues at the lateral hearing axis.

The integration of multiple modalities into a unified representation has mostly been studied in animals with specialized behavior. While this strategy has been very fruitful in the past, it may have biased analysis away from the hearing generalist‘s necessity to achieve sufficient sensory precision. Finding that aSRFs in the chicken tectum are annular suggest that auditory integration might not always occur through map alignment, as in the barn owl, but could be sufficient by just signaling the spatial distance in respect to the hearing axis and consequently the prime distance sense, the visual axis.

4.11 Comparing auditory systems in tetrapods

Accurate sound localization is not only essential to birds but to all tetrapods. Interestingly tympanic hearing evolved independently among tetrapods. Consequently they all differ in certain aspects of sound localization (Carr and Christensen-Dalsgaard 2016), some of them clearly connected to their ecology.

The most striking behaviour of snakes is their way of moving on the ground. No wonder that they are specialized in perceiving sounds transmitted through the ground. Their lower jaw transmits such ground vibrations to their inner ear (Friedel et al. 2008). Consequently the canal that connects the middle ear to the air in most tetrapods is missing in snakes.

In contrast, in some turtles, in adaptation to their aquatic and terrestrial life, a hearing evolved that works both in water and air. However their eardrums transduce sound

waves more efficiently in water (Christensen-Dalsgaard et al. 2012).

The animals probably most comparable to birds are lizards which also lack external ear structures, have similar sized heads, a lateral vision and eardrums that are also connected by an interaural canal (Christensen-Dalsgaard 2005b). The sensitivity of their hearing is also in a rather low-frequency range, comparable to birds (Fay 1988). It would therefore be quite possible that they process the auditory world similar to birds. Unfortunately, in lizards there is no data on sound localization along elevation available and aSRFs have not been measured along elevation as well. However they also enhance their cues by internally coupled ears (Carr and Christensen-Dalsgaard 2016).

The mammalian auditory system is in stark contrast to the avian. A great difference can be derived from the evolution of their night-living ancestors. Night activity in mammals leads to an increased binocularity to maximize light input (Vega-Zuniga et al. 2013). However, following the argumentation put forward in this thesis, this leads to a mismatch between hearing and seeing, which is why the evolution of pinnae makes sense. They allow sound localization in front, again aligning vision and hearing. Furthermore they also differ in the neuronal processing of their localization cues (Grothe et al. 2010).

Overall, sound localization with symmetrical ears seems to work remarkably well and has proven its worth over the course of evolution. Birds dominate the airspace: in fact, during daytime the most abundant vertebrates to be seen are birds, with mammals still mostly occupying nocturnal or at least hidden ecological niches.

4.12 Conclusion

Until recently it was assumed that sound localization in elevation requires external structures and a high frequency hearing, both of which are absent in most birds. In mammals and the barn owl external ears modify high frequency components of sound to induce cues that change along elevation. Here I show that the avian head diffracts sound to induce IIDs that depend on the elevation of the source. In addition, diffraction induces these cues already at relatively low frequencies. This fits perfectly with the avian hearing, since it specializes in the perception of lower frequencies. Interestingly, the best hearing of birds seems to follow the occurrence of such cues. This could explain why pinnae have never evolved in most birds and consequently why there was no need for the avian hearing to shift to higher frequencies. Sound localization based on lower frequencies has also some advantages. Since lower frequencies are carried further in air, birds could locate sounds at greater distances. Furthermore, based on previous findings, it was assumed that aSRFs in birds with symmetrical ears are unconfined in elevation. This was quite puzzling, as this would not explain how most birds locate sounds in elevation. However here I show that the birds' auditory units, which respond to sound direction, display aSRFs that are spatially confined both in azimuth and elevation. This was only possible because in contrast to previous attempts, I have not limited my measurements to the frontal hemisphere. Instead I extended them to more lateral positions, covering the complete surround of the animal. In general, the more lateral a sound was presented, the smaller the aSRF of the responding neuron was. As a consequence, laterally presented sounds have the lowest ambiguity for the bird. The localization of sound would therefore be most accurate to the side, which is supported by our simulation and observations from nature (Schnyder et al. 2014, Nelson and Suthers 2004). Overall, birds have two areas where they could locate best. Such a bilateral hearing not only covers a fuller extent of their surroundings, it also aligns with their laterally positioned eyes. In conclusion avian sound localization has to be seen in stark contrast to sound localization in mammals and the barn owl (Figure 4.5).

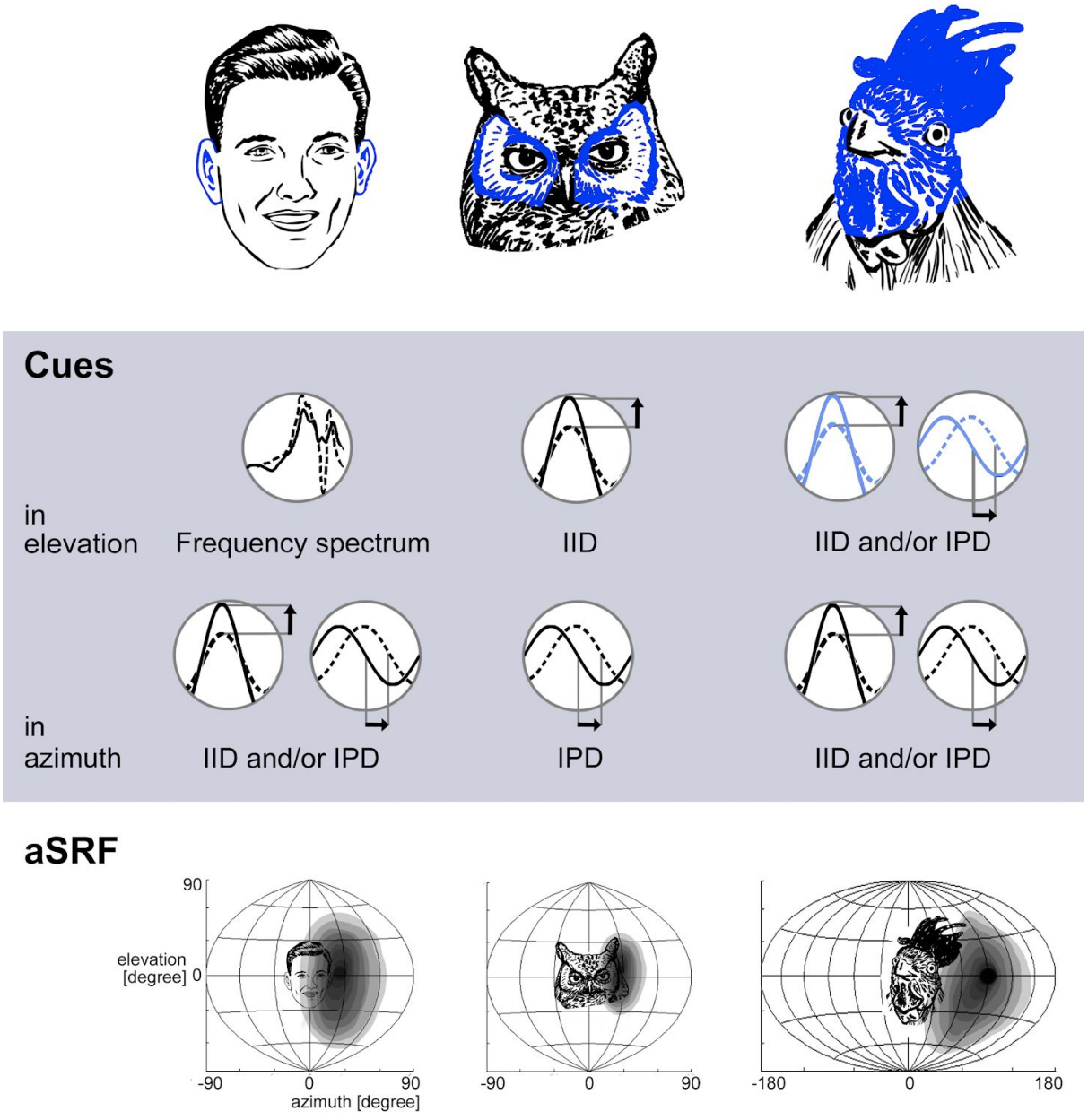

Figure 4.5: In birds with symmetrical ears the entire head induces cues for sound localization in elevation and their aSRFs are spatially confined in both azimuth and elevation. The head diffracts sounds at lower frequencies (compared to mammals and owls with asymmetrical ears) and induces IIDs to the side of the animal. In contrast to mammals and owls with asymmetrical ears, the spatially confined aSRFs in birds with symmetrical ears are always centered to the side of the head. It is likely that elevation is encoded exactly like azimuth on the basis of IIDs and/or IPDs. (Illustration: Ulrike Schnyder)

Bibliography

Anglea, S. M., Geist, D. R., Brown, R. S., Deters, K. A., & McDonald, R. D. (2004). Effects of acoustic transmitters on swimming performance and predator avoidance of juvenile chinook salmon. *North American Journal of Fisheries Management*, *24*(1), 162–170. http://doi.org/10.1577/M03-065

Au, W. W. L. (2012). *The sonar of dolphin*. Springer Science & Business Media. Retrieved from https://books.google.de/books?hl=de&lr=&id=NEXTBwAAQBAJ&oi=fnd&pg=PR7&dq=echolocation+in+cetaceans&ots=gzn5BOWnqh&sig=p0Esrl7fof58D9BjPdh3BFda6Fc

Blauert, J. (1997). *Spatial Hearing: The Psychophysics of Human Sound Localization*. *Cambridge, MA: Massachusetts Institute of Technology*. Cambridge, MA: MIT Press.

Brinkløv, S., Fenton, M. B., Ratcliffe, J. M., Brinkløv, S., Fenton, M. B., & Ratcliffe, J. M. (2013). Echolocation in Oilbirds and swiftlets. *Frontiers in Physiology*, *4*(May), 123. http://doi.org/10.3389/fphys.2013.00123

Calford, M. B., Wise, L. Z., & Pettigrew, J. D. (1985). Coding of sound location and frequency in the auditory midbrain of diurnal birds of prey, families accipitridae and falconidae. *Journal of Comparative Physiology A*, *157*(2), 149–160. http://doi.org/10.1007/BF01350024

Carr, C. E., & Boudreau, R. E. (1991). Central projections of auditory nerve fibers in the barn owl. *The Journal of Comparative Neurology*, *314*(2), 306–318. http://doi.org/10.1002/cne.903140208

Carr, C. E., & Christensen-Dalsgaard, J. (2016). Evolutionary trends in directional hearing. Current Opinion in Neurobiology, 40, 111–117. http://doi.org/10.1016/j.conb.2016.07.001

Carr, C. E., & Konishi, M. (1988). Axonal delay lines for time measurement in the owl's brainstem. *Proceedings of the National Academy of Sciences of the United States of America*, *85*(21), 8311–8315.

http://doi.org/10.1073/pnas.85.21.8311

Carr, C. E., & Konishi, M. (1990). A circuit for detection of interaural time differences in the brain stem of the barn owl. *The Journal of Neuroscience*, *10*(10), 3227–3246. Retrieved from http://www.jneurosci.org/content/10/10/3227.short

Cazettes, F., Fischer, B. J., & Pena, J. L. (2014). Spatial cue reliability drives frequency tuning in the barn Owl's midbrain. *eLife*, *3*, e04854. http://doi.org/10.7554/eLife.04854

Christensen-Dalsgaard, J. (2005a). Directional Hearing in Nonmammalian Tetrapods. In A. N. Popper & R. R. Fay (Eds.), *Sound Source Localization* (pp. 67–123). New York, NY: Springer.

Christensen-Dalsgaard, J. (2005b). Directionality of the lizard ear. *Journal of Experimental Biology*, *208*(6), 1209–1217. http://doi.org/10.1242/jeb.01511

Christensen-Dalsgaard, J., Brandt, C., Willis, K. L., Christensen, C. B., Ketten, D., Edds-Walton, P., … Carr, C. E. (2012). Specialization for underwater hearing by the tympanic middle ear of the turtle, Trachemys scripta elegans. *Proceedings of the Royal Society B: Biological Sciences*, *279*(1739), 2816–2824. http://doi.org/10.1098/rspb.2012.0290

Coles, R. B., & Aitkin, L. M. (1979). The response properties of auditory neurones in the midbrain of the domestic fowl (Callus gallus) to monaural and binaural stimuli. *Journal of Comparative Physiology A*, *134*(3), 241–251. http://doi.org/10.1007/BF00610398

Coles, R., Konishi, M., & Pettigrew, J. (1987). Hearing and echolocation in the Australian grey swiftlet, Collocalia Spodiopygia. *Journal of Experimental Biology*, *371*, 365–371. Retrieved from http://jeb.biologists.org/content/129/1/365.short

Dooling, R., Lohr, B., & Dent, M. (2000). Hearing in birds and reptiles. In R. J. Dooling, R. R. Fay, & A. N. Popper (Eds.), *Comparative hearing: birds and reptiles* (pp. 308–360). New York, NY: Springer.

du Lac, S., & Knudsen, E. I. (1990). Neural maps of head movement vector and speed in the optic tectum of the barn owl. *Journal of Neurophysiology*, *63*(1), 131–146. http://doi.org/10.1152/jn.01142.2009.

Dyson, M. L., Klump, G. M., & Gauger, B. (1998). Absolute hearing thresholds and critical masking ratios in the European barn owl: a comparison with other owls. *Journal of Comparative Physiology A: Sensory, Neural, and Behavioral Physiology*, *182*(5), 695–702. http://doi.org/10.1007/s003590050214

Engelmann, W. (1928). Untersuchungen zur Schallokalisation bei Tieren. *Zeitschrift Für Psychologie*, (106).

Fay, R. R. (1988). *Hearing in vertebrates: a psychophysics databook*. Winnetka, Illinois, USA: Hill-Fay Associates.

Firzlaff, U., & Schuller, G. (2003). Spectral directionality of the external ear of the lesser spear-nosed bat, Phyllostomus discolor. *Hearing Research*, *185*(1–2), 110–122. http://doi.org/10.1016/S0378-5955(03)00281-8

Fischer, F. P., Köppl, C., & Manley, G. A. (1988). The basilar papilla of the barn owl Tyto alba: A quantitative morphological SEM analysis. *Hearing Research*, *34*(1), 87–101. http://doi.org/10.1016/0378-5955(88)90053-6

Forster, B., Cavina-Pratesi, C., Aglioti, S. M., & Berlucchi, G. (2002). Redundant target effect and intersensory facilitation from visual-tactile interactions in simple reaction time. *Experimental Brain Research*, *143*(4), 480–487. http://doi.org/10.1007/s00221-002-1017-9

Friedel, P., Young, B. A., & van Hemmen, J. L. (2008). Auditory localization of ground-borne vibration in snakes. *The American Physical Society*, *100*(4), 4871.

Fukui, I., Burger, R. M., Ohmori, H., & Rubel, E. W. (2010). GABAergic inhibition sharpens the frequency tuning and enhances phase locking in chicken nucleus magnocellularis neurons. *Journal of Neuroscience*, *30*(36), 12075–12083. http://doi.org/10.1523/JNEUROSCI.1484-10.2010

Gardner, M. B., & Gardner, R. S. (1973). Problem of localization in the median plane: effect of pinnae cavity occlusion. *The Journal of the Acoustical Society of America*, *53*(2), 400–408. http://doi.org/10.1121/1.1981556

Giard, M. H., & Peronnet, F. (1999). Auditory-Visual Integration during Multimodal Object Recognition in Humans: A Behavioral and Electrophysiological Study. *Journal of Cognitive Neuroscience*, *11*(5),

473–490. http://doi.org/10.1162/089892999563544

Gleich, O., Dooling, R. J., & Manley, G. A. (2005). Audiogram, body mass, and basilar papilla length: correlations in birds and predictions for extinct archosaurs. *Die Naturwissenschaften*, *92*(12), 595–8. http://doi.org/10.1007/s00114-005-0050-5

Gleich, O., & Manley, G. A. (2000). The Hearing Organ of Birds and Crocodilia. In *Comparative hearing: Birds and reptiles* (pp. 70–138). New York: Springer.

Grothe, B., Pecka, M., & McAlpine, D. (2010). Mechanisms of sound localization in mammals. *Physiological Reviews*, *90*(3), 983–1012. http://doi.org/10.1152/physrev.00026.2009

Güntürkün, O. (1997). Avian visual lateralization: A review. NeuroReport, 8(6), R3–R11.

Hagstrum, J. T. (2000). Infrasound and the avian navigational map. *The Journal of Experimental Biology*, *203*(Pt 7), 1103–1111. http://doi.org/10.1017/S037346330100145X

Harmening, W. M., & Wagner, H. (2011). From optics to attention: visual perception in barn owls. *Journal of Comparative Physiology. A, Neuroethology, Sensory, Neural, and Behavioral Physiology*, *197*(11), 1031–42. http://doi.org/10.1007/s00359-011-0664-3

Hausmann, L., von Campenhausen, M., Endler, F., Singheiser, M., & Wagner, H. (2009). Improvements of sound localization abilities by the facial ruff of the barn owl (Tyto alba) as demonstrated by virtual ruff removal. *PLOS ONE*, *4*(11), e7721. http://doi.org/10.1371/journal.pone.0007721

Heffner, H. E., & Heffner, R. S. (2008). High-frequency hearing. *Handbook of the Senses: Audition*. Retrieved from http://www.utoledo.edu/al/psychology/pdfs/comphearaudio/High_Freq_Hearing_preprint_version.pdf

Hill, E. M., Koay, G., Heffner, R. S., & Heffner, H. E. (2014). Audiogram of the chicken (Gallus gallus domesticus) from 2 Hz to 9 kHz. *Journal of Comparative Physiology. A, Neuroethology, Sensory, Neural, and Behavioral Physiology*, *200*(10), 863–870.

http://doi.org/10.1007/s00359-014-0929-8

Hofman, P., Riswick, J. Van, & Opstal, A. Van. (1998). Relearning sound localization with new ears. *Nature Neuroscience*, *1*(5), 417–421.

Iwaniuk, A. N., Heesy, C. P., Hall, M. I., & Wylie, D. R. W. (2008). Relative Wulst volume is correlated with orbit orientation and binocular visual field in birds. *Journal of Comparative Physiology. A, Neuroethology, Sensory, Neural, and Behavioral Physiology*, *194*(3), 267–82. http://doi.org/10.1007/s00359-007-0304-0

Jensen, K. K., & Klokker, S. (2006). Hearing sensitivity and critical ratios of hooded crows (Corvus corone cornix). *The Journal of the Acoustical Society of America*, *119*(2), 1269. http://doi.org/10.1121/1.2159431

Keller, C., Hartung, K., & Takahashi, T. T. (1998). Head-related transfer functions of the barn owl: measurement and neural responses. *Hearing Research*, *118*(1–2), 13–34.

Klump, G. (2000). Sound Localization in Birds. In R. J. Dooling, R. R. Fay, & A. N. Popper (Eds.), *Comparative Hearing: Birds and Reptiles* (pp. 249–307). New York, NY: Springer.

Knudsen, E. I. (1982). Auditory and visual maps of space in the optic tectum of the owl. *The Journal of Neuroscience*, *2*(9), 1177–1194.

Knudsen, E. I. (1984). Auditory properties of space-tuned units in owl's optic tectum. *Journal of Neurophysiology*, *52*(4), 709–723.

Knudsen, E. I., & Brainard, M. S. (1995). Creating a unified representation of visual and auditory space in the brain. *Annual Review of Neuroscience*, *18*(1), 19–43. http://doi.org/10.1146/annurev.neuro.18.1.19

Knudsen, E. I., & Konishi, M. (1978). A neural map of auditory space in the owl. *Science (New York, N.Y.)*, *200*(4343), 795–797.

Knudsen, E. I., & Konishi, M. (1978). Center-surround organization of auditory receptive fields in the owl. *Science (New York, N.Y.)*, *202*(4369), 778–780.

Koka, K., Jones, H. G., Thornton, J. L., Lupo, J. E., & Tollin, D. J. (2011). Sound pressure transformations by the head and pinnae of the adult Chinchilla (Chinchilla lanigera). *Hearing Research*, *272*(1–2), 135–47. http://doi.org/10.1016/j.heares.2010.10.007

Konishi, M. (2000). Study of sound localization by owls and its relevance to humans. *Comparative Biochemistry and Physiology Part A: Molecular & Integrative Physiology*, (126.4), 459–469.

Konishi, M., & Knudsen, E. I. (1979). The oilbird: hearing and echolocation. *Science (New York, N.Y.)*, *204*(4391), 425–7. Retrieved from http://www.ncbi.nlm.nih.gov/pubmed/441731

Kretzschmar, E. (1982). *Wie hört ein Sperber (Accipiter nisus L.) Alarmrufe seiner Beutevögel*. Ruhr Universität Bochum.

Larsen, O. N. (2004). Does the environment constrain avian sound localization? *Anais Da Academia Brasileira de Ciências*, *76*(2), 267–73. http://doi.org//S0001-37652004000200013

Lewald, J. (1987). Interaural time and intensity difference tresholds of the pigeon (Columba livia). *Naturwissenschaften*, *74*, 449–451.

Lewald, J. (1990). Neural mechanisms of directional hearing in the pigeon. *Experimental Brain Research*, *82*(2), 423–436. http://doi.org/10.1007/BF00231262

Lewald, J. (2002). Vertical sound localization in blind humans. *Neuropsychologia*, *40*(12), 1868–1872. http://doi.org/10.1016/S0028-3932(02)00071-4

Lewald, J., & Dörrscheidt, G. (1998). Spatial-tuning properties of auditory neurons in the optic tectum of the pigeon. *Brain Research*, *790*(1–2), 339–342.

Manley, G. A. (1990). *Peripheral Hearing Mechanisms in Reptiles and Birds* (Vol. 26). Berlin: Springer Science & Business Media. http://doi.org/10.1007/978-3-642-83615-2

Manley, G. A., Köppl, C., & Konishi, M. (1988). A neural map of interaural intensity differences in the brain stem of the barn owl. *The Journal of Neuroscience*, *8*(8), 2885–2878. Retrieved from http://www.jneurosci.org/content/8/8/2665.short

Marti, C. D. (1974). Feeding Ecology of Four Sympatric Owls. *The Condor*, *76*(1), 45–61.

Mason, M. J. (2016). Internally coupled ears in living mammals. *Biological*

Cybernetics, *110*(4–5), 345–358. http://doi.org/10.1007/s00422-015-0675-1

McAlpine, D., & Grothe, B. (2003). Sound localization and delay lines--do mammals fit the model? *Trends in Neurosciences*, *26*(7), 347–50. http://doi.org/10.1016/S0166-2236(03)00140-1

Middlebrooks, J. C., & Green, D. M. (1991). Sound localization by human listeners. *Annual Review of Psychology*, *42*(1), 135–159. http://doi.org/10.1146/annurev.ps.42.020191.001031

Middlebrooks, J. C., & Knudsen, E. I. (1984). A neural code for auditory space in the cat's superior colliculus. *J Neurosci*, *4*(10), 2621–2634. Retrieved from http://www.jneurosci.org/content/4/10/2621.short

Miller, L. A., & Surlykke, A. (2001). How Some Insects Detect and Avoid Being Eaten by Bats: Tactics and Countertactics of Prey and Predator. *BioScience*, *51*(7), 570. http://doi.org/10.1641/0006-3568(2001)051[0570:HSIDAA]2.0.CO;2

Mills, A. (1972). *Auditory localization*. (J. V Tobias, Ed.)*Foundations of Modern Auditory Theory*. New York, NY: Academic Press.

Mogdans, J., & Knudsen, E. I. (1994). Representation of interaural level difference in the VLVp, the first site of binaural comparison in the barn owl's auditory system. *Hearing Research*, *74*(1–2), 148–164. http://doi.org/10.1016/0378-5955(94)90183-X

Moiseff, A. (1989). Binaural disparity cues available to the barn owl for sound localization. *Journal of Comparative Physiology A*, *164*(5), 629–636. http://doi.org/10.1007/BF00614505

Moiseff, A. (1989). Binaural disparity cues available to the barn owl for sound localization. *Journal of Comparative Physiology. A, Sensory, Neural, and Behavioral Physiology*, *164*(5), 629–36.

Moiseff, A., & Konishi, M. (1981). Neuronal and behavioral sensitivity to binaural time differences in the owl. *The Journal of Neuroscience*, *1*(1), 40–48.

Moiseff, A., Pollack, G. S., & Hoy, R. R. (1978). Steering responses of flying crickets to sound and ultrasound: Mate attraction and predator avoidance*. *Neurobiology*, *75*(8), 4052–4056. http://doi.org/10.1073/pnas.75.8.4052

Moore, B. C., Oldfield, S. R., & Dooley, G. J. (1989). Detection and

discrimination of spectral peaks and notches at 1 and 8 kHz. *The Journal of the Acoustical Society of America*, *85*(2), 820–36. Retrieved from http://www.ncbi.nlm.nih.gov/pubmed/2925997

Nelken, I. (2004). Processing of complex stimuli and natural scences in the auditory cortex. *Current Opinion in Neurobiology*. http://doi.org/10.1016/j.conb.2004.06.005

Nelson, B. S., & Suthers, R. A. (2004). Sound localization in a small passerine bird: discrimination of azimuth as a function of head orientation and sound frequency. *The Journal of Experimental Biology*, *207*(Pt 23), 4121–33. http://doi.org/10.1242/jeb.01230

Niederleitner, B., Gutierrez-Ibanez, C., Krabichler, Q., Weigel, S., & Luksch, H. (2017). A novel relay nucleus between the inferior colliculus and the optic tectum in the chicken (Gallus gallus). *Journal of Comparative Neurology*, *525*(3), 513–534. http://doi.org/10.1002/cne.24082

Norberg, R. (1977). Occurrence and Independent Evolution of Bilateral Ear Asymmetry in Owls and Implications on Owl Taxonomy. *Philosophical Transactions of the Royal Society B: Biological Sciences*, *280*(973), 375–408. http://doi.org/10.1098/rstb.1977.0116

Olsen, J. F., Knudsen, E. I., & Esterly, S. D. (1989). Neural maps of interaural time and intensity differences in the optic tectum of the barn owl. *The Journal of Neuroscience*, *9*(7), 2591–2605.

Payne, R. S. (1962). How the Barn Owl Locates Prey by Hearing. *The Living Bird, First Annual of the Cornell Laboratory of Ornithology*, 151–159.

Payne, R. S. (1971). Acoustic location of prey by barn owls (Tyto alba). *The Journal of Experimental Biology*, *54*(3), 535–73.

Peña, J. L., & Konishi, M. (2001). Auditory spatial receptive fields created by multiplication. *Science (New York, N.Y.)*, *292*(5515), 249–252. http://doi.org/10.1126/science.1059201

Popper, A. N., Plachta, D. T. T., Mann, D. A., & Higgs, D. (2004). Response of clupeid fish to ultrasound: A review. In *ICES Journal of Marine Science* (Vol. 61, pp. 1057–1061). http://doi.org/10.1016/j.icesjms.2004.06.005

Pytte, C., Ficken, M., & Moiseff, A. (2004). Ultrasonic singing by the

blue-throated hummingbird: a comparison between production and perception. *Journal of Comparative Physiology A*, 665–673. http://doi.org/10.1007/s00359-004-0525-4

Rauschecker, J. P., & Tian, B. (2000). Mechanisms and streams for processing of “what” and “where” in auditory cortex. *Proceedings of the National Academy of Sciences*, *97*(22), 11800–11806. http://doi.org/10.1073/pnas.97.22.11800

Reijniers, J., Vanderelst, D., Jin, C., Carlile, S., & Peremans, H. (2014). An ideal-observer model of human sound localization. *Biological Cybernetics*, (ILD). http://doi.org/10.1007/s00422-014-0588-4

Reijniers, J., Vanderelst, D., & Peremans, H. (2010). Morphology-Induced Information Transfer in Bat Sonar. *Physical Review Letters*, *105*(14), 148701. http://doi.org/10.1103/PhysRevLett.105.148701

Rek, P. (2014). Acoustic location of conspecifics in a nocturnal bird: The corncrake Crex crex. *Acta Ethologica*, *17*(1), 31–35. http://doi.org/10.1007/s10211-013-0155-3

Rice, W. (1982). Acoustical location of prey by the marsh hawk: adaptation to concealed prey. *The Auk*, *99*(3), 403–413.

Roeder, K. D. (1962). The behaviour of free flying moths in the presence of artificial ultrasonic pulses. *Animal Behaviour*, *10*(3–4), 300–304. http://doi.org/10.1016/0003-3472(62)90053-2

Roffler, S. K., & Butler, R. A. (1968). Factors that influence the localization of sound in the vertical plane. *The Journal of the Acoustical Society of America*, *43*(December 1967), 1255–1259. http://doi.org/10.1121/1.1910976

Schermuly, L., & Klinke, R. (1990). Infrasound sensitive neurones in the pigeon cochlear ganglion. *J. Comp. Physiol. A.*, *166*, 355–363. http://doi.org/10.1007/BF00204808

Schnitzler, H.-U., & Kalko, E. K. V. (2001). Echolocation by Insect-Eating Bats We define four distinct functional groups of bats and find differences in signal structure that correlate with the typical echolocation tasks faced by each group Perceptual problems for foraging bats. *Source: BioScience*,

51(7), 557–569. http://doi.org/10.1641/0006-3568(2001)051[0557:ebieb]2.0.co;2

Schnupp, J. W. H., & Carr, C. E. (2009). On hearing with more than one ear: lessons from evolution. *Nature Neuroscience*, *12*(6), 692–7. http://doi.org/10.1038/nn.2325

Schnyder, H. A., Vanderelst, D., Bartenstein, S., Firzlaff, U., & Luksch, H. (2014). The Avian Head Induces Cues for Sound Localization in Elevation. *PLoS ONE*, *9*(11), e112178. http://doi.org/10.1371/journal.pone.0112178

Snow, D. (1961). The natural history of the oilbird, Steatornis caripensis, inTrinidad. *Zoologica*, (46), 27–48.

Stein, B. E., Meredith, M. A., & Wallace, M. T. (1993). The visually responsive neuron and boyond : multisensory integration in cat and monkey. *Progress in Brain Research*, *95*, 79–90. http://doi.org/10.1016/S0079-6123(08)60359-3

Sullivan, W. E., & Konishi, M. (1984). Segregation of stimulus phase and intensity coding in the cochlear nucleus of the barn owl. *The Journal of Neuroscience*, *4*(7), 1787–1799. Retrieved from http://www.jneurosci.org/content/4/7/1787.short

Takahashi, T. T. (1989). Construction of an Auditory Space Map. *Annals of the New York Academy of Sciences*, *563*(1), 101–113. http://doi.org/10.1111/j.1749-6632.1989.tb42193.x

Takahashi, T. T., Moiseff, A., & Konishi, M. (1984). Time and intensity cues are processed independently in the auditory system of the owl. *The Journal of Neuroscience*, *4*(7), 1781–1786. Retrieved from http://www.jneurosci.org/content/4/7/1781.short

Theurich, M., Langner, G., & Scheich, H. (1984). Infrasound responses in the midbrain of the guinea fowl. *Neuroscience Letters*, *49*(1–2), 81–86. http://doi.org/10.1016/0304-3940(84)90140-X

Thomassen, H., Gea, S., Maas, S., Bout, R. G., Dirckx, J. J. J., Decraemer, W. F., & Povel, G. D. E. (2007). Do Swiftlets have an ear for echolocation? The functional morphology of Swiftlets' middle ears. *Hearing Research*, *225*(1–2), 25–37. http://doi.org/10.1016/j.heares.2006.11.013

Vallortigara, G., Cozzutti, C., Tommasi, L., & Rogers, L. J. (2001). How birds use their eyes: Opposite left-right specialization for the lateral and frontal visual hemifield in the domestic chick. Current Biology, 11(1), 29–33. http://doi.org/10.1016/S0960-9822(00)00027-0

Vanderelst, D., Reijniers, J., Firzlaff, U., & Peremans, H. (2011). Dominant glint based prey localization in horseshoe bats: a possible strategy for noise rejection. *PLoS Computational Biology*, *7*(12), e1002268. http://doi.org/10.1371/journal.pcbi.1002268

Vedurmudi, A. P., Young, B. A., & van Hemmen, J. L. (2016). Internally coupled ears: mathematical structures and mechanisms underlying ICE. *Biological Cybernetics*, *110*(4–5), 359–382. http://doi.org/10.1007/s00422-016-0696-4

Vega-Zuniga, T., Medina, F. S., Fredes, F., Zuniga, C., Severín, D., Palacios, A. G., … Mpodozis, J. (2013). Does nocturnality drive binocular vision? Octodontine rodents as a case study. *PloS One*, *8*(12), e84199. http://doi.org/10.1371/journal.pone.0084199

Verhaal, J., & Luksch, H. (2013). Mapping of the Receptive Fields in the Optic Tectum of Chicken (Gallus gallus) Using Sparse Noise. *PLoS ONE*, *8*(4), e60782. http://doi.org/10.1371/journal.pone.0060782

Verhaal, J., & Luksch, H. (2015). Multimodal integration in behaving chickens. *Journal of Experimental Biology*, *49*(November), 90–95. http://doi.org/10.1242/jeb.129387

Viete, S., Peña, J. L., & Konishi, M. (1997). Effects of interaural intensity difference on the processing of interaural time difference in the owl's nucleus laminaris. *The Journal of Neuroscience : The Official Journal of the Society for Neuroscience*, *17*(5), 1815–24. Retrieved from http://www.ncbi.nlm.nih.gov/pubmed/9030640

Volman, S. F., & Konishi, M. (1990). Comparative physiology of sound localization in four species of owls. *Brain, Behavior and Evolution*, *36*, 196–215. http://doi.org/10.1159/000316083

Volman, S., & Konishi, M. (1989). Spatial selectivity and binaural responses in the inferior colliculus of the great horned owl. *The Journal of Neuroscience*, *9*(9), 3083–3096.

von Campenhausen, M., & Wagner, H. (2006). Influence of the facial ruff on the sound-receiving characteristics of the barn owl's ears. *Journal of Comparative Physiology. A, Neuroethology, Sensory, Neural, and Behavioral Physiology*, *192*(10), 1073–82. http://doi.org/10.1007/s00359-006-0139-0

Vonderschen, K., & Wagner, H. (2009). Tuning to Interaural Time Difference and Frequency Differs Between the Auditory Arcopallium and the External Nucleus of the Inferior Colliculus. *Journal of Neurophysiology*, *101*(March 2009), 2348–2361. http://doi.org/10.1152/jn.91196.2008

Wagner, H., Takahashi, T., & Konishi, M. (1987). Representation of interaural time difference in the central nucleus of the barn owl's inferior colliculus. *The Journal of Neuroscience*, *7*(10), 3105–3116.

Wang, L., Devore, S., Delgutte, B., & Colburn, H. S. (2014). Dual sensitivity of inferior colliculus neurons to ITD in the envelopes of high-frequency sounds: experimental and modeling study. *Journal of Neurophysiology*, *111*(1), 164–81. http://doi.org/10.1152/jn.00450.2013

Wang, Y., & Karten, H. J. (2010). Three subdivisions of the auditory midbrain in chicks (Gallus gallus) identified by their afferent and commissural projections. *Journal of Comparative Neurology*, *518*(8), 1199–1219. http://doi.org/10.1002/cne.22269

Welch, T. E., & Dent, M. L. (2011). Lateralization of acoustic signals by dichotically listening budgerigars (Melopsittacus undulatus). *The Journal of the Acoustical Society of America*, *130*(4), 2293–301. http://doi.org/10.1121/1.3628335

Wiener, F. (1947). Sound diffraction by rigid spheres and circular cylinders. *The Journal of the Acoustical Society of America*, *6*(62), 444–451. Retrieved from http://link.aip.org/link/?JASMAN/19/444/1

Witten, I. B., Bergan, J. F., & Knudsen, E. I. (2006). Dynamic shifts in the owl's auditory space map predict moving sound location. *Nature Neuroscience*, *9*(11), 1439–45. http://doi.org/10.1038/nn1781

Witten, I. B., & Knudsen, E. I. (2005). Why seeing is believing: merging auditory and visual worlds. *Neuron*, *48*(3), 489–96.

http://doi.org/10.1016/j.neuron.2005.10.020

Witten, I. B., Knudsen, P. F., & Knudsen, E. I. (2010). A dominance hierarchy of auditory spatial cues in barn owls. *PloS One*, *5*(4), e10396. http://doi.org/10.1371/journal.pone.0010396

Wright, D., Hebrank, J., & Wilson, B. (1974). Pinna reflections as cues for localization. *The Journal of the Acoustical Society of America*, *56*, 957–962.

Yodlowski, M. L., Kreithen, M. L., & Keeton, W. T. (1977). Detection of atmospheric infrasound by homing pigeons. *Nature*, *265*(5596), 725–726. http://doi.org/10.1038/265725a0

Young, E. D., Rice, J. J., & Tong, S. C. (1996). Effects of pinna position on head-related transfer functions in the cat. *The Journal of the Acoustical Society of America*, *99*(5), 3064–76. Retrieved from http://www.ncbi.nlm.nih.gov/pubmed/8642117

Appendix

Declaration of author contributions

Chapter 2: The Avian Head Induces Cues for Sound Localization in Elevation

Authors: Schnyder Hans A., Vanderelst Dieter, Bartenstein Sophia, Firzlaff Uwe, Luksch Harald (2014) PLoS ONE

Contributions: Conceived and designed the experiments: HAS UF HL. Performed the experiments: HAS. Analyzed the data: HAS DV UF. Contributed reagents/materials/analysis tools: HAS DV SB UF. Contributed to the writing of the manuscript: HAS DV UF HL.

Chapter 3: Auditory spatial receptive fields in the midbrain of the domestic chicken (Gallus gallus domesticus)

Contributors: Vanderelst Dieter, Verhaal Josine, Firzlaff Uwe, Luksch Harald

Contributions: Conceived and designed the experiments: HAS UF HL. Performed the experiments: HAS. Analyzed the data: HAS DV UF. Contributed reagents/materials/analysis tools: HAS DV JV UF. Contributed to the writing of the manuscript: HAS DV UF HL.

Ethics statement

We performed all our experiments according to the German animal welfare law. This study has been approved by the government of Upper Bavaria, Germany (Gz. 55.2-1-54-2532-40-11). We kept our animals deeply anesthetized during all surgical procedures and recordings.

Eidesstattliche Erklärung

Ich erkläre an Eides statt, dass ich die bei der promotionsführenden Einrichtung der Fakultät Wissenschaftszentrum Weihenstephan für Ernährung, Landnutzung und Umwelt der Technischen Universität München zur Promotionsprüfung vorgelegte Arbeit mit dem Titel:
“Sound Localization in Birds - Physical and Neurophysiological Mechanisms of Sound Localization in the Chicken”
in Freising am Lehrstuhl für Zoologie, unter der Anleitung und Betreuung durch Univ.-Prof. Harald Luksch ohne sonstige Hilfe erstellt und bei der Abfassung nur die gemäß § 6 Ab. 6 und 7 Satz 2 angebotenen Hilfsmittel benutzt habe.

Ich habe keine Organisation eingeschaltet, die gegen Entgelt Betreuerinnen und Betreuer für die Anfertigung von Dissertationen sucht, oder die mir obliegenden Pflichten hinsichtlich der Prüfungsleistungen für mich ganz oder teilweise erledigt.

Ich habe die Dissertation in dieser oder ähnlicher Form in keinem anderen Prüfungsverfahren als Prüfungsleistung vorgelegt.

Ich habe den angestrebten Doktorgrad noch nicht erworben und bin nicht in einem früheren Promotionsverfahren für den angestrebten Doktorgrad endgültig gescheitert.

Die öffentlich zugängliche Promotionsordnung der TUM ist mir bekannt, insbesondere habe ich die Bedeutung von § 28 (Nichtigkeit der Promotion) und § 29 (Entzug des Doktorgrades) zur Kenntnis genommen. Ich bin mir der Konsequenzen einer falschen Eidesstattlichen Erklärung bewusst.

Mit der Aufnahme meiner personenbezogenen Daten in die Alumni-Datei bei der TUM bin ich einverstanden.

Ort, Datum, Unterschrift

Danksagung

Danke Harald, für das Wagnis ein Problem mit mir zu bearbeiten, an dem sich einige bislang die Zähne ausgebissen hatten.

Danke Uwe, für Rat und Tat zu jeder Zeit.

Danke Uli, für die vielfältige Unterstützung, gerade im letzten Jahr.

Danke Brian, für dein tiefes Verständnis der Geräuschlokalisation normaler Vögel.

Danke Josine, für die Einweihung in die Kunst der in-vivo Elektrophysiologie.

Danke Dieter, für deinen objektiven Blick fürs Wesentliche.

Danke Gaby, Birgit und Yvonne, für eure Hilfe.

Danke Simon, für dein Wissen und Verstand.

Danke Berti, für den Glauben an mich.

Danke Papa, für die Beratung.

Danke Hühner, ohne euch wäre diese Arbeit unmöglich gewesen. Ihr habt für immer meinen Respekt verdient.

Danke Susanne, Tomás, Michael, Max, Wolfgang, Tobi, Stefan, Stephan, Barbara, Ulrike, Arne, Mama, Bernhard und Elmar.

Danke Bernstein Center for Computational Neuroscience Munich (BMBF) (FKZ01GQ1004B), für die finanzielle Unterstützung.

Ohne euch alle wäre ich aufgeschmissen gewesen.